

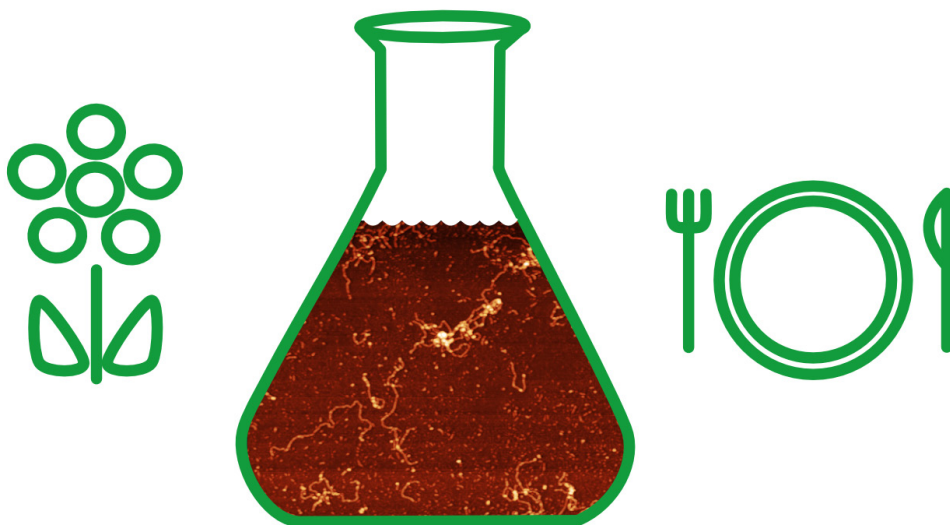


DOCTORAL THESIS NO. 2022:44
FACULTY OF NATURAL RESOURCES AND AGRICULTURAL SCIENCES

Plant protein nanofibrils

- Characterising properties for future foo

ANJA HERNEKE



Plant protein nanofibrils

- Characterising properties for future food

Anja Herneke

Faculty of Natural Resources and Agricultural Sciences

Molecular Sciences

Uppsala



SWEDISH UNIVERSITY
OF AGRICULTURAL
SCIENCES

DOCTORAL THESIS

Uppsala 2022

Acta Universitatis Agriculturae Sueciae
2022:44

Cover: Schematic drawing of a flower, an e-flask with protein nanofibrils and a plate with cutlery.

(Photo and illustration: Anja Herneke)

ISSN 1652-6880

ISBN (print version) 978-91-7760-963-6

ISBN (electronic version) 978-91-7760-964-3

© 2022 Anja Herneke, Swedish University of Agricultural Sciences

Uppsala

Print: SLU Grafisk Service, Uppsala 2022

Plant protein nanofibrils

Abstract

This thesis explores the potential of protein nanofibrils (PNFs) as an ingredient to generate structure in food. Proteins from whey and from plants were used to form PNFs, with particular focus on proteins extracted from plants. PNFs were formed by heating (85-90 °C) the proteins at pH 2 for 24-96 h. Various microstructural features were observed on casting whey-based PNFs with nanoscale variations (length, morphology) into films. Length of the PNFs, rather than morphology, had the greatest effect on microstructural attributes.

Whey is a well-studied food protein with good ability to form PNFs. Whey-based and plant-based PNFs were compared to understand better how plant proteins can be used to form PNFs with similar length. Characterisation of the secondary structure and morphology of PNFs made from plant-based sources, such as legumes, cereals, oilseeds and tubers, showed that all proteins could form PNFs, but with some variation in morphology (curved/straight).

Analysis of extracted protein size and purity to investigate their effects on formation of PNFs revealed that smaller and purer proteins gave better PNFs production. Increased pH after fibril formation affected PNF morphology and the viscosity of fibrillated samples of fava bean, fava bean globular fractions 11S and 7S, and mung bean. Straight PNFs from fava beans and curved PNFs from mung beans were examined for their ability to form and stabilise foams. At relatively low concentrations, fibrillated proteins (independent of PNF morphology) generated more voluminous and more stable foam than the corresponding protein at the same concentration. At very low concentrations, only curved PNFs gave stable foams at pH close to the isoelectric point of the protein.

Preliminary results indicated that curved PNFs from mung beans can also be assembled into microfibrils with the help of a flow-focusing method, which has potential for use in creating meat-like textures in future food applications.

Keywords: amyloids, fava bean, mung bean, lupin, oat, rapeseed, vicilin, legumin, secondary structure, nanostructure

Author's address: Anja Herneke, Department of Molecular Sciences, Swedish University of Agricultural Sciences, Uppsala, Sweden.

Nanofibriller från växtprotein

Sammanfattning

Denna avhandling undersöker möjligheten att använda protein-baserade nanofibriller (PNF:er) som en ingrediens för att skapa struktur i mat. Protein från vassle och växter användes för att bilda PNF:er, där störst fokus var på proteiner extraherade från växter. Fibrillerna bildades genom att värma (85-90 °C) proteinet vid pH 2 i 24-96 timmar. Mikrostrukturella skillnader kunde observeras när PNF från vassle med olika nanostrukturer (längd och morfologi) gjöts till filmer. Det var längden på PNF snarare än morfologin som hade den största påverkan på filmernas mikrostruktur.

Vassle är det mest studerade livsmedelsrelaterade proteinet för sin förmåga att bilda PNF:er. Vassle- med växtbaserade PNF:er jämfördes i syfte att bättre förstå hur växtproteiner kan användas för att bilda PNF:er med liknande längd. Karakterisering av sekundärstrukturen och morfologin av PNFs tillverkade från protein extraherat från baljväxter, spannmål, oljeväxter och rotfrukter visade att alla proteiner kunde bilda PNF:er dock med visa morfologiska skillnader (krulliga/raka).

Analys av de extraherade proteinernas storlek och renhet visade att mindre och renare protein förbättrade PNF produktion. Höjt pH efter fibrillering påverkade fibrillernas morfologi och lösningens viskositet för prover innehållande fibrillerat protein från åkerböna, åkerböna 11S, åkerböna 7S och mungböna. Raka PNF:er från åkerböna och krulliga PNF:er från mungböna undersöktes för deras förmåga att skapa och stabilisera skum. Vid relativt låga koncentrationer genererar fibrillerade proteiner (oberoende av PNFs morfologi) stabilare skum med större volym än motsvarande protein vid samma koncentration. Vid mycket låga koncentrationer var det endast krulliga PNF:er som bidrog till ett stabilt skum vid pH nära proteinets isoelektriska punkt.

Preliminära resultat visar att krulliga PNF:er från mungbönor också kan linjeras med hjälp av en flödescell till mikrofibrer, som har potential att användas för att skapa köttliknande texturer i framtida livsmedelstillämpningar.

Nyckelord: amyloider, åkerböna, mungböna, lupin, havre, raps, vicilin, legumin, sekundärstruktur, nanostruktur

Författaren adress: Anja Herneke, Sveriges Lantbruksuniversitet, Institutionen för molekylära vetenskaper, Uppsala, Sverige

Contents

List of publications.....	7
Abbreviations	9
1. Introduction.....	11
2. Background.....	13
2.1 PNFs from food proteins.....	13
2.1.1 In vitro formation of PNFs.....	15
2.2 PNF structure.....	15
2.2.1 Molecular structure	15
2.2.2 Nanostructure	16
2.2.3 Microstructure	17
2.3 PNF detection and characterisation.....	17
2.4 Are PNFs safe to eat?.....	18
2.5 PNFs as texture initiators in food.....	19
2.5.1 Foams.....	19
2.5.2 Microfibres	20
3. Objectives and Hypotheses	23
4. Materials and Methods.....	25
4.1 Food proteins.....	25
4.1.1 Protein extraction.....	25
4.1.2 Protein composition analyses.....	26
4.2 Protein nanofibrils	28
4.2.1 Preparation	28

4.2.2	Secondary structure.....	29
4.2.3	Nanostructure and microstructure of PNFs	30
4.2.4	Change in pH.....	31
4.2.5	Viscosity.....	31
4.3	Food model systems.....	32
4.3.1	Foams.....	32
4.3.2	Microfibres	32
5.	Research outcomes	35
5.1	Nanostructure to microstructure - the role of PNF morphology ..	35
5.2	Plant-based PNFs.....	37
5.2.1	Secondary structure of plant-based PNFs.....	37
5.2.2	Nanoscale morphology of plant-based PNFs	40
5.2.3	Protein size matters	41
5.2.4	Protein purity matters.....	44
5.2.5	Effect of changes in pH on PNFs.....	46
5.2.6	Viscosity of plant-based PNFs.....	47
5.3	Food model systems.....	49
5.3.1	Foams.....	49
5.4	Microfibres	54
6.	Conclusions	57
7.	Future work.....	59
	References.....	61
	Popular science summary	71
	Populärvetenskaplig sammanfattning	73
	Acknowledgements	75

List of publications

This thesis is based on the work contained in the following papers, referred to by Roman numerals in the text:

- I. Ayaka Kamada, Anja Herneke, Patricia Lopez-Sanchez, Constantin Harder, Eirini Ornithopoulou, Qiong Wu, Xinfeng Wei, Matthias Schwartzkopf, Peter Müller-Buschbaum, Stephan V. Roth, Mikael S. Hedenqvist, Maud Langton and Christofer Lendel (2022). Hierarchical propagation of structural features in protein nanomaterials. *Nanoscale* 14, 2502-2510.
- II. Anja Herneke, Christofer Lendel, Daniel Johansson, William Newson, Mikael Hedenqvist, Saeid Karkehabadi, David Jonsson, and Maud Langton (2021). Protein nanofibrils for sustainable food—characterization and comparison of fibrils from a broad range of plant protein isolates. *ACS Food Science & Technology* 1 (5), 854-864.
- III. Anja Herneke, Christofer Lendel, Saeid Karkehabadi, Jing Lu, Maud Langton. Protein nanofibrils from fava bean and its major storage protein: Formation and ability to stabilize foam (submitted).
- IV. Anja Herneke, Saeid Karkehabadi, Jing Lu, Christofer Lendel, Maud Langton. Protein nanofibrils from mung bean: The effect of pH on morphology and the ability to form and stabilise foams (submitted).

Papers I and II are reproduced with the permission of the publishers.

The contribution of Anja Herneke to the papers included in this thesis was as follows:

- I. Prepared microscopy images of films and participated in writing the manuscript, together with the co-authors.
- II. Designed the study together with the co-authors. Performed the majority of the laboratory work and was mainly responsible for writing the manuscript.
- III. Designed the study together with the co-authors. Performed the majority of the laboratory work and was mainly responsible for evaluating the results and writing the manuscript.
- IV. Designed the study together with the co-authors. Performed the majority of the laboratory work and was mainly responsible for evaluating the results and writing the manuscript.

Abbreviations

AFM	Atomic force microscope
CD	Circular dichroism
FPI	Fava bean protein isolate
FTIR	Fourier-transform infrared spectroscopy
LPI	Lupin protein isolate
MPI	Mung bean protein isolate
OPI	Oat protein isolate
PPI	Potato protein isolate
RPI	Rapeseed protein isolate
SDS-PAGE	Sodium dodecyl sulphate-polyacrylamide gel electrophoresis
SEC	Size exclusion chromatography
SEM	Scanning electron microscopy
SPI	Soybean protein isolate
TEM	Transmission electron microscopy
ThT	Thioflavin T
PNFs	Protein nanofibrils
WPI	Whey protein isolate

1. Introduction

Food production is one of the major causes of global environmental change. It is responsible for 30% of global greenhouse gas emissions (Willett *et al.*, 2019) and 70% of global water use (Graça, Calheiros and Oliveira, 2014). Lowering intake of animal-based products and instead eating more plant-based foods would decrease the impact of the food supply chain on the environment (Willett *et al.*, 2019). However, consumption of animal-based products is deeply rooted in many cultures (Graça, Calheiros and Oliveira, 2014). By developing novel plant-based foods mimicking animal-based products in appearance and texture, consumers can be encouraged to change to a more sustainable diet (Lonkila and Kaljonen, 2021).

Food proteins are important in the human diet for supplying essential amino acids and imparting important structural properties to many foods (such as meat and cheese) (Foegeding and Davis, 2011). However, the ability to create these textural properties is highly dependent on protein structure and ability to interact with other food ingredients. Plant proteins can have a good amino acid profile, but are usually inferior to animal proteins in creating texture in food applications, limiting their use. A possible solution to overcome this limitation of plant proteins is to reassemble these proteins into stiffer structures such as amyloid-like protein nanofibrils (PNFs).

This thesis work covers assembly and characterisation of plant-based PNFs from several sources and the functional properties of PNFs in food model systems such as foams and fibres (Figure 1). The overall aim was to explore how PNFs can be used to create texture in future sustainable food applications.

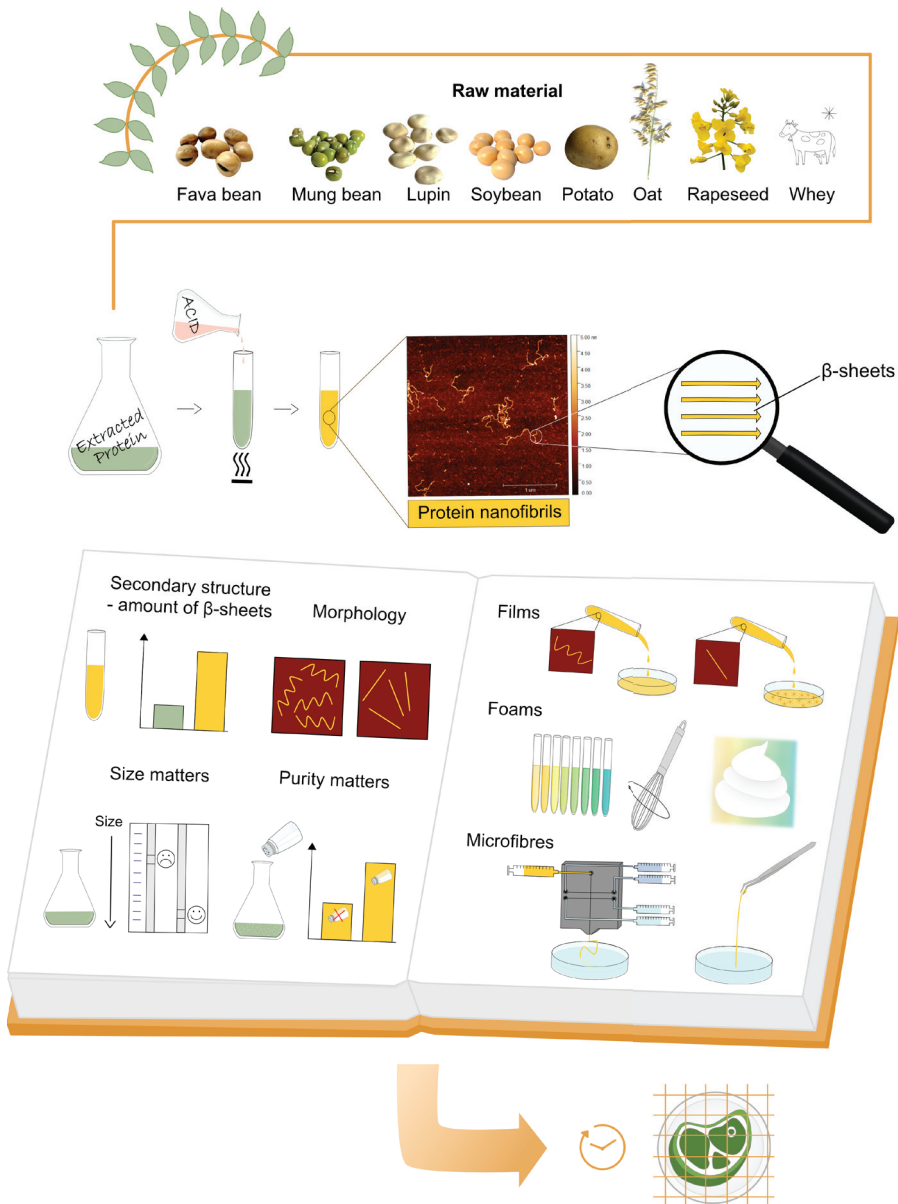


Figure 1. Plant-based protein nanofibrils from protein source to application.

2. Background

Protein nanofibrils are well-organised protein aggregates defined by having a cross β -sheet diffraction pattern when examined under X-ray (Eisenberg and Sawaya, 2017). William Astbury first reported this in 1935 when he studied poached egg white exposed to X-rays (Astbury, Dickinson and Bailey, 1935). Astbury speculated that all proteins have both a fibrous and a globular state, a suggestion later confirmed by Goldschmidt *et al.* (2010) who concluded that 98.7% of all proteins have the genetic capacity to form PNFs. This is probably why PNF structures are found in many biological systems. A well-established association is the involvement of PNF structures (amyloids) in several pathological conditions such as Alzheimer's, Parkinson's and Jacob-Creutzfeldt disease (Sipe *et al.*, 2016). Many eukaryotic organisms, from bacteria and yeasts to humans, also use PNF structures in functional biological systems (Otzen and Riek, 2019). Functional PNFs have applications as mechanical protection and adhesion in biofilms, epigenetic transfer and catalytic scaffolds. An ability to form PNFs with no connection to natural function has been reported for denatured proteins, including several of food protein origin (Cao and Mezzenga, 2019).

2.1 PNFs from food proteins

The most studied food protein in terms of ability to form PNFs is the bovine whey protein β -lactoglobulin (Lendel and Solin, 2021). Whey is a side-stream product from the cheese industry, which generates a large amount of protein that could be suitable for use in creating novel food and materials (Jelen, 1979). Whey is a mixture of several proteins, among which the β -

lactoglobulin fraction is most frequently studied for its ability to form PNFs (Ye *et al.*, 2018; Bolder *et al.*, 2006). The suitability of β -lactoglobulin for this application is due to its small size (18 kDa (Pereira *et al.*, 2007)) and high solubility (Lendel and Solin, 2021). Substantial knowledge about the fibril formation ('fibrillation') mechanism by which PNFs are produced has been gained from studies of whey and other animal-origin proteins. However, the sustainable and ethical points of view provide an even stronger motive to study the ability of plant proteins to form PNFs. For this reason, plant-based PNFs have been a growing research field in recent years.

Research to date on plant proteins has usually focused on plant storage proteins (Yang and Sagis, 2021). These can be divided according to solubility using Osborne classification system into: 1) globulins (salt-soluble), 2) albumins (water-soluble), 3) prolamins (alcohol-soluble) and 4) glutelins (dilute acid/alkali-soluble) (Osborne, 1924). Globulins are usually the most abundant storage protein in legumes and oilseeds (Yang and Sagis, 2021). The most commonly reported method for plant protein extraction is isoelectric precipitation (Sari *et al.*, 2015). In this wet-extraction method, the protein is extracted by first exposing the plant source to alkaline pH to increase the solubility of globulins and albumins, which are then separated from the insoluble fraction by centrifugation. The supernatant is adjusted to the isoelectric point of the globulins, which is usually around pH 4-5. The globulins aggregate and are collected by centrifugation, while the albumins remain in the supernatant, which is usually discarded (J. Yang *et al.*, 2022). Based on their sedimentation coefficient, globulins are usually divided into two major protein fractions, known as legumin-type (11-12S) and vicilin-type (7S-8S) globulins. Legumes usually have both legumin-type and vicilin-type globulins, while legumin-type globulins are dominant in brassicas, rice and oats (Shewry, Napier and Tatham, 1995). Legumin-type globulins from several plant species are reported to comprise a hexameric structure with molecular weight between 300 and 380 kDa (Chéreau *et al.*, 2016). Vicilin-type globulins are smaller proteins usually found in the shape of a trimer with molecular weight between 150 and 190 kDa.

Most plant-based PNFs described to date are from either whole or fractionated globulin proteins from legumes (Akkermans *et al.*, 2007; Josefsson *et al.*, 2019; Munialo *et al.*, 2014; Li *et al.*, 2020; Li *et al.*, 2019;

Herneke *et al.*, 2021; Liu and Tang, 2013). There are also some reports of legumin-type globulins from cereals (Herneke *et al.*, 2021; Zhou *et al.*, 2021) and oilseeds (Herneke *et al.*, 2021; Soon *et al.*, 2022). Gluten from wheat (Monge-Morera *et al.*, 2021) and patatin and protease inhibitors from potato (Josefsson *et al.*, 2020) are among the few reported PNFs made from plant-based proteins other than globulins.

2.1.1 In vitro formation of PNFs

Two different pathways for the formation of PNFs have been proposed. One is denaturation of the native protein's globular structure, followed by hydrolysis into peptide fragments where some contribute to formation of the fibril structure (Akkermans *et al.*, 2008). The other pathway is based on observations that the core region of the native protein is incorporated directly into the fibril in some cases, suggesting partial unfolding of the native protein where redundant peptides are 'shaved off' to form a more stable fibril structure (Mishra *et al.*, 2007). Native proteins are usually relatively stable and need to be subjected to harsh conditions, such as changes in the chemical environment and temperature, to unfold and form PNFs. Denaturation chemicals such as urea and alcohols have been used to form PNFs (Lendel and Solin, 2021). Many food proteins have been found to form PNFs at low pH (1.5-3) and high temperature (70-90 °C), conditions that help to speed up hydrolysis of the native protein into small peptides, which are assembled into more ordered PNFs structures (Hill *et al.*, 2011). Low pH makes most proteins positively charged, generating repulsive forces between the molecules, which prohibits unfavourable aggregation. However, PNFs, with their highly organised structure, can overcome these repulsive forces by providing sufficient binding energy.

2.2 PNF structure

2.2.1 Molecular structure

Many factors affect the morphology of PNFs, but at molecular scale all PNFs are very similar. All PNFs have a large amount of β -sheets, where the strands are aligned parallel or anti-parallel to each other (Figure 2). These β -sheets

form a so-called cross- β structure in which the strands are orientated perpendicular to the axis of the fibril and the protein chains are linked together with a network of hydrogen bonds and van der Waals forces (Eisenberg and Sawaya, 2017). A hallmark of the cross- β structure is the characteristic X-ray diffraction pattern given by an inter-strand distance of around 4.8 Å, corresponding to the hydrogen bond between the peptide backbones and the inter-sheet distance of 6-12 Å, which varies depending on the size and packaging arrangement of the side groups. The cross- β structure further elongates into protofilaments, and two or more protofilaments twisted together form a fibril (Figure 2). Due to variations in the number of protofilaments that form a fibril and in inter-sheet packing arrangements, the width of a mature fibril can vary from 8 to 20 nm (Eisenberg and Sawaya, 2017). However, there are reports of mature fibrils being even wider, up to 173 nm (Lara *et al.*, 2011).

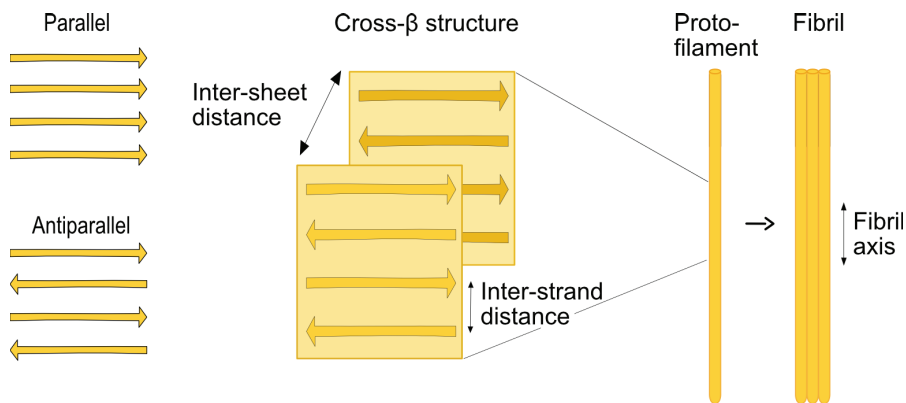


Figure 2. (Left) β -strands aligned parallel or antiparallel, (centre) cross- β structure of β -sheets along the perpendicular axis of the fibre and (right) two or more protofilaments twisted together to form a fibril.

2.2.2 Nanostructure

The packing arrangement of the protofilaments defines the final morphology of the fibril structure (Adamcik and Mezzenga, 2018). Protofilaments are assembled either in a twisted or helical ribbon manner. In the past, mature PNFs were classified based on their morphological attributes as long and straight, or semi-flexible (Lendel and Solin, 2021). However, an additional

shape, namely fibril structures with much higher curvature, has been reported to assemble from several full-length protein sources (Ye *et al.*, 2018, Josefsson *et al.*, 2019, Herneke *et al.*, 2021, Josefsson *et al.*, 2020). These worm-like curly fibrils are usually thinner and shorter and exhibit lower Young's modulus than other reported PNF structures. There are several theories on how this curly structure is built (Lendel and Solin, 2021). It could be formed from protofilaments that have not yet assembled fully into fibrils, or from a completely different architecture of the β -sheet core. However, the latter suggestion is contradicted by findings in fibre diffraction experiments that some curved fibrils have the characteristic cross- β structure. A third theory is that the curly PNFs are assembled with a similar β -sheet core as straight PNFs, but have large disordered parts outside the core.

2.2.3 Microstructure

In order to use PNFs as structuring ingredients in food and biomaterials, it is essential to determine how morphologically different PNFs structures assemble on microscopic level. This was investigated in this thesis work by monitoring the assembly of two morphologically different PNFs (curved and straight) from whey into films. Functional properties such as the foaming ability of similar curved and straight PNFs from plant-based protein sources were also explored in this thesis work. The overall aim was to increase knowledge on the complexity of PNF morphology and on relevant areas of use.

2.3 PNF detection and characterisation

In addition to detecting PNFs by their characteristic cross- β X-ray diffraction pattern, several other methods are widely used for structure characterisation. Among these, thioflavin T (ThT) fluorescence is a convenient method for detecting PNFs due to the high affinity of this dye for the fibril structure, leading to increased fluorescence intensity. Complementary methods for secondary structure characterisation and quantification include circular dichroism (CD) and Fourier-transform infrared spectroscopy (FTIR). To capture the morphological characteristics of PNFs, several different microscopic techniques can be used, such as atomic force microscopy

(AFM), scanning electron microscopy (SEM) and transmission electron microscopy (TEM) (Cao and Mezzenga, 2019).

2.4 Are PNFs safe to eat?

If PNFs are to be used in future food applications, it is important to know that they are safe for humans to eat. One problem is that the fibrillation process can increase the bioavailability of some allergenic food proteins, due to denaturation and hydrolysis of the protein (Tavano, 2013). A recent genetic screening study of several legume storage proteins identified genes for proteins, especially 7S globulin, that have a high probability of forming PNFs in the genome (Antonets and Nizhnikov, 2017). The authors interpreted these results as indicating that the functional PNFs in plants are probably beneficial for seeds during dehydration, where they can provide structural support. This would suggest that humans already consume PNFs when eating legumes. A later study by Antonets *et al.* (2020) demonstrated that 7S globulin from pea exhibits PNF-related properties *in vivo* and *in vitro* (Antonets *et al.*, 2020). These PNFs were demonstrated to be toxic to yeast and human cell cultures in high concentrations, indicating that PNFs may be part of the defence mechanism of seeds. However, PNFs should be safe for human consumption because the concentration of PNFs in seeds is much lower than the level tested in that study. Nevertheless, if PNFs are to be used in future foods at higher concentrations than found in nature, it is crucial to investigate the food safety aspect of PNFs.

Some years earlier Lassé *et al.* (2016), investigated the digestibility and cell toxicity of PNFs made from whey, soybean, kidney bean and egg white protein found that a concentration up to 0.25 mg/mL exerted low or no toxicity on human cell lines (Caco-2 and Hec-1). This concentration is 50 times higher than that in the study by Antonets *et al.* (2020), on PNFs from pea 7S globulin, where the highest concentration was 0.5 µg/mL. In the same study, Lassé *et al.* (2016) investigated the digestibility of PNFs made from whey, soybean, kidney bean and egg white protein in an *in vitro* model, by incubating the PNFs with three different proteases (Proteinase K, pepsin and pancreatin). The results showed that some of the PNFs formed from food protein were able to resist proteolysis in the stomach model. The digestibility

differed depending on the morphology of the PNFs (curly or straight). Straight PNFs from whey seemed more resistant to pepsin and pancreatin than curly PNFs from soybean and kidney bean. In conclusion, there is still a need to investigate whether PNFs are safe for human consumption. Proper *in vivo* animal model testing has to be conducted before upscaling PNF production for food applications.

2.5 PNFs as texture initiators in food

The hierarchical order and electrostatic forces make PNFs some of the stiffest protein-based structures known (Smith *et al.*, 2006). This feature, together with the typical variation in length to diameter ratio of the fibrils (several μm to some nm), makes PNFs efficient thickeners and stabilisers of foams and emulsions (Cao and Mezzenga, 2019). These functional properties have resulted in PNFs becoming a growing field of interest among scientists during the past decade as they seek to create new functional and sustainable materials and food applications (Lendel and Solin, 2021, Cao and Mezzenga, 2019).

2.5.1 Foams

Stable bubbles are important in many food products, such as bread and other baked products, whipped cream, ice cream, cheese and meringues, to mention a few (Campbell and Mougeot, 1999). Introducing bubbles alters the texture and rheological properties of food, giving it a different mouthfeel and appearance (Murray, 2020). There is increasing interest from the food industry in using proteins to stabilise foams to create new textures (Amagliani and Schmitt, 2017). The foaming ability of a protein depends on its ability to reduce surface tension when making interfacial films encapsulating the bubbles. The surface tension reduction depends in turn on the protein structure, with hydrophilic and flexible proteins usually being better foam stabilisers than more rigid and hydrophobic molecules (Lam, Velikov and Velev, 2014). Foam stability depends on the liquid drainage rate in the continuous phase located between the bubbles. Liquid drainage is controlled by capillarity forces and gravity and can be dampened by increased viscosity in the continuous phase (Weaire and Phelan, 1996).

Fibrillated protein from β -lactoglobulin (Oboroceanu *et al.*, 2014) and soybean (Wan, Yang and Sagis, 2016a) has been observed to increase foaming capacity and stability compared with non-fibrillated protein from the same sources.

Plant-based PNFs have the potential to be used to stabilise texture in aerated food applications, such as dairy analogues or gluten-free bread. However, there is a need for further investigations on the foaming properties of plant-based PNFs, to determine whether differences in PNF morphology, solution pH and/or concentration affect the ability to stabilise foams. To expand knowledge in this field, the foaming properties at high and low concentration of two morphologically different PNF systems, made from mung bean (curly) and fava bean (straight) protein, were explored in this thesis. For the mung bean samples, the foams were made at several different pH levels (2-8), while the fava bean foams were made at a food-related pH (7).

2.5.2 Microfibres

In nature, there are many examples of highly structured protein-based biomaterials with remarkable mechanical attributes. One example is spider silk, which is constructed of fibrils aligned along the axis into a strong microfibre (Qiu *et al.*, 2019). Different spinning techniques, such as wet spinning, for controlling the assembly of PNFs into fibres have been tested (Lendel and Solin, 2021). For instance, Kamada *et al.* (2017) were able to form microfibrils from both curved and straight whey-based PNFs by using a flow-focusing method without any other additives (Kamada *et al.*, 2017). The microfibrils were formed by flow elongation of the PNFs, with the help of sheath flows with water and acetate buffer controlling the alignment and gelation of the PNFs by approaching the isoelectric point of the protein. Interestingly, only the curved PNFs formed coherent microfibrils. The straight PNFs also formed fibres, but these could not resist the surface tension of the acetate bath when picked up (Kamada *et al.*, 2017).

The ability of curved mung bean PNFs to form microfibrils was explored in this thesis using a similar flow-focusing technique to that described by Kamada *et al.* (2017). To my knowledge, this is first attempt at microfibre

assembly from plant-based PNFs. Microfibres made from plant-based PNFs have potential for use as a bottom-up method to create similar textured structures as made by the muscle fibres in meat. The ability to control the length of the fibres means that a meat analogue made from microfibres could be a good complement to existing plant-based meat replacement products, which are mainly made by extrusion cooking (Dekkers, Boom and van der Goot, 2018).

3. Objectives and Hypotheses

The overall aim of this thesis was to explore the ability to form PNFs from different plant-based sources and assess how these can be processed for use as stabilisers/thickeners in future food applications.

Specific objectives of the work were:

- To evaluate the effects of nanostructurally different PNFs (curved/straight, long/short) on the microstructure of films/materials. The hypothesis tested was that the nanostructure of PNFs affects their ability to assemble on microstructural level (Paper I).
- To determine the ability to form PNFs from legumes, cereals, oilseeds and tubers, by evaluating the secondary structure and morphology of these PNFs. The hypothesis tested was that PNFs can be made from a wide range of plant proteins and that these PNFs are detectable with methods that determine protein secondary structure and nanostructure (Paper II).
- To evaluate the effect of protein size and purity on PNF formation. The hypothesis tested was that smaller and purer protein isolates are superior in their ability to form PNFs (Papers II, III and VI).
- To define the effects of chemical environment on PNF stability. The hypothesis tested was that PNFs are affected to some extent by elevated pH, but remain sufficiently stable

to contribute structuring ability at food-related pH (Paper IV).

- To evaluate the viscosity and foaming properties of plant-based PNFs with different morphology. The hypothesis tested was that PNFs are better foam stabilisers than native plant proteins and that curved PNFs form more viscous samples than straight PNFs and are therefore better foam stabilisers (Papers III and IV).
- To define the effect of chemical environment on the ability of PNFs to stabilise foams. The hypothesis tested was that pH affects the ability of PNFs to stabilise foams (Paper IV).
- To investigate the ability of plant-based PNFs to form microfibrils. The hypothesis tested was that PNFs can be aligned into coherent microfibrils (work still in progress).

4. Materials and Methods

This chapter describes how the protein sources used to form PNFs were collected/extracted, how PNFs were created and evaluated, and how the PNFs were treated to investigate functional properties. The methods are only described briefly here; see materials and methods sections in Papers I-IV for more detailed descriptions.

4.1 Food proteins

Different types of protein were evaluated for their ability to form PNFs, including five proteins extracted in-house and three obtained as pre-extracted protein isolate. In-house protein extraction was performed on fava bean (*Vicia faba minor* cv. Gloria), mung bean (*Vigna radiate*), lupin seed (*Lupinus angustifolius* cv. Boregine), rapeseed (*Brassica napus*) and oat (*Avena sativa* cv. Mathilda). Protein isolates from soybean (*Glycine max*), potato (*Solanum tuberosum*) and whey (Lacprodan DI-9224) were kindly provided by Solae (Belgium), Lyckeby Starch AB (Sweden) and Arla Food Ingredients (Denmark), respectively.

4.1.1 Protein extraction

All protein isolates generated in-house were extracted with pH gradients. Depending on the raw material, there was some variation in processing steps before and after the pH alterations (Table 1). The variations in processing steps were as follows: defatting (only lupin, oat and rapeseed), dehulling (only fava bean and lupin), air classification (only oat) and addition of salt (sodium chloride, NaCl) (only mung bean and fava bean). All raw materials

were milled into flour and dissolved in de-ionised water before being exposed to pH alterations.

In brief, the protein extraction process was as follows. First, the pH of all dissolved flours was adjusted to alkaline pH (8-9.2) and insoluble material was removed. Next, the proteins were collected by lowering the pH (4-5) to the isoelectric point where the respective proteins exhibit no net charge and become insoluble. Isoelectric precipitation pH was based either on literature reports or in-house solubility experiments. Finally, further purification experiments were performed on some of the raw materials. By adding salt (NaCl) at different concentrations (Table 1) during the extraction process, a pure protein isolate from mung bean and the globular fractions 8S (mung bean), 11S (fava bean), and 7S (fava bean) were collected.

4.1.2 Protein composition analyses

Protein concentration was evaluated as nitrogen content in protein isolates, using either the Kjeldahl or Dumas method (conversion factor 6.25). In addition, protein composition was evaluated by size-exclusion liquid chromatography and sodium dodecyl sulphate-polyacrylamide gel electrophoresis (SDS-PAGE).

Table 1. General processing steps applied (A) or not applied (N/A) for extracting protein isolates in-house in this thesis. Roman numerals in brackets refer to the paper (I-IV) in which the protein isolates were used.

Source	Defatted	Dehulled	Milled	Air-classified	Alkali (pH)	Isoelectric precipitation (pH)	NaCl (M)	Freeze-dried	Protein isolate
Fava bean (II, III)	N/A	A	A	N/A	9	4	N/A	A	FPI
Mung bean (II)	N/A	N/A	A	N/A	8	4.6	N/A	A	MPI
Lupin (II)	A	A	A	N/A	8	4	N/A	A	LPI
Oat (II)	A	N/A	A	A	9.2	5	N/A	A	OPI
Rapeseed (II)	A	N/A	A	N/A	8	5	N/A	A	RPI
Fava bean (III)	N/A	A	A	N/A	8	4.8	0.3	A	11S
Fava bean (III)	N/A	A	A	N/A	8	4.8	0.15	A	7S
Mung bean (IV)	N/A	N/A	A	N/A	8	4.6	0.6	N/A	MPI
Mung bean (II, IV)	N/A	N/A	A	N/A	8	4.6	0.2	N/A	8S

4.2 Protein nanofibrils

4.2.1 Preparation

All PNFs analysed were prepared using approximately the same procedure. Dissolved proteins were adjusted to pH 2 and passed through a 0.45 μm filter. Concentration, temperature and heating time varied for the proteins treated in Papers I-IV (Table 2). The reason for this variation was mainly due to differences in protein solubility. In Paper I, the PNFs were made at two different concentrations, to obtain PNFs with distinctly different morphologies (curly/straight). The protein concentration used in Paper III for fava bean and its globular fractions 11S and 7S (10 mg/mL) was selected due to limited access to protein isolates, which restricted the ability to test the critical pH concentrations. Mung bean PNFs were made at a higher concentration (25 mg/mL) in Paper IV than in Paper II (10-20 mg/mL). This was because the protein in Paper III was purer (see protein extraction above) and did not result in aggregation during heating. Approximately 50% of the purified mung bean protein was converted to PNFs after fibrillation.

Table 2. Concentration, temperature and heating time used to form protein nanofibrils (PNFs) from the proteins reported in Papers I-IV. Roman numerals in brackets refer to the paper (I-IV) in which the respective protein isolates were used.

Protein Source	Concentration (mg/mL)	Temperature (°C)	Heating time (h)
Whey (I)	40 or 70-80	90	72
Fava bean (II)	20	85	24
Mung bean (II)	10, 12, 15, 20	85	24
Lupin (II)	20	85	24
Oat (II)	20	85	24
Rapeseed (II)	2	85	24
Soybean (II)	14	90	72
Potato (II)	14	90	96
Whey (II)	40	85	72
8S (II)	10	85	24
Fava bean (III)	10	85	24
11S (III)	10	85	24
7S (III)	10	85	24
Mung bean (IV)	25	85	2, 4, 6, 24, 48
8S (IV)	25	85	2, 4, 6, 24, 48

4.2.2 Secondary structure

The characteristic secondary structure of PNFs with a high amount of β -sheets makes it possible to quantify the ability of proteins with a diverse secondary structure to re-form into PNFs. In all papers, ThT fluorescence assay was used as a detection method for PNF formation. Thioflavin T is a fluorescent dye with a high affinity for the specific cross β -sheet structure of PNFs, which causes increased fluorescence intensity, making it the standard method for PNF detection (Figure 3) (Cao and Mezzenga, 2019).

In Papers II and IV, the β -sheet rich PNFs were also detected with the help of CD spectroscopy, a method used to measure the absorption of circularly polarised light (Figure 3) (Greenfield, 2006). Proteins with a well-defined cross β -sheet structure have a spectral minimum (negative peak) at 218 nm

and disordered proteins at 195 nm. To avoid interference from non-fibrillated proteins and peptides, the fibrillated samples were further purified using a spin membrane or dialysis membrane with a cut-off at 100 kDa.

In Paper II, the secondary structure of the PNFs from all proteins was further quantified with the help of FTIR spectroscopy, a method based on sample absorption of infrared light at several different wavelengths (Figure 3) (S. Yang *et al.*, 2022). Nine different absorption bands are usually collected for measurements of protein and peptides (amides A and B, amides I-VII). In the present case, amide band I gave the most information on the secondary structure of the protein-based sample. Before starting the FTIR measurements, the PNFs were purified with a spin membrane or dialysis membrane with a cut-off of 100 kDa and freeze-dried to remove the interference of water molecules.

4.2.3 Nanostructure and microstructure of PNFs

The morphology of the PNFs generated was analysed in all papers (I-IV) by AFM (Bruker device), operating in tapping mode or Scanasyt-air (Figure 3). A drop of 10-15 μL of PNF sample, diluted 1:1000-1:10000 fold, was allowed to dry for 1 h on a freshly cleaved mica surface. The images were analysed using Gwyddion 2.45 software.

In Paper I, morphologically different whey PNFs (short curly, long straight, and short straight) were investigated for their effect on the microstructural features of cast films. The short and straight PNFs were generated by sonicating samples containing long PNFs. The microstructural features of the films were investigated with several microscopic methods, such as light microscopy, confocal laser scanning microscopy, SEM, AFM and synchrotron-based X-ray scattering (small- and wide-angle X-ray scattering). The film was made by pouring fibrillated protein into a glass petri dish and leaving it to dry, or by spray deposition. Spray deposition of the PNFs as thin films was used to investigate the effect of reduced evaporation time on film microstructure.

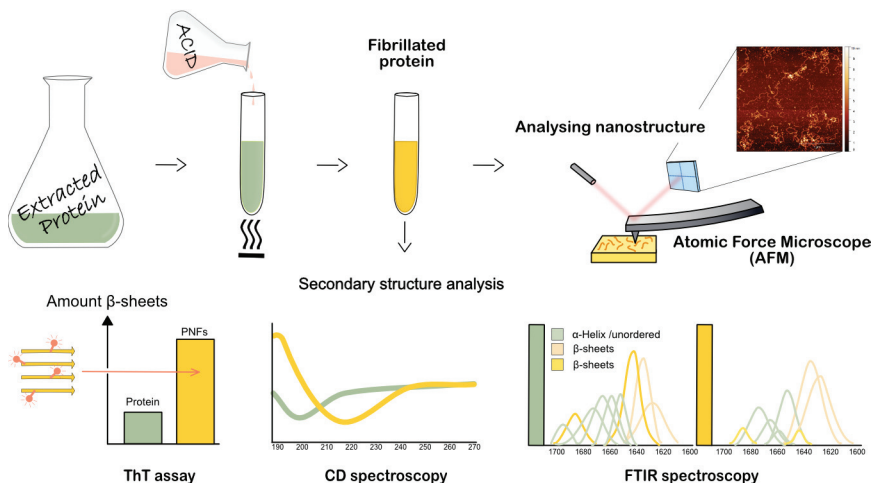


Figure 3. Methods used to characterise the nanostructure and secondary structure of protein nanofibrils (PNFs) generated in this thesis.

4.2.4 Change in pH

In Paper III, the stability of mung bean PNFs was examined over a wide pH range (2-9), to determine how the PNFs behaved at food-related pH values. The pH was adjusted by addition of 0.5 M and 4 M NaOH while monitoring with a pH meter.

4.2.5 Viscosity

Viscosity over increased shear rate was investigated in Papers III and IV, to determine the ability of PNFs to increase the thickness of a solution and the impact of PNF morphology on the viscosity behaviour of samples. In Paper IV, viscosity over increased shear rate was investigated for non-fibrillated and fibrillated protein in a pH range of 2-8. The same method was applied in Paper III on fibrillated protein from fava bean and its 11S and 7S globular fractions at pH 2 and 7.

4.3 Food model systems

4.3.1 Foams

Fibrillated and non-fibrillated proteins from fava bean, fava bean globular fractions 11S and 7S (Paper III) and mung bean (Paper IV) were whipped using an Ultra Turrax t 25 homogeniser at 13,500 rpm for 5 min. Foaming capacity, foam stability and foam half-life time were investigated for the mung bean samples at a concentration of 15 mg/mL and pH 2-8, and for the fava bean, 11S and 7S samples at concentrations of 10 and pH 7. Same foaming properties were also investigated for fibrillated and non-fibrillated samples from mung bean and fava bean, fava bean 11S and fava bean 7S at a concentration of 1 mg/mL at pH 2, 5 and 7.

The foam generated from the mung bean samples (Paper IV) was dyed with ThT and the microstructure was analysed by confocal microscopy. The features in the micrographs were analysed to obtain statistical information about bubble size distribution and area fraction. The foam made from fava bean and its 11S and 7S globular fractions (Paper III) at a concentration of 1 mg/mL was also dyed with ThT and imaged with confocal microscopy.

4.3.2 Microfibres

Fibrillated mung bean protein prepared according to the same protocol as in Paper IV was dialysed with a 100 kDa membrane for seven days against 0.01 M HCl. The final concentration of purified mung bean PNFs was approximately 14 mg/mL. The flow-focusing experiments were performed according to the method described by Kamada *et al.* (2017), with some modifications. Figure 4 provides a schematic overview of the flow-focusing set-up. Mung bean PNFs were injected into the core flow at a flow rate of 4.0 mL/h. The PNFs were further aligned with the help of sheath flows with de-ionised water at a flow rate of 9.9 mL/h, and acetate buffer (pH 4.6) at a flow rate of 24.88 mL/h. Finally, the microfibrils were extruded into a bath, with acetate buffer at pH 4.6. The microfibrils were lifted from the acetate bath with tweezers to collect an image.

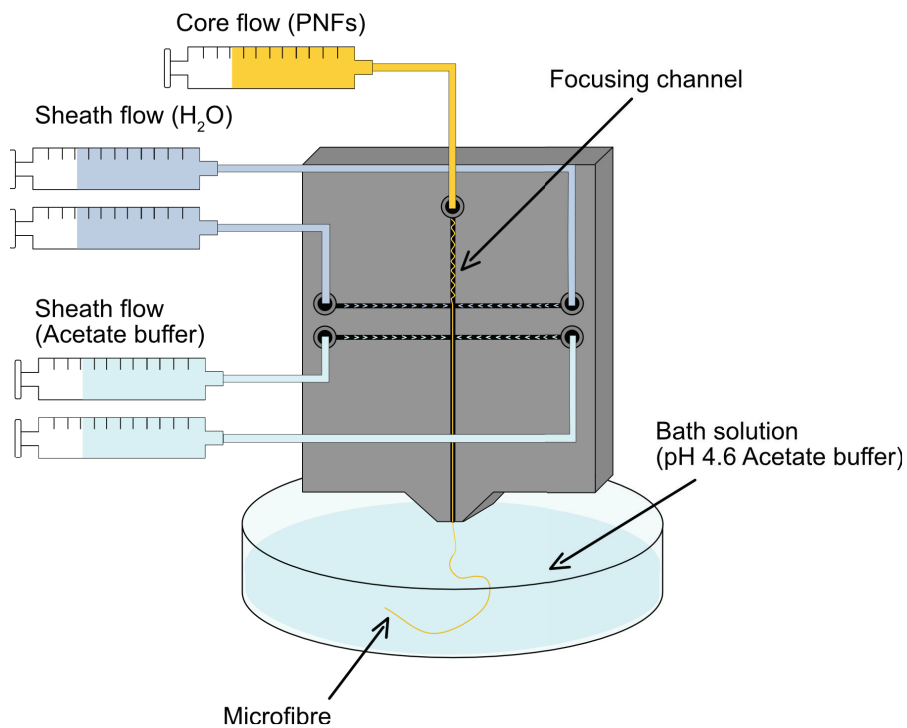


Figure 4. Schematic overview of microfibre formation from protein nanofibrils.

5. Research outcomes

Whey was used in Paper I in this thesis to explore how PNF morphology affects microstructural features. The ability of proteins extracted from legumes, cereals, oilseeds and tubers to form PNFs and the effects of external factors such as protein size and purity on PNF formation were examined in Paper II. The plant-based PNFs obtained were then compared with PNFs from whey, to test the generalisability of the extensive knowledge available on PNFs from whey.

The PNFs from whole and fractionated fava bean and mung bean were investigated in detail in Papers III and IV. In both papers, the ability of these PNFs as foam stabilisers was investigated. In Paper IV, a more in-depth characterisation of the stability of curved mung bean PNFs at different pH and an investigation into how changes in pH affect foam properties were performed. Finally, mung bean PNFs were also explored for their ability to form microfibrils in a flow-focusing set-up (preliminary data).

5.1 Nanostructure to microstructure - the role of PNF morphology

Whey protein can form PNFs with different distinct nanostructures depending on the concentration (Ye *et al.*, 2018). At high protein concentrations (70-80 mg/mL), the PNFs had a curved worm-like morphology, while at a low concentration (below 40 mg/mL), the PNFs were long and straight. These distinct morphological differences in PNF nanostructure also affect the microscale features (Paper I), which can easily be observed by casting the fibrillated material into films, as seen in Figure 5. In this case curved PNFs formed a smooth, transparent film and straight

PNFs formed heterogeneous film with a mixture of coarse structures and more homogenous regions. These features were evident even if the non-fibrillated peptides had been removed by dialysis and the curved PNFs had been diluted to the same concentration as the straight PNFs. These observations lead to the assumption that PNF nanostructure affects the microstructural features. The two populations of PNFs identified differed in morphology, length, and diameter. Curved PNFs were around ~ 300 nm in length and had diameter of around 1.7 nm. Straight PNFs were considerably longer and thicker, around $1 \mu\text{m}$ in length and 3.4 nm in diameter. Sonicating the long PNFs resulted in shorter rods, with the majority of the particles having length below 200 nm. Films generated from the sonicated PNFs had a homogenous microstructure similar to that of films created from the short and curved PNFs (Figure 5). This led to the conclusion that it was the length scale of the PNFs that determined microstructure features.

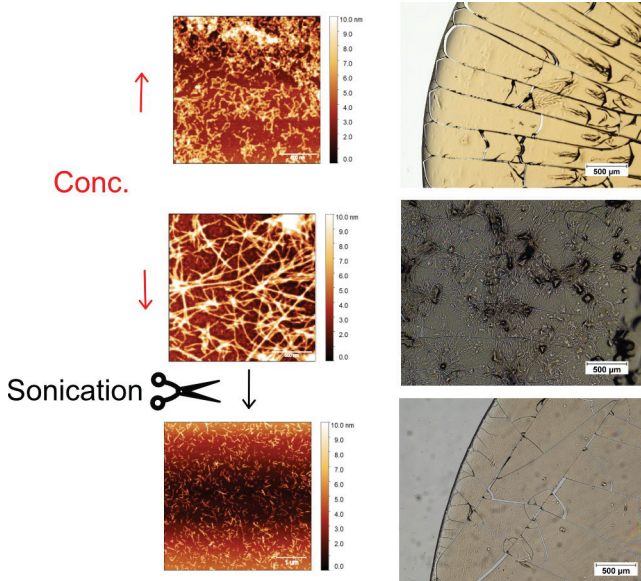


Figure 5. (Left) Effect of whey protein concentration on protein nanofibril (PNF) morphology. Atomic force micrographs of curved PNFs generated at high whey protein concentration and long straight PNFs generated at low whey protein concentration. Long straight PNFs were shortened by sonication. (Right) Light microscopy images of cast film from curved, long straight, and short straight PNFs showing their different microstructural features.

5.2 Plant-based PNFs

To apply existing knowledge about whey-based PNFs to the more sustainable resource of plant PNFs, the ability to produce PNFs from seven different plant-based protein isolates (fava bean (FPI), mung bean (MPI), lupin (LPI), oat (OPI), rapeseed (RPI), soy (SPI), potato (PPI)) was investigated (Paper II). The plant-based PNFs were compared against the long straight PNFs made from whey protein (WPI) (see Figure 5) in terms of secondary structure and nanostructure. These properties were also investigated for purified and fractionated protein from fava bean and mung bean (Papers II-IV).

5.2.1 Secondary structure of plant-based PNFs

All protein isolates tested in Paper II were able to form PNFs. The secondary structure of these PNFs was analysed using ThT, CD and FTIR spectroscopy. Figure 6 shows the relative increase in fluorescence for all seven protein isolates after fibrillation. After heating, all protein isolates except those from oat and rapeseed showed an increase in fluorescence. This is in line with previous findings on ThT fluorescence of plant-based PNFs from soy (Akkermans *et al.*, 2007) and pea (Munialo *et al.*, 2014) protein. The lack of increase in fluorescence after heat treatment of oat and rapeseed protein isolates is not fully understood, but it could be due to limitations with the ThT assay. There have been reports that the ThT dye can interact with native protein structures; for example, serum albumin has been seen to bind to the ThT dye (Sen *et al.*, 2009). Many plant storage proteins have a high density of β -sheets, (Marcone, Kakuda and Yada, 1998) which is the case for oat and rapeseed proteins (Liu *et al.*, 2009; Perera, McIntosh and Wanasundara, 2016). Undissolved native protein rich in β -sheets might also explain the lack of increase in fluorescence for the oat and rapeseed isolates. These domains may bind to the ThT dye, generating high initial ThT fluorescence, but may be destroyed during the fibrillation process due to protein unfolding and hydrolysis, together with low turnover from proteins to PNFs, generating lower ThT fluorescence after fibrillation. To summarise, these results indicate that the ThT assay should be used with care as a sole indicator of PNF structures and use of other complementary methods for secondary structure characterisation can be recommended.

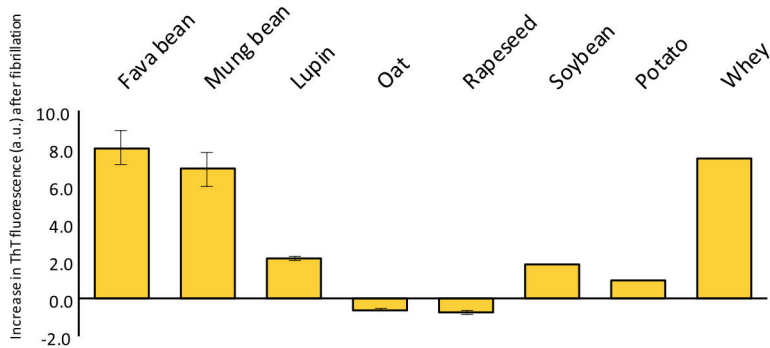


Figure 6. Relative increase in thioflavin T (ThT) fluorescence (a.u.) after heat incubation of protein from fava bean, mung bean, lupin, oat, rapeseed, soybean, potato and whey.

Figure 7 shows some examples of CD spectra for non-fibrillated, fibrillated, and purified fibrillated protein from mung bean, oat, rapeseed and whey (for CD spectra of all proteins investigated, see Figure 2 in Paper II). After being purified through 100 kDa spin or dialysis membranes, all fibrillated plant-based proteins had a spectrum minimum that moved to the right on the horizontal axis, becoming closer to the minimum for β -sheet-rich structures (Greenfield, 2006). These results confirm that all plant-based proteins, after heating, had an increased amount of β -sheet structures, clearly indicating presence of PNFs in the samples. However, for the whey protein samples a shift in spectrum to the β -sheet minimum was observed already after fibrillation, without any further purification, indicating that the whey samples had higher protein turnover to PNFs than the plant-based proteins.

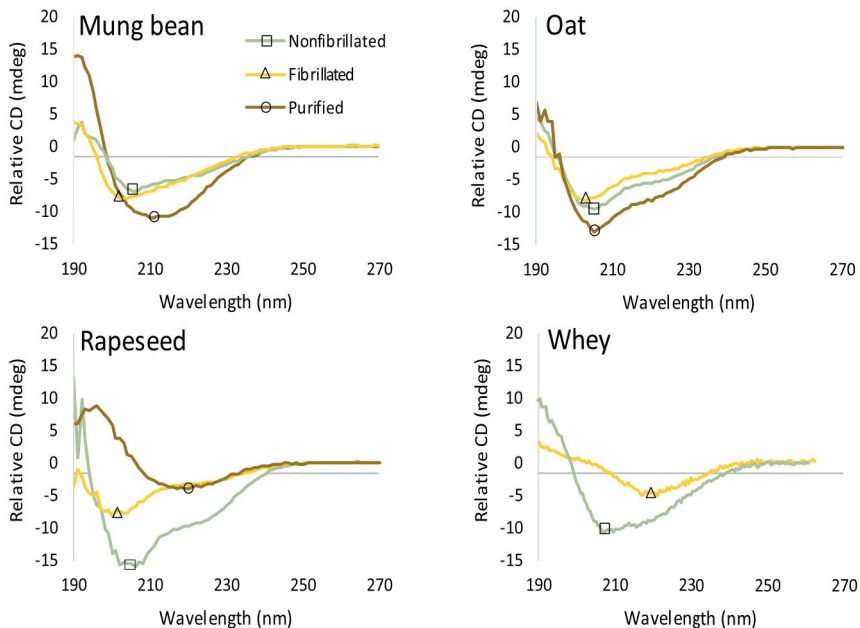


Figure 7. Circular dichroism spectra of nonfibrillated protein (green, squares), fibrils (yellow, triangles), and purified fibrils (brown, circles) from mung bean, oat, rapeseed and whey.

Figure 8 shows the secondary structure content of purified PNFs from all plant proteins investigated in Paper II, which was determined with FTIR spectroscopy. The secondary structure of the PNFs was divided into four groups: strongly hydrogen-bonded β -sheets, weakly hydrogen-bonded β -sheets, α -helix/unordered and β -turns. The FTIR data were in agreement with the results obtained from CD spectra, confirming that all the purified and dialysed plant-based samples had a high ratio of β -sheet structures. The fibrillated protein samples from potato and whey were purified with a 100 kDa dialysis membrane, instead of being filtered through a 100 kDa spin membrane, which might explain why these two samples had more strongly hydrogen-bonded β -sheets than the other plant-based samples. However, no quantification was made of the efficiency of the two different purification methods.

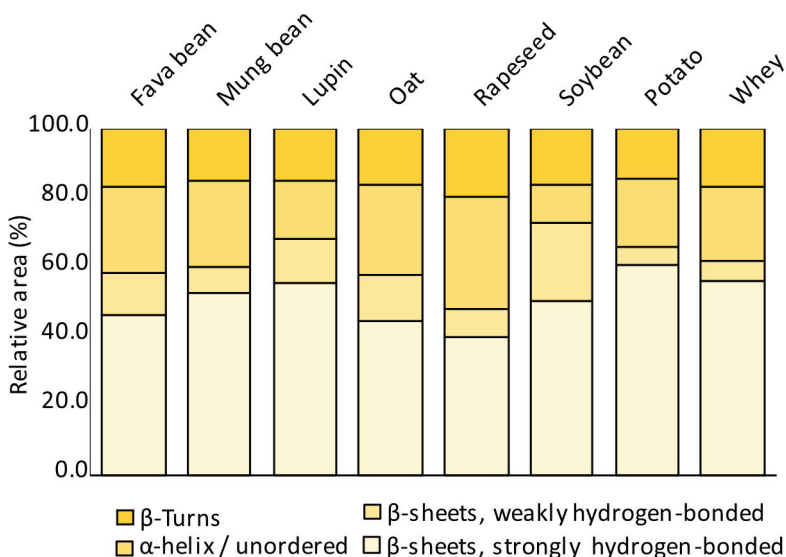


Figure 8. Relative size of resolved infrared peaks from purified protein nanofibrils (PNFs) from fava bean, mung bean, lupin, oat, rapeseed, soybean, potato and whey, grouped into β -turns, α -helix/unordered, β -sheets, weakly hydrogen-bonded β -sheets and strongly hydrogen-bonded β -sheets.

5.2.2 Nanoscale morphology of plant-based PNFs

Atomic force morphology analysis of all fibrillated proteins investigated in Paper II confirmed that PNFs were formed in all samples, but that they differed in length and morphology (Figure 9). Those from fava bean, mung bean, soybean and potato had a worm-like curved morphology, similar to that of other reported plant-based PNFs such as pea (Munialo *et al.*, 2014) and PNFs from high-concentration whey protein (see Figure 4). The curved PNFs had an average length of \sim 220-720 nm. The PNFs from lupin, oat and rapeseed had a straighter, semi-flexible morphology. The longest PNFs in these samples varied between \sim 390 and 910 nm in length. None of the plant-based PNFs obtained in Paper II was able to form PNFs as long as those from whey protein, which were up to several μ m in length. The reason why whey protein is superior in its PNF-forming ability to the plant proteins investigated in Paper II is not fully understood, but some possible explanations are discussed in the next section.

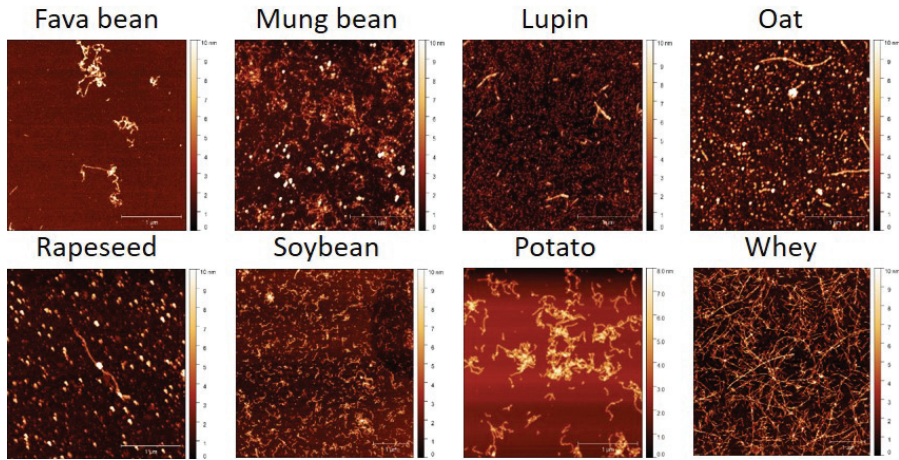


Figure 9. Atomic force microscopy images of protein nanofibrils (PNFs) from fava bean, mung bean, lupin, oat, rapeseed, soybean, potato and whey. The scale bar is 1 μm in all images. Figure adopted from Paper II, with permission.

5.2.3 Protein size matters

Protein size may explain why whey protein is superior to plant proteins in its ability to form PNFs. The distribution and size of the major proteins examined in this work are summarised in Table 3. Whey protein consists of two major small monomeric proteins, which were the smallest (18.3 and 14.2 kDa) proteins investigated for PNF formation in this thesis (Pereira *et al.*, 2007). Among the plant-based protein isolates investigated, the potato isolate had the smallest proteins (40-45 kDa and >25 kDa) (Racusen and Weller, 1984; Løkra and Strætkevren, 2009). Purified PNFs from potato and whey had a high amount of β -sheets when investigated with FTIR (Figure 8), which might be correlated to the small proteins being more easily denatured and hydrolysed into peptides when exposed to fibrillation conditions (high temperature and low pH).

The other plant-based proteins investigated in Paper II consist mainly of globulins, although with some diversity in the distribution of the smaller vicilin (7-8S) and larger legumin (11-12S) fractions (Table 3). Both oat and rapeseed protein consist of majority proteins belonging to the 12S protein

family (Mäkinen *et al.*, 2016; Wanasundara *et al.*, 2012). Extracted protein from soybean, fava bean and lupin consists of a mixture of 7S (143-260 kDa) and 11S (353-430 kDa) fractions (Barac *et al.*, 2004; Langton *et al.*, 2020; Duranti *et al.*, 2008). Among the legumes investigated in Paper II, only mung bean had a majority (89%) of the smaller (200 kDa) vicilin fraction (8S) (Mendoza *et al.*, 2001). The 7S and 11S fractions comprise only 3.4 and 7.6 % of total storage protein in mung beans. The fact that the majority of the mung bean isolate consisted of a smaller protein can explain the high increase in ThT fluorescence after heating (Figure 6). Of the proteins investigated in Paper II, only heated fava bean protein isolate showed a greater increase in fluorescence after fibrillation, but this can be explained by its protein concentration being twice that of the mung bean isolate.

Table 3. Summary of major protein families present, protein distribution and protein size for all protein isolates examined in this thesis.

Protein isolate	Protein family	Protein content (%) in extract	Protein size (kDa)	References
Fava bean	11S / 7S	50 / 27	353 / 150	(Langton <i>et al.</i> , 2020, Warsame <i>et al.</i> , 2020)
Mung bean	8S	89	200	(Mendoza <i>et al.</i> , 2001)
Lupin	11S / 7S	44-45 / 35-37	330-430 / 143-260	(Duranti <i>et al.</i> , 2008)
Oat	12S	80	320	(Mäkinen <i>et al.</i> , 2016)
Rapeseed	12S	60	300-360	(Wanasundara <i>et al.</i> , 2012)
Soybean	11S / 7S	52 / 32	360 / 150-180	(Barac <i>et al.</i> , 2004)
Potato	Patatin / protease inhibitors	35-40 / 25-50	40-45 / >25	(Racusen and Weller, 1984, Løkra and Strætkvern, 2009)
Whey	β -lactoglobulin / α -lactalbumin	58 / 20	18.3 / 14.2	(Pereira <i>et al.</i> , 2007)

Comparisons of the PNF-forming ability of the 7S and 11S fractions from fava bean (Paper III) based on ThT fluorescence measurements revealed that

7S samples displayed a high increase in fluorescence after heating, but the 11S samples showed no increase at all (Figure 10A). On imaging the fibrillated samples with AFM, straight PNF structures were detected in both samples (Figure 10B-D). However, the fibrils that originated from 7S proteins were detected in larger quantities, although the imaged samples had equal concentrations. These results are in line with findings in a study by Tang and Wang (2010) on the ability of soybean 7S and 11S to form PNFs, which showed that 7S had a much greater increase in ThT fluorescence than 11S after heating. There are clear indications that the hypothesis that lower molecular weight protein is superior in forming PNFs (see Chapter 3) is true. Smaller size proteins may denature more easily to form small peptides during the hydrolysis process than proteins with a larger structure.

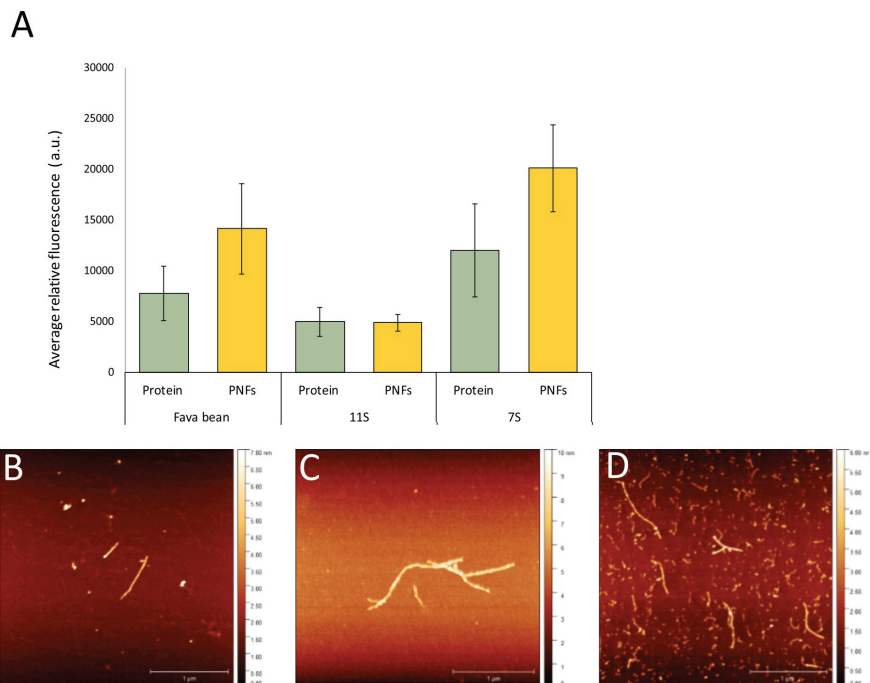


Figure 10. (A) Average relative fluorescence for non-fibrillated (protein) and fibrillated (protein nanofibrils, PNFs) samples from fava bean protein isolate and fava bean fractions 11S and 7S at a concentration of 10 mg/mL. Atomic force microscopy images of PNFs from (B) fava bean (C), fraction 11S and (D) fraction 7S.

There are indications that only small segments of the full-length protein chain contribute to formation of PNFs (Baldwin *et al.*, 2011). In a study by Josefsson *et al.* (2019), the PNF-forming segments in soy (identified with MALDI-TOF) were further explored and compared with PNFs formed from the native soybean protein. The results showed that peptide fragments originating from both 7S and 11S could form PNFs. Interestingly, the PNFs formed from the small synthetic peptides were all several μm long and straight, whereas the PNFs formed from the native protein were a mixture of primarily small curved PNFs with some elements of long and straight PNFs. Based on these results, Josefsson *et al.* (2019) concluded that it is probably peptide length, and not the specific sequences, that contribute to PNF morphology. Since native 7-8S and 11-12S both have PNF-forming segments in their protein sequence, other factors must contribute to the difference in PNF formation between these fractions.

One possible explanation for 7-8S more easily forming PNFs than 11-12S could be the thermal stability of the respective protein. Unfolding protein by heating enables more efficient hydrolysis, due to exposure of previously buried residues (Cao and Mezzenga, 2019). The denaturation midpoint temperature for 11S and 7S proteins from fava bean is reported to be 85 °C and 76.5 °C, respectively (Kimura *et al.*, 2008). In Paper III, all proteins fibrillated at 85 °C (see Table 2), which might have resulted in more efficient denaturation of the 7S fraction than the 11S fraction, resulting in 7S having more optimal conditions for PNF formation.

5.2.4 Protein purity matters

For soybean protein, a clear correlation has been reported between protein concentration and amount of PNFs formed (Akkermans *et al.*, 2007). To scale up PNF production, it is important to be able to form large quantities of PNFs. In Paper II, it was speculated that extract purity might affect protein solubility, due to the interaction of non-protein residues. A purer protein extract will thus form more and longer PNFs.

For the protein isolate produced in-house and extracted with pH alteration (see Table 1), gel formation was observed at a relatively low concentration when heated (85 °C) at pH 2. For example, the mung bean protein isolate

examined in Paper II started to form solid gels at a concentration of around 10 mg/mL. The protein isolate obtained had a yellow colour (Figure 11A), and the protein content was estimated to be 84.5% (w/w) by Dumas nitrogen measurements. Previous chemical analyses on mung bean protein isolate using a similar extraction protocol have shown that it contains a relatively high amount (8.7%) of carbohydrates (Brishti *et al.*, 2017). The gelling of mung bean protein isolate during heating in acid conditions was probably caused by a combination of formation of curved PNFs and carbohydrate aggregates. These aggregates were evident in the AFM images as particles still present after filtration (100 kDa spin membranes) of the mung bean PNF samples (Figure 11B). In Paper IV, an optimised extraction protocol for mung bean protein was developed. A small modification, involving addition of 0.6 M NaCl during the extraction process, resulted in a much whiter protein isolate (Figure 11C). With this purified mung bean protein isolate, it was possible to generate PNFs up to 25 mg/mL without gel formation during heating. No aggregates were detected on analysing these PNFs with AFM. The PNFs formed from purified mung bean protein (Figure 11D) were still curved, but longer than the PNFs from less pure mung bean protein (Figure 11B). Similar improvements in PNF formation have recently been reported for the 12S globulin fraction from oat (Zhou *et al.*, 2021). For an oat protein isolate obtained by adding NaCl in the extraction process, that study reported formation of PNFs up to 5.3 μm in length. This is five times longer than the longest fibril observed for oat protein extracted without addition of NaCl in Paper II (see Figure 9). The fibrils formed from the purified oat protein were of similar length to those reported for whey protein, confirming the theory that high-purity protein is important for good PNF formation.

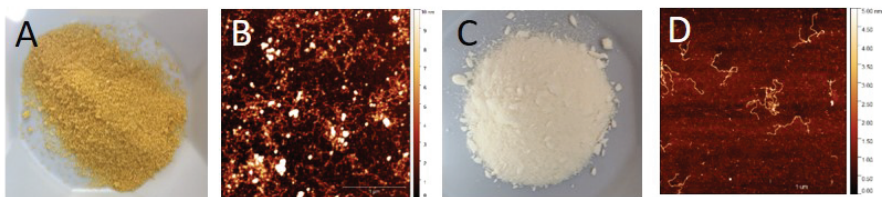


Figure 11. (A) Mung bean protein isolate extracted without NaCl and (B) atom force microscopy (AFM) image of protein nanofibrils (PNFs) made from the same isolate. (C) Mung bean protein isolate extracted with NaCl and (D) AFM images of PNFs made from the same isolate

5.2.5 Effect of changes in pH on PNFs

Food products usually have higher pH (4-7) than the acidic conditions used for PNF formation. Fibrils formed at high temperature and acidic pH are positively charged on the surface, which causes electrostatic repulsion between the PNFs (Loveday *et al.*, 2012). Theoretically, increasing the pH will alter the charges on PNFs and cause aggregation and disturbances (Jones and Mezzenga, 2012). However, it is not fully clear how pH affects PNF structure in practice. An effect of pH on PNFs of food protein origin has been reported for β -lactoglobulin and soybean protein, (Kroes-Nijboer *et al.*, 2012; Wan and Guo, 2019) with the PNFs from both aggregating as the isoelectric point of the original protein was approached.

Paper IV investigated the impact of increasing the pH from 2 to 9 on the nanostructure of curved mung bean PNFs (Figure 12). At pH 3 the PNFs still had their characteristic morphology, but the fibrils had started to disassemble into shorter fragments. This fragmentation of PNFs increased at pH 4. Between pH 5 and 6 the PNFs appeared more aggregated, which is in line with earlier observations for β -lactoglobulin and soybean at similar pH (Kroes-Nijboer *et al.*, 2012; Wan and Guo, 2019). At pH 7, the mung bean PNFs were shorter than at the original pH, but the curved morphology remained. These characteristics persisted at pH 8, but the PNFs seemed to be more entangled. Finally, at pH 9 the samples contained mostly small aggregates, without the characteristic curved PNFs.

In Paper III, the pH was altered to 7 for PNF solutions containing fava bean and the two globular fractions 11S and 7S from the same source. Analysis of the nanostructure with AFM showed that the straight semi-flexible PNFs from fractions 11S and 7S were mainly disassembled into small fragments (see Figure 3 in Paper III). The PNFs made from the less purified protein isolate from whole fava bean contained mostly globular aggregates that could be carbohydrates still present in the sample. In contrast, the curved mung bean PNFs appeared to be more stable at neutral pH than the semi-flexible PNFs made from fava bean and its fractions.

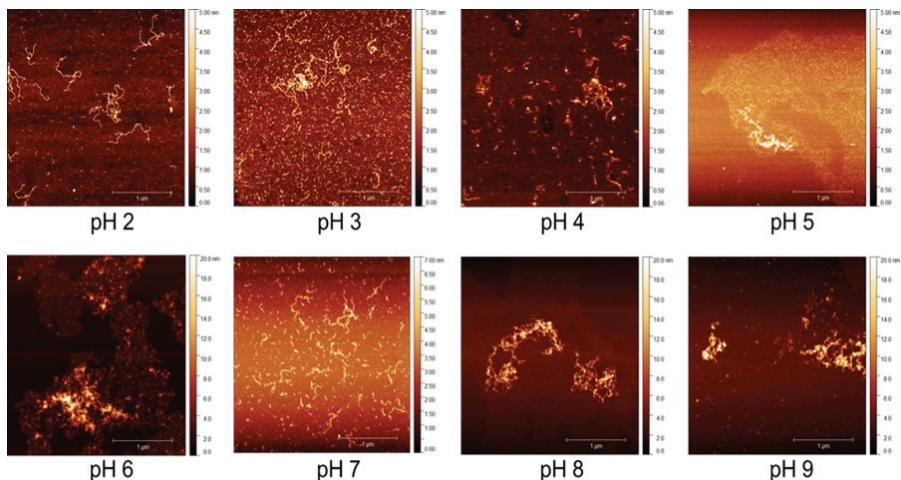


Figure 12. Atomic force microscopy images of mung bean protein nanofibrils (PNFs) at pH 2-9. Figure adopted from paper IV, with permission from editor.

5.2.6 Viscosity of plant-based PNFs

Viscosity is a critical parameter in understanding an ingredient's ability to introduce texture within a food application (Bourne, 1982). It has been shown that PNFs with curved morphology, similar to those formed at high concentration in Paper I, can be produced by addition of 80 mM CaCl_2 to whey protein when incubated at low pH and high temperature (Loveday *et al.*, 2011). Loveday *et al.* (2012) found that these short curved PNFs were much more viscous than long straight PNFs from the same source, temperature and concentration and suggested that curved PNFs could play a greater role than straight PNFs as a texture-introducing ingredient in future food applications.

Viscosity profiles of plant-based PNFs with similar morphological differences were investigated in Papers III and IV (Figure 13). Comparisons of the straight semi-flexible PNFs made from fava bean, fava bean fraction 11S and fava bean fraction 7S with the more curved PNFs obtained from mung bean protein at the same pH and concentration showed that the mung bean PNFs had 6.3 times higher viscosity than fraction 7S PNFs, 3.5 times higher than fraction 11S PNFs and 1.7 times higher than fava bean PNFs at

low shear rate (0.1/s). The reason for fava bean PNFs having relatively high viscosity in this case was probably the less pure protein isolate used, resulting in PNFs co-existing with carbohydrate aggregates. At increased shear rate, all PNFs decreased in viscosity, but the initial advantages of the curved PNFs still persisted.

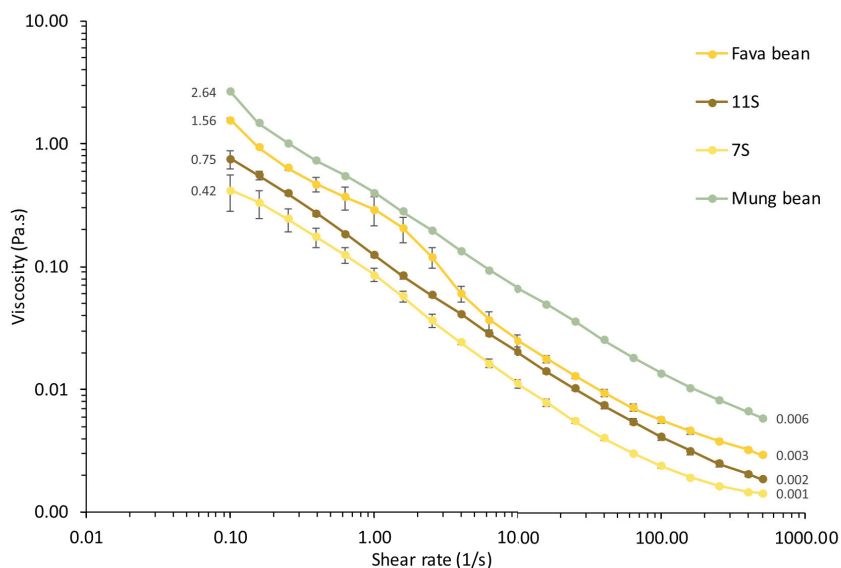


Figure 13. Viscosity versus shear rate (0.1-500/s) for curved protein nanofibrils (PNFs) from mung bean and straight PNFs from fava bean and its fractions 11S, and 7S, at a concentration of 10 mg/mL and pH 2.

In Paper IV, viscosity profiles were obtained for non-fibrillated and fibrillated mung bean protein in the pH range 2 to 8. Figure 14 shows the increase in viscosity at different shear rates (0.1-500/s) for mung bean protein after fibrillation at pH 2, 5 and 7 and a concentration of 15 mg/mL. At low shear rate (0.1/s), the fibrillated samples had 3.3 times (pH 2), 84.6 times (pH 5) and 347.8 (pH 7) times higher viscosity than the native non-fibrillated protein. This large increase in viscosity after fibrillation indicates that at food-related pH, curved PNFs can be used at low concentrations to impart texture in future food applications. These results are in agreement with the conclusion of Loveday *et al.* (2012), based on their study on the

viscosity of curved and straight PNFs from whey, that there is a future for generic curved PNFs to generate samples with high viscosity.

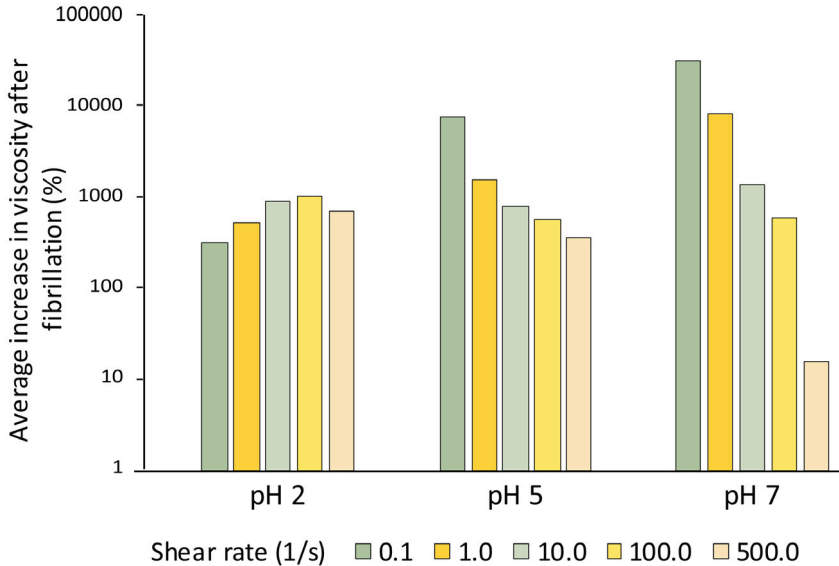


Figure 14. Average increase (%) in viscosity at shear rate 0.1, 1.0, 10, 100 and 500 /s after heat incubation of mung bean protein at pH 2, 5 and 7. The adjustments to pH 5 and 7 were made after heat incubation.

5.3 Food model systems

5.3.1 Foams

In recent years, numerous studies on the ability of plant proteins to stabilise foams have emerged (Amagliani *et al.*, 2021). Surface active proteins can form stable foams by lowering the surface tension and forming an interfacial film around bubbles (Lam, Velikov and Velez, 2014). Foam stability is affected by liquid drainage, which causes thinning of the interfacial film and ultimately rupture (Narsimhan and Xiang, 2018). This rupture can be hindered by increasing the bulk viscosity of the solution (Apostolidis and McLeay, 2016). The foaming properties of plant-globulin proteins are

usually poor due to their large size and rigid structure, making them less surface active (Amagliani *et al.*, 2021). Some studies have shown that foaming properties can be improved by modifying proteins into PNFs, *e.g.* this has been reported for fibril systems from whey and soybean protein (Oboroceanu *et al.*, 2014; Peng *et al.*, 2017; Wan, Yang and Sagis, 2016b).

Papers III and IV investigated foaming capacity, foam stability and foam volume half-life for non-fibrillated and fibrillated protein from fava bean isolate, fava bean 11S, fava bean 7S and mung bean protein isolate (Figures 15 and 16). Fibrillated fava bean, fava bean 11S and fava bean 7S protein at pH 7 and a concentration of 10 mg/mL generated more foam volume that was stable for a longer time than non-fibrillated protein from the same sources (Figure 15A-C). In particular, the fibrillated samples from fava bean 11S formed very stable foams over time (Figure 15C).

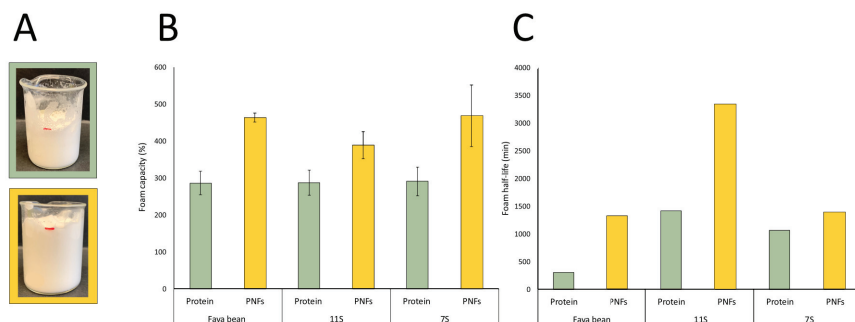


Figure 15. A) Examples of foams made from fava bean 7S protein (green box) and fava bean 7S protein nanofibrils (PNFs) (yellow box). Fibrillated and non-fibrillated protein from fava bean, fava bean 11S and fava bean 7S analysed for (B) foaming capacity and (C) foam half-life at pH 7 and a concentration of 10 mg/mL.

The foaming properties of PNFs are strongly affected by changes in pH, as demonstrated for long straight PNFs from whey (Peng *et al.*, 2017). Paper IV further explored the foaming ability of the curved PNFs from mung bean at pH 2-9 and a concentration of 15 mg/mL (Figure 16 A-B). The increase in foam volume was 40-110% higher for all fibrillated samples than for non-fibrillated samples at the same pH. At pH 4, 5, 7, 8 and 9, the fibrillated samples were more stable over time than the non-fibrillated samples. The low foam stability for fibrillated samples at pH 2 and 3 was probably due to repulsing forces between the PNFs, which made it difficult to generate a

stable interfacial film (Loveday *et al.*, 2012). This was confirmed by imaging the foams with the help of confocal microscopy (Figure 16C). The fibrillated sample at pH 2 had larger bubbles than the non-fibrillated samples, indicating faster rupture of the interfacial films. When the pH increased, the fibrillated samples showed a more significant fraction of small bubbles, indicating slower liquid drainage and bubble collapse.

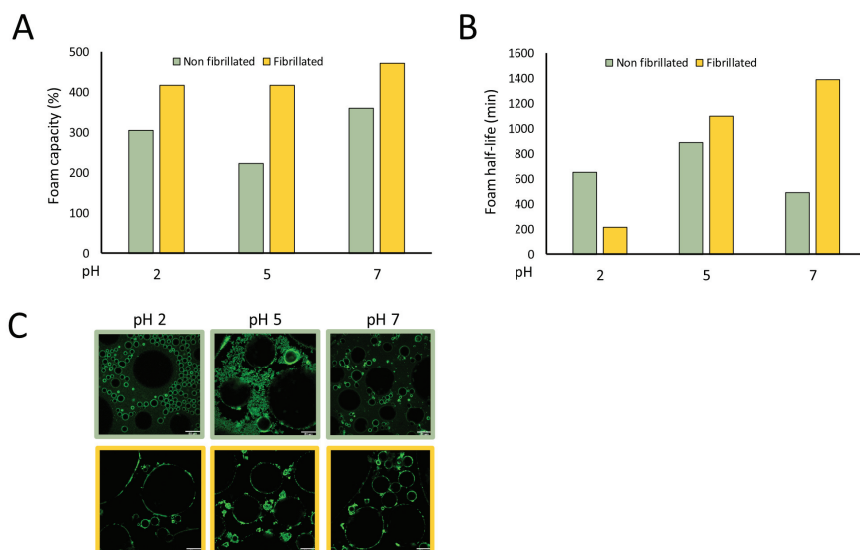


Figure 16. A) Foaming capacity and B) foam half-life of non-fibrillated and fibrillated protein from mung bean at a concentration of 15 mg/mL. C) Confocal images of bubbles stabilised by non-fibrillated (green boxes) and fibrillated (yellow boxes) whole mung bean protein isolate at pH 2, 5 and 7 stained with ThT fluorescent dye (scale bar 50 μ m).

The foam experiments reported in Papers III and IV were performed on samples containing a mixture of PNFs and peptides. It is still not fully understood whether the small peptides or the larger PNFs contribute most to the increase in foam volume and stability. A study by Wan, Yang and Sagis (2016a) investigated this further by comparing the foaming properties of a mixture of PNFs and peptides, purified PNFs and purified peptides made from the 11S globular fraction of soybean, and concluded that the pure PNFs had the poorest foaming properties. This conclusion is supported by

observations of decreased surface tension of fibrillated samples of β -lactoglobulin consisting of a mixture of PNFs and peptides, which was not seen for purified PNFs (Jung, Gunes and Mezzenga, 2010). This indicates that the peptides within the mixed fibrillated samples contributed most to the formation of a thicker interfacial film that stabilised the bubbles. In contrast, Peng *et al.* (2017) found that purified PNFs made from β -lactoglobulin generated more stable foams around the isoelectric point compared with untreated protein in the same conditions.

To further investigate whether the peptides or the curved mung bean-based PNFs obtained in Paper IV contributed most to the improved foam properties, fibrillated mung bean protein was purified into two fractions, containing pure PNFs and pure peptides. Foaming capacity and half-life were investigated at pH 2, 5 and 7 for the mixed system, pure PNFs and pure peptides. The mixed system and the pure PNFs both generated more voluminous foam than the pure peptides at all pH values tested (Figure 17A-B). At pH 7, the foams generated from the mixed system and PNFs were stable for the first 30 min, then the stability dropped to the same level as seen for the pure peptides. The mixed and pure PNF samples were both more stable over time at pH 5 than the pure peptides. Based on this result, it was concluded that the PNFs contributed to the improved foam properties, not the peptide fraction.

However, it is still not fully understood whether PNFs are small enough to stabilise foams by forming a thick interfacial film. Instead, they most likely contribute to stability by creating a gel-like network in the continuous phase, which will prevent drainage (Oboroceanu *et al.*, 2014). The foams made of fibrillated samples from mung bean protein discussed above were all made at 1 mg/mL concentration, showing that the latter explanation probably applies for mung bean PNFs. At pH 5, close to the isoelectric point for mung bean protein, the foams generated from mixed and pure protein were much more stable than at pH 7. This is probably because the PNFs acquire a net charge around pH 5 and start to aggregate (Figure 13), generating a more gel-like viscous sample (see Figure 4 in Paper IV) that hinders the collapse of the bubbles. Based on the earlier observation that samples with curved PNFs were more viscous than samples with straight PNFs, it was hypothesised that curved PNFs have superior foaming properties.

This hypothesis was tested by diluting the samples containing fibrillated and non-fibrillated fava bean protein, fava bean 11S and fava bean 7S protein to the same concentration (1 mg/mL) and examining foaming capacity and foam volume half-life at pH 2, 5 and 7 (Figure 17C-D). The results showed that none of the fibrillated samples was able to form stable foams at any pH value tested, while non-fibrillated samples generated more stable foams at pH 5 and 7. This was confirmed by confocal microscopy of the foams made at pH 7, which showed that the non-fibrillated protein had formed thicker films around the bubbles than the fibrillated samples, indicating that the protein was superior in creating thick interfacial films (see Figure 6C in Paper III). These results indicate that the ability to stabilise foams is concentration-dependent for straight PNFs generated from fava bean and its globular fractions.

How PNFs with different morphology contribute to foam stability is complex. Further research still needs to be done but, based on the results discussed above, curved PNFs seem to be better able to stabilise foams than straight PNFs at low concentrations, especially at pH close to the isoelectric point of the original protein.

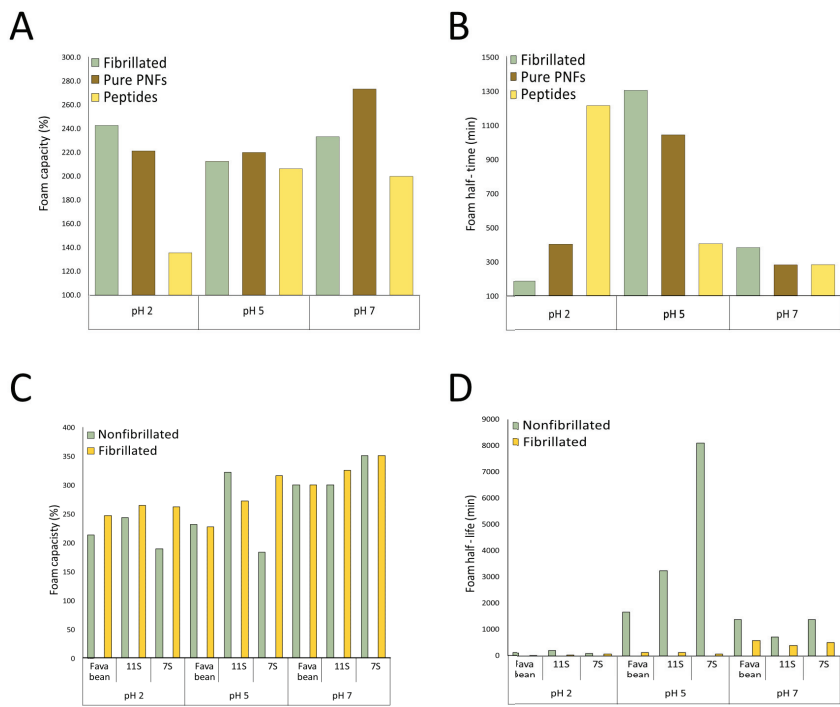


Figure 17. A) Foaming capacity and B) volume half-life for fibrillated, purified PNFs and peptides from mung bean protein. C) Foaming capacity and D) volume half-life for nonfibrillated and fibrillated protein from fava bean, fava bean fraction 11S and fava bean fraction 7S. All samples were made at pH 2, 5 and 7 and a concentration of 1 mg/mL.

5.4 Microfibrils

Microfibrils were formed from purified mung bean PNFs using a flow-focusing technique. With the addition of sheath flows of water and acetate buffer, the PNFs were aligned and aggregated into microfibrils stable enough to be picked up from the acetate bath (Figure 18). However, these mung bean-based microfibrils were too brittle to persist in drying conditions, making it impossible to perform any tensile measurements. The reason for this brittleness is still unknown, but it is probably related to the fact that it is

difficult to align curved PNFs within the flow channel. Small-angle X-ray scattering measurements on curved and straight PNFs from whey in a similar flow set-up have shown that curved PNFs have very poor alignment within the channel compared with straight PNFs (Kamada *et al.*, 2017). The reason why the curved PNFs were able to form microfibrils strong enough to break the surface tension was probably because they formed an entangled network within the channel. A potential explanation for the weak microfibrils formed from the straight PNFs from whey is that high alignment in the flow channel decreases their ability to interact.

Both these theories probably apply to the curved PNFs from mung beans, because these were considerably longer (around 20 times longer) than the curved PNFs formed from whey. The long curved PNFs from mung beans might have entangled with each other to some extent in the flow channel, but were too long to interact sufficiently well enough to form stable microfibrils that could resist drying conditions. A possible treatment to improve the microfibrils generated from mung bean PNFs is to shorten the fibrils by ultrasonication, which was found to be an efficient method to break long PNFs generated from whey in Paper I. Spinning microfibrils from other plant-based PNFs with less curved structure can be considered, *e.g.* the straight and relatively short PNFs that can be generated from fava bean and its globular fractions are candidates.

Taken together, the results presented in this thesis prove for the first time that it is possible to spin microfibrils based on plant-based PNFs. However, this work is still in progress and further research will have to be conducted before plant-based PNF microfibrils can be used to create texture in future food applications.

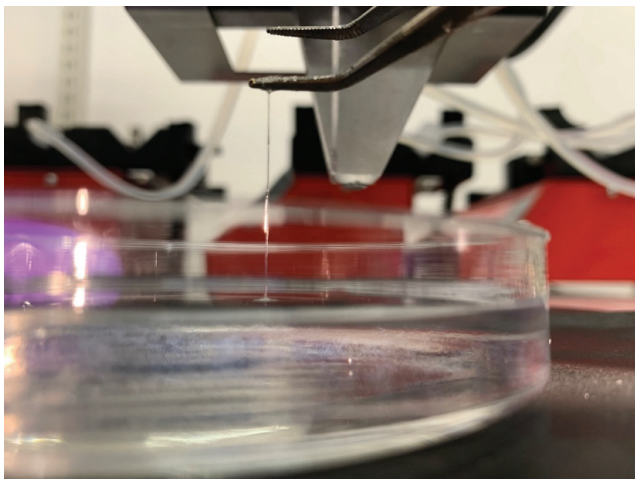


Figure 18. Microfibres formed from mung bean protein nanofibrils.

6. Conclusions

- Films cast with whey-based PNFs of different length and morphology had different microstructure. The length distribution of the fibrils seemed to contribute more to microstructure features than PNF morphology.
- A wide range of different plant-based proteins from legumes, cereals, oilseed and tubers can form PNFs when heated at 85-90 °C and pH 2 for 24-96 h. Secondary structure characterisation and detection of these PNFs with ThT assay has limitations, so the recommendation is to use complementary methods such as CD spectroscopy and nanostructure imaging by AFM.
- Small-sized and purified proteins form PNFs more easily than larger, more rigid and less purified protein structures.
- Changes in pH affect PNF morphology. Curved PNFs from mung bean protein form aggregates around pH 4-6. At pH 7 they still have curved morphology, but are shorter than at the original pH (2). Straight PNFs from fava bean protein and its major globular fractions (11S and 7S) degrade into smaller rods at pH 7.

- Fibrillated protein from fava bean and its 11S and 7S globular fractions forms more voluminous foam and more stable foam at pH 7 than non-fibrillated protein from the same source.
- Curved PNFs create more viscous samples than straight PNFs.
- Fibrillated protein from mung beans forms more voluminous foams at pH 2-9 than non-fibrillated protein from the same source. These foams are more stable over time than those made from non-fibrillated protein at pH 4, 5, 7, 8 and 9.
- In fibrillated samples from mung bean protein, it is the curved PNFs, and not the peptides, that contribute to foam stability. At pH 5 and low concentration (1 mg/mL), the curved PNFs from mung bean protein form stable foam, which is not the case for straight PNFs from fava bean protein, fava bean fraction 11S and fava bean fraction 7S. Curved PNFs are probably better at stabilising foams at low concentrations because of higher viscosity of the continuous phase, which hinders rupture of the air bubbles.
- Curved PNFs from mung bean protein can form microfibrils that are stable enough to be picked up by tweezers.

7. Future work

The intention with the work presented in this thesis was to obtain new knowledge on the potential of plant-based PNFs in future food applications. However, some work still remains to be done before PNFs can be used in food applications. For instance, it is critical to get a broader understanding of the effect of PNFs generated *in vitro* on human health, how they are digested and whether they contribute to the bioavailability of essential nutrients.

Another factor to take into consideration is the scalability of PNF production and whether it can be economically sustainable. Plant-based PNFs formed from raw material/protein sources that represent low-value or side streams today could be of great interest. These sources include fava beans, which are mostly used as animal feed (Crépon *et al.*, 2010), and mung bean protein, which is a large waste stream from production of glass noodles (Charoensuk *et al.*, 2018). However, production of plant-based PNFs needs to be further optimised so that PNFs which remain stable within food-related pH intervals can be generated in large quantities. It would be interesting to investigate pre-treatment methods for plant proteins to make them more soluble or easier to hydrolyse into smaller peptides. One option could be to sonicate the protein before fibrillation, a method that has been reported to improve protein solubility (Kamada *et al.*, 2021), which might generate higher protein conversion to PNFs. Pre-treating the protein with hydrolysing enzymes to generate more available peptides that can form PNFs is another possibility (Gao *et al.*, 2013; Mohammadian and Madadlou, 2016).

One way to decrease the susceptibility of PNFs to pH changes is to add a surfactant. A naturally occurring surfactant is lecithin, a zwitterion composed

of a mixture of phospholipids found in plant cell membranes (Alhaji *et al.*, 2020). A study by Mantovani *et al.* (2016) found that PNFs from β -lactoglobulin were more stable at increased pH when a small amount of lecithin was added during the fibrillation process.

Apart from their potential use as texture initiators in food application, PNFs could be made into more high-value food ingredients by being used as a carrier of essential nutrients such as iron. Iron deficiency is a growing health problem, which has increased interest in producing iron-enriched food applications. One promising candidate is iron nanoparticles, which have high bioavailability, but which have been reported to be unstable due to rapid oxidation and aggregation (Kumari and Chauhan, 2021). According to Shen *et al.* (2017) PNFs from β -lactoglobulins are an efficient carrier of iron nanoparticles by helping to reduce oxidation and aggregation. The authors investigated this hybrid system of PNFs and iron nanoparticles *in vitro* and *in vivo* models, which demonstrated good digestibility and bioavailability. Therefore hybrid systems with PNFs and iron nanoparticles could be a promising candidate for fortifying future food applications with iron. Plant-based iron-enriched PNFs could be used to improve iron intake of people consuming a vegetarian or vegan diet. Li *et al.* (2019) generated magnetic PNFs from fava bean by adding iron nanoparticles during the fibrillation process. Magnetic plant-based PNFs could thus be a viable method for introducing stable iron particles into food applications, while exposing them to a magnetic field might also make it possible to control the alignment of the PNFs, hence controlling the texture.

To extend the preliminary work presented in this thesis, it would be interesting to investigate whether it is possible to spin microfibrils with better mechanical attributes. For this to be done, there is a need for a better understanding of how PNFs with different morphology align in flow and whether the entanglement of PNFs can be improved by adding food-acceptable cross-linkers.

References

- Adamcik, J. and Mezzenga, R. (2018) 'Amyloid Polymorphism in the Protein Folding and Aggregation Energy Landscape', *Angewandte Chemie - International Edition*, 57(28), pp. 8370–8382. Available at: <https://doi.org/10.1002/anie.201713416>.
- Akkermans, C., Van Der Goot, A.J., Venema, P., Gruppen, H., Vereijken, J.M., Van Der Linden, E. and Boom, R.M. (2007) 'Micrometer-sized fibrillar protein aggregates from soy glycinin and soy protein isolate', *Journal of Agricultural and Food Chemistry*, 55(24), pp. 9877–9882. Available at: <https://doi.org/10.1021/jf0718897>.
- Akkermans, C., Venema, P., van der Goot, A.J., Gruppen, H., Bakx, E.J., Boom, R.M. and van der Linden, E. (2008) 'Peptides are building blocks of heat-induced fibrillar protein aggregates of β -lactoglobulin formed at pH 2', *Biomacromolecules*, pp. 1474–1479. Available at: <https://doi.org/10.1021/bm7014224>.
- Alhajj, M.J., Montero, N., Yarce, C.J. and Salamanca, C.H. (2020) 'Lecithins from vegetable, land, and marine animal sources and their potential applications for cosmetic, food, and pharmaceutical sectors', *Cosmetics*, 7(4), pp. 1–19. Available at: <https://doi.org/10.3390/cosmetics7040087>.
- Amagliani, L. and Schmitt, C. (2017) 'Globular plant protein aggregates for stabilization of food foams and emulsions', *Trends in Food Science and Technology*, 67, pp. 248–259. Available at: <https://doi.org/10.1016/j.tifs.2017.07.013>.
- Amagliani, L., Silva, J.V.C., Saffon, M. and Dombrowski, J. (2021) 'On the foaming properties of plant proteins: Current status and future opportunities', *Trends in Food Science and Technology*, 118(PA), pp. 261–272. Available at: <https://doi.org/10.1016/j.tifs.2021.10.001>.
- Antonets, K.S., Belousov, M. V., Sulatskaya, A.I., Belousova, M.E., Kosolapova, A.O., Sulatsky, M.I., Andreeva, E.A., Zykin, P.A., Malovichko, Y. V., Shtark, O.Y., Lykholay, A.N., Volkov, K. V., Kuznetsova, I.M., Turoverov, K.K., Kochetkova, E.Y., Bobylev, A.G., Usachev, K.S., Demidov, O.N.,

- Tikhonovich, I.A. and Nizhnikov, A.A. (2020) *Accumulation of storage proteins in plant seeds is mediated by amyloid formation*, *PLoS Biology*. Available at: <https://doi.org/10.1371/journal.pbio.3000564>.
- Antonets, K.S. and Nizhnikov, A.A. (2017) 'Predicting amyloidogenic proteins in the proteomes of plants', *International Journal of Molecular Sciences*, 18(10), pp. 1–22. Available at: <https://doi.org/10.3390/ijms18102155>.
- Apostolidis, C. and McLeay, F. (2016) 'Should we stop eating like this? Reducing meat consumption through substitution', *Food Policy*, 65, pp. 74–89. Available at: <https://doi.org/10.1016/j.foodpol.2016.11.002>.
- Astbury, W.T., Dickinson, S. and Bailey, K. (1935) 'The X-ray interpretation of denaturation and the structure of the seed globulins', *Biochemical Journal*, 29(10), pp. 2351–2360.1. Available at: <https://doi.org/10.1042/bj0292351>.
- Baldwin, A.J., Knowles, T.P.J., Tartaglia, G.G., Fitzpatrick, A.W., Devlin, G.L., Shamma, S.L., Waudby, C.A., Mossuto, M.F., Meehan, S., Gras, S.L., Christodoulou, J., Anthony-Cahill, S.J., Barker, P.D., Vendruscolo, M. and Dobson, C.M. (2011) 'Metastability of native proteins and the phenomenon of amyloid formation', *Journal of the American Chemical Society*, 133(36), pp. 14160–14163. Available at: <https://doi.org/10.1021/ja2017703>.
- Barac, M., Stanojevic, S., Jovanovic, S. and Pesic, M. (2004) 'Soy protein modification: A review', *Acta Periodica Technologica*, 280(35), pp. 3–16. Available at: <https://doi.org/10.2298/apt0435003b>.
- Bolder, S.G., Hendrickx, H., Sagis, L.M.C. and Van Der Linden, E. (2006) 'Fibril assemblies in aqueous whey protein mixtures', *Journal of Agricultural and Food Chemistry*, 54(12), pp. 4229–4234. Available at: <https://doi.org/10.1021/jf060606s>.
- Bourne, M.C. (1982) 'Texture, Viscosity, and Food', *Food Texture and Viscosity*, pp. 1–23. Available at: <https://doi.org/10.1016/b978-0-12-119060-6.50006-x>.
- Brishti, F.H., Zarei, M., Muhammad, S.K.S., Ismail-Fitry, M.R., Shukri, R. and Saari, N. (2017) 'Evaluation of the functional properties of mung bean protein isolate for development of textured vegetable protein', *International Food Research Journal*, 24(4), pp. 1595–1605.
- Campbell, G.M. and Mougeot, E. (1999) 'Creation and characterisation of aerated food products', *Trends in Food Science and Technology*, 10(9), pp. 283–296. Available at: [https://doi.org/10.1016/S0924-2244\(00\)00008-X](https://doi.org/10.1016/S0924-2244(00)00008-X).
- Cao, Y. and Mezzenga, R. (2019) 'Food protein amyloid fibrils: Origin, structure, formation, characterization, applications and health implications', *Advances in Colloid and Interface Science*, 269, pp. 334–356. Available at: <https://doi.org/10.1016/j.cis.2019.05.002>.
- Charoensuk, D., Brannan, R.G., Chanasattru, W. and Chaiyasit, W. (2018) 'Physicochemical and emulsifying properties of mung bean protein isolate as influenced by succinylation', *International Journal of Food Properties*,

- 21(1), pp. 1633–1645. Available at: <https://doi.org/10.1080/10942912.2018.1502200>.
- Chéreau, D., Videcoq, P., Ruffieux, C., Pichon, L., Motte, J.C., Belaid, S., Venturaireira, J. and Lopez, M. (2016) ‘Combination of existing and alternative technologies to promote oilseeds and pulses proteins in food applications’, *OCL - Oilseeds and fats, Crops and Lipids*, 41(1). Available at: <https://doi.org/10.1051/ocl/2016020>.
- Crépon, K., Marget, P., Peyronnet, C., Carrouée, B., Arese, P. and Duc, G. (2010) ‘Nutritional value of faba bean (*Vicia faba* L.) seeds for feed and food’, *Field Crops Research*, 115(3), pp. 329–339. Available at: <https://doi.org/10.1016/j.fcr.2009.09.016>.
- Dekkers, B.L., Boom, R.M. and van der Goot, A.J. (2018) ‘Structuring processes for meat analogues’, *Trends in Food Science and Technology*, 81(August), pp. 25–36. Available at: <https://doi.org/10.1016/j.tifs.2018.08.011>.
- Duranti, M., Consonni, A., Magni, C., Sessa, F. and Scarafoni, A. (2008) ‘The major proteins of lupin seed: Characterisation and molecular properties for use as functional and nutraceutical ingredients’, *Trends in Food Science and Technology*, 19(12), pp. 624–633. Available at: <https://doi.org/10.1016/j.tifs.2008.07.002>.
- Eisenberg, D.S. and Sawaya, M.R. (2017) ‘Structural studies of amyloid proteins at the molecular level’, *Annual Review of Biochemistry*, 86, pp. 69–95. Available at: <https://doi.org/10.1146/annurev-biochem-061516-045104>.
- Foegeding, E.A. and Davis, J.P. (2011) ‘Food Hydrocolloids Food protein functionality : A comprehensive approach’, *Food hydrocolloids*, 25(8), pp. 1853–1864. Available at: <https://doi.org/10.1016/j.foodhyd.2011.05.008>.
- Gao, Y.Z., Xu, H.H., Ju, T.T. and Zhao, X.H. (2013) ‘The effect of limited proteolysis by different proteases on the formation of whey protein fibrils’, *Journal of Dairy Science*, 96(12), pp. 7383–7392. Available at: <https://doi.org/10.3168/jds.2013-6843>.
- Goldschmidt, L., Teng, P.K., Riek, R. and Eisenberg, D. (2010) ‘Identifying the amyloids, proteins capable of forming amyloid-like fibrils’, *Proceedings of the National Academy of Sciences of the United States of America*, 107(8), pp. 3487–3492. Available at: <https://doi.org/10.1073/pnas.0915166107>.
- Graça, J., Calheiros, M.M. and Oliveira, A. (2014) ‘Moral Disengagement in Harmful but Cherished Food Practices? An Exploration into the Case of Meat’, *Journal of Agricultural and Environmental Ethics*, 27(5), pp. 749–765. Available at: <https://doi.org/10.1007/s10806-014-9488-9>.
- Greenfield, N.J. (2006) ‘Using circular dichroism spectra to estimate protein secondary structure’, *Nature Protocols*, 1(6), pp. 2876–2890. Available at: <https://doi.org/10.1038/nprot.2006.202>.
- Herneke, A., Lendel, C., Johansson, D., Newson, W., Hedenqvist, M., Karkehabadi, S., Jonsson, D. and Langton, M. (2021) ‘Protein Nanofibrils for Sustainable

- Food–Characterization and Comparison of Fibrils from a Broad Range of Plant Protein Isolates’, *ACS Food Science & Technology*, 1(5), pp. 854–864. Available at: <https://doi.org/10.1021/acfoodscitech.1c00034>.
- Hill, S.E., Miti, T., Richmond, T. and Muschol, M. (2011) ‘Spatial extent of charge repulsion regulates assembly pathways for lysozyme amyloid fibrils’, *PLoS ONE*, 6(4). Available at: <https://doi.org/10.1371/journal.pone.0018171>.
- Jelen, P. (1979) ‘Industrial Whey Processing Technology : An Overview’, *Journal of Agricultural and Food Chemistry*, 27(4), pp. 658–661. Available at: <https://doi.org/10.1021/jf60224a037>.
- Jones, O.G. and Mezzenga, R. (2012) ‘Inhibiting, promoting, and preserving stability of functional protein fibrils’, *Soft Matter*, 8(4), pp. 876–895. Available at: <https://doi.org/10.1039/c1sm06643a>.
- Josefsson, L., Cronhamn, M., Ekman, M., Widehammar, H., Emmer, Å. and Lendel, C. (2019) ‘Structural basis for the formation of soy protein nanofibrils’, *RSC Advances*, 9(11), pp. 6310–6319. Available at: <https://doi.org/10.1039/c8ra10610j>.
- Josefsson, L., Ye, X., Brett, C.J., Meijer, J., Olsson, C., Sjögren, A., Sundlöf, J., Davydok, A., Langton, M., Emmer, Å. and Lendel, C. (2020) ‘Potato Protein Nanofibrils Produced from a Starch Industry Sidestream’, *ACS Sustainable Chemistry and Engineering* [Preprint]. Available at: <https://doi.org/10.1021/acssuschemeng.9b05865>.
- Jung, J.M., Gunes, D.Z. and Mezzenga, R. (2010) ‘Interfacial activity and interfacial shear rheology of native β -lactoglobulin monomers and their heat-induced fibers’, *Langmuir*, 26(19), pp. 15366–15375. Available at: <https://doi.org/10.1021/la102721m>.
- Kamada, A., Mittal, N., Söderberg, L.D., Ingverud, T., Ohm, W. and Roth, S. V (2017) ‘Flow-assisted assembly of nanostructured protein microfibers’, *Proc Natl Acad Sci USA*, 114(6), pp. 1232–1237. Available at: <https://doi.org/10.1073/pnas.1617260114>.
- Kamada, A., Rodriguez-Garcia, M., Ruggeri, F.S., Shen, Y., Levin, A. and Knowles, T.P.J. (2021) ‘Controlled self-assembly of plant proteins into high-performance multifunctional nanostructured films’, *Nature Communications*, 12(1), pp. 1–10. Available at: <https://doi.org/10.1038/s41467-021-23813-6>.
- Kimura, A., Takako, F., Meili, Z., Shiori, M., Maruyama, N. and Utsumi, S. (2008) ‘Comparison of physicochemical properties of 7S and 11S globulins from pea, fava bean, cowpea, and French bean with those of soybean-french bean 7S globulin exhibits excellent properties’, *Journal of Agricultural and Food Chemistry*, 56(21), pp. 10273–10279. Available at: <https://doi.org/10.1021/jf801721b>.
- Kroes-Nijboer, A., Sawalha, H., Venema, P., Bot, A., Flöter, E., Den Adel, R., Bouwman, W.G. and Van Der Linden, E. (2012) ‘Stability of aqueous food

- grade fibrillar systems against pH change', *Faraday Discussions*, 158, pp. 125–138. Available at: <https://doi.org/10.1039/c2fd20031g>.
- Kumari, A. and Chauhan, A.K. (2021) 'Iron nanoparticles as a promising compound for food fortification in iron deficiency anemia: a review', *Journal of Food Science and Technology* [Preprint]. Available at: <https://doi.org/10.1007/s13197-021-05184-4>.
- Lam, S., Velikov, K.P. and Velez, O.D. (2014) 'Pickering stabilization of foams and emulsions with particles of biological origin', *Current Opinion in Colloid and Interface Science*, 19(5), pp. 490–500. Available at: <https://doi.org/10.1016/j.cocis.2014.07.003>.
- Langton, M., Ehsanzamir, S., Karkehabadi, S., Feng, X., Johansson, M. and Johansson, D.P. (2020) 'Gelation of faba bean proteins - Effect of extraction method, pH and NaCl', *Food Hydrocolloids*, 103, p. 105622. Available at: <https://doi.org/10.1016/J.FOODHYD.2019.105622>.
- Lara, C., Adamcik, J., Jordens, S. and Mezzenga, R. (2011) 'General self-assembly mechanism converting hydrolyzed globular proteins into giant multistranded amyloid ribbons', *Biomacromolecules*, 12(5), pp. 1868–1875. Available at: <https://doi.org/10.1021/bm200216u>.
- Lassé, M., Ulluwishewa, D., Healy, J., Thompson, D., Miller, A., Roy, N., Chitchohan, K. and Gerrard, J.A. (2016) 'Evaluation of protease resistance and toxicity of amyloid-like food fibrils from whey, soy, kidney bean, and egg white', *Food Chemistry*, 192, pp. 491–498. Available at: <https://doi.org/10.1016/j.foodchem.2015.07.044>.
- Lendel, C. and Solin, N. (2021) 'Protein nanofibrils and their use as building blocks of sustainable materials', *RSC Advances*, 11(62), pp. 39188–39215. Available at: <https://doi.org/10.1039/d1ra06878d>.
- Li, J., Pylypchuk, I., Johansson, D.P., Kessler, V.G., Seisenbaeva, G.A. and Langton, M. (2019) 'Self-assembly of plant protein fibrils interacting with superparamagnetic iron oxide nanoparticles', *Scientific Reports*, 9(1), pp. 1–18. Available at: <https://doi.org/10.1038/s41598-019-45437-z>.
- Li, T., Wang, L., Zhang, X., Geng, H., Xue, W. and Chen, Z. (2020) 'Assembly behavior, structural characterization and rheological properties of legume proteins based amyloid fibrils', *Food Hydrocolloids*, 111(October 2020), p. 106396. Available at: <https://doi.org/10.1016/j.foodhyd.2020.106396>.
- Liu, G., Li, J., Shi, K., Wang, S., Chen, J., Liu, Y. and Huang, Q. (2009) 'Composition, secondary structure, and self-assembly of oat protein isolate', *Journal of Agricultural and Food Chemistry*, 57(11), pp. 4552–4558. Available at: <https://doi.org/10.1021/jf900135e>.
- Liu, J. and Tang, C.H. (2013) 'Heat-induced fibril assembly of vicilin at pH2.0: Reaction kinetics, influence of ionic strength and protein concentration, and molecular mechanism', *Food Research International*, 51(2), pp. 621–632. Available at: <https://doi.org/10.1016/j.foodres.2012.12.049>.

- Løkra, S. and Strætkvern, K.O. (2009) 'Industrial Proteins from Potato Juice. A Review', *Food*, 3(1), pp. 88–95.
- Lonkila, A. and Kaljonen, M. (2021) 'Promises of meat and milk alternatives: an integrative literature review on emergent research themes', *Agriculture and Human Values*, 38(3), pp. 625–639. Available at: <https://doi.org/10.1007/s10460-020-10184-9>.
- Loveday, S.M., Su, J., Rao, M.A., Anema, S.G. and Singh, H. (2011) 'Effect of calcium on the morphology and functionality of whey protein nanofibrils', *Biomacromolecules*, 12(10), pp. 3780–3788. Available at: <https://doi.org/10.1021/bm201013b>.
- Loveday, Simon M., Su, J., Rao, M.A., Anema, S.G. and Singh, H. (2012) 'Whey protein nanofibrils: The environment-morphology-functionality relationship in lyophilization, rehydration, and seeding', *Journal of Agricultural and Food Chemistry*, 60(20), pp. 5229–5236. Available at: <https://doi.org/10.1021/jf300367k>.
- Loveday, S. M., Wang, X.L., Rao, M.A., Anema, S.G. and Singh, H. (2012) 'β-Lactoglobulin nanofibrils: Effect of temperature on fibril formation kinetics, fibril morphology and the rheological properties of fibril dispersions', *Food Hydrocolloids*, pp. 242–249. Available at: <https://doi.org/10.1016/j.foodhyd.2011.07.001>.
- Mäkinen, O.E., Sozer, N., Ercili-Cura, D. and Poutanen, K. (2016) *Protein From Oat: Structure, Processes, Functionality, and Nutrition, Sustainable Protein Sources*. Available at: <https://doi.org/10.1016/B978-0-12-802778-3.00006-8>.
- Mantovani, R.A., Fattori, J., Michelon, M. and Cunha, R.L. (2016) 'Formation and pH-stability of whey protein fibrils in the presence of lecithin', *Food Hydrocolloids*, 60, pp. 288–298. Available at: <https://doi.org/10.1016/j.foodhyd.2016.03.039>.
- Marcone, M.F., Kakuda, Y. and Yada, R.Y. (1998) 'Salt soluble seed globulins of dicotyledonous and monocotyledonous plants II. Structural characterization', *Food Chemistry*, 63(2), pp. 265–274. Available at: [https://doi.org/10.1016/S0308-8146\(97\)00159-3](https://doi.org/10.1016/S0308-8146(97)00159-3).
- Mendoza, E.M.T., Adachi, M., Bernardo, A.E.N. and Utsumi, S. (2001) 'Mungbean [*Vigna radiata* (L.) Wilczek] globulins: Purification and characterization', *Journal of Agricultural and Food Chemistry*, 49(3), pp. 1552–1558. Available at: <https://doi.org/10.1021/jf001041h>.
- Mishra, R., Sörgjerd, K., Nyström, S., Nordigården, A., Yu, Y.C. and Hammarström, P. (2007) 'Lysozyme Amyloidogenesis Is Accelerated by Specific Nicking and Fragmentation but Decelerated by Intact Protein Binding and Conversion', *Journal of Molecular Biology*, 366(3), pp. 1029–1044. Available at: <https://doi.org/10.1016/j.jmb.2006.11.084>.

- Mohammadian, M. and Madadlou, A. (2016) 'Characterization of fibrillated antioxidant whey protein hydrolysate and comparison with fibrillated protein solution', *Food Hydrocolloids*, 52, pp. 221–230. Available at: <https://doi.org/10.1016/j.foodhyd.2015.06.022>.
- Monge-Morera, M., Lambrecht, M.A., Deleu, L.J., Louros, N.N., Rousseau, F., Schymkowitz, J. and Delcour, J.A. (2021) 'Heating Wheat Gluten Promotes the Formation of Amyloid-like Fibrils', *ACS Omega*, 6(3), pp. 1823–1833. Available at: <https://doi.org/10.1021/acsomega.0c03670>.
- Munialo, C.D., Martin, A.H., Van Der Linden, E. and De Jongh, H.H.J. (2014) 'Fibril formation from pea protein and subsequent gel formation', *Journal of Agricultural and Food Chemistry*, 62(11), pp. 2418–2427. Available at: <https://doi.org/10.1021/jf4055215>.
- Murray, B.S. (2020) 'Recent developments in food foams', *Current Opinion in Colloid and Interface Science*, 50. Available at: <https://doi.org/10.1016/j.cocis.2020.101394>.
- Narsimhan, G. and Xiang, N. (2018) 'Role of Proteins on Formation, Drainage, and Stability of Liquid Food Foams', *Annual Review of Food Science and Technology*, 9, pp. 45–63. Available at: <https://doi.org/10.1146/annurev-food-030216-030009>.
- Oboroceanu, D., Wang, L., Magner, E. and Auty, M.A.E. (2014) 'Fibrillization of whey proteins improves foaming capacity and foam stability at low protein concentrations', *Journal of Food Engineering*, 121(1), pp. 102–111. Available at: <https://doi.org/10.1016/j.jfoodeng.2013.08.023>.
- Osborne T.B. (1924) 'The Vegetable Proteins', *Nature*, 114(2875), p. 822. Available at: <https://doi.org/10.1038/114822c0>.
- Otzen, D. and Riek, R. (2019) 'Functional amyloids', *Cold Spring Harbor Perspectives in Biology*, 11(12). Available at: <https://doi.org/10.1101/cshperspect.a033860>.
- Peng, D., Yang, J., Li, J., Tang, C. and Li, B. (2017) 'Foams Stabilized by β -Lactoglobulin Amyloid Fibrils: Effect of pH', *Journal of Agricultural and Food Chemistry*, pp. 10658–10665. Available at: <https://doi.org/10.1021/acs.jafc.7b03669>.
- Pereira, I., Gomes, A.M.P., Pintado, M.E., Madureira, A.R. and Malcata, F.X. (2007) 'Bovine whey proteins – Overview on their main biological properties', *Food Research International*, 40(10), pp. 1197–1211. Available at: <https://doi.org/10.1016/j.foodres.2007.07.005>.
- Perera, S.P., McIntosh, T.C. and Wanasundara, J.P.D. (2016) 'Structural properties of cruciferin and napin of Brassica napus (canola) show distinct responses to changes in pH and temperature', *Plants*, 5(3), pp. 64–74. Available at: <https://doi.org/10.3390/plants5030036>.
- Qiu, W., Patil, A., Hu, F. and Liu, X.Y. (2019) 'Hierarchical Structure of Silk Materials Versus Mechanical Performance and Mesoscopic Engineering

- Principles', *Small*, 15(51), pp. 1–45. Available at: <https://doi.org/10.1002/smll.201903948>.
- Racusen, D. and Weller, D.L. (1984) 'Molecular Weight of Patatin, a Major Potato Tuber Protein', *Journal of Food Biochemistry*, pp. 103–107. Available at: <https://doi.org/10.1111/j.1745-4514.1984.tb00318.x>.
- Sari, Y.W., Mulder, W.J., Sanders, J.P.M. and Bruins, M.E. (2015) 'Towards plant protein refinery: Review on protein extraction using alkali and potential enzymatic assistance', *Biotechnology Journal*, 10(8), pp. 1138–1157. Available at: <https://doi.org/10.1002/biot.201400569>.
- Sen, P., Fatima, S., Ahmad, B. and Khan, R.H. (2009) 'Interactions of thioflavin T with serum albumins: Spectroscopic analyses', *Spectrochimica Acta - Part A: Molecular and Biomolecular Spectroscopy*, 74(1), pp. 94–99. Available at: <https://doi.org/10.1016/j.saa.2009.05.010>.
- Shen, Y., Posavec, L., Bolisetty, S., Hilty, F.M., Nyström, G., Kohlbrecher, J., Hilbe, M., Rossi, A., Baumgartner, J., Zimmermann, M.B. and Mezzenga, R. (2017) 'Amyloid fibril systems reduce, stabilize and deliver bioavailable nanosized iron', *Nature Nanotechnology*, 12(7), pp. 642–647. Available at: <https://doi.org/10.1038/nnano.2017.58>.
- Shewry, P.R., Napier, J.A. and Tatham, A.S. (1995) 'Seed storage proteins: Structures and biosynthesis', *Plant Cell*, 7(7), pp. 945–956. Available at: <https://doi.org/10.2307/3870049>.
- Sipe, J.D., Benson, M.D., Buxbaum, J.N., Ikeda, S., Saraiva, M.J.M., Westermark, P., Sipe, J.D., Benson, M.D., Buxbaum, J.N., Ikeda, S., Saraiva, M.J.M. and Westermark, P. (2016) 'Amyloid fibril proteins and amyloidosis : chemical identification and clinical classification International Society of Amyloidosis 2016 Nomenclature Guidelines Amyloid fibril proteins and amyloidosis : chemical identification and clinical classification I', *Amyloid*, 6129. Available at: <https://doi.org/10.1080/13506129.2016.1257986>.
- Smith, J.F., Knowles, T.P.J., Dobson, C.M., MacPhee, C.E. and Welland, M.E. (2006) 'Characterization of the nanoscale properties of individual amyloid fibrils', *Proceedings of the National Academy of Sciences of the United States of America*, 103(43), pp. 15806–15811. Available at: <https://doi.org/10.1073/pnas.0604035103>.
- Soon, W.L., Peydayesh, M., Mezzenga, R. and Miserez, A. (2022) 'Plant-Based Amyloids from Food Waste for Removal of Heavy Metals from Contaminated Water', *SSRN Electronic Journal*, 445(April), p. 136513. Available at: <https://doi.org/10.2139/ssrn.4032325>.
- Tang, C.H. and Wang, C.S. (2010) 'Formation and characterization of amyloid-like fibrils from soy β -conglycinin and glycinin', *Journal of Agricultural and Food Chemistry*, pp. 11058–11066. Available at: <https://doi.org/10.1021/jf1021658>.

- Tavano, O.L. (2013) 'Protein hydrolysis using proteases: An important tool for food biotechnology', *Journal of Molecular Catalysis B: Enzymatic*, 90, pp. 1–11. Available at: <https://doi.org/10.1016/j.molcatb.2013.01.011>.
- Wan, Y. and Guo, S. (2019) 'The Formation and Disaggregation of Soy Protein Isolate Fibril: Effects of pH', *Food Biophysics*, 14(2), pp. 164–172. Available at: <https://doi.org/10.1007/s11483-019-09567-1>.
- Wan, Z., Yang, X. and Sagis, L.M.C. (2016a) 'Contribution of Long Fibrils and Peptides to Surface and Foaming Behavior of Soy Protein Fibril System', *Langmuir*, 32(32), pp. 8092–8101. Available at: <https://doi.org/10.1021/acs.langmuir.6b01511>.
- Wan, Z., Yang, X. and Sagis, L.M.C. (2016b) 'Nonlinear Surface Dilatational Rheology and Foaming Behavior of Protein and Protein Fibrillar Aggregates in the Presence of Natural Surfactant', *Langmuir*, 32(15), pp. 3679–3690. Available at: <https://doi.org/10.1021/acs.langmuir.6b00446>.
- Wanasundara, J.P.D., Abeysekera, S.J., McIntosh, T.C. and Falk, K.C. (2012) 'Solubility differences of major storage proteins of brassicaceae oilseeds', *JAOCS, Journal of the American Oil Chemists' Society*, 89(5), pp. 869–881. Available at: <https://doi.org/10.1007/s11746-011-1975-9>.
- Warsame, A.O., Michael, N., O'Sullivan, D.M. and Tosi, P. (2020) 'Identification and Quantification of Major Faba Bean Seed Proteins', *Journal of Agricultural and Food Chemistry*, 68(32), pp. 8535–8544. Available at: <https://doi.org/10.1021/acs.jafc.0c02927>.
- Weaire, D. and Phelan, R. (1996) 'The physics of foam', *Journal of Physics Condensed Matter*, 8(47), pp. 9519–9524. Available at: <https://doi.org/10.1088/0953-8984/8/47/055>.
- Willett, W., Rockström, J., Loken, B., Springmann, M., Lang, T., Vermeulen, S., Garnett, T., Tilman, D., DeClerck, F., Wood, A., Jonell, M., Clark, M., Gordon, L.J., Fanzo, J., Hawkes, C., Zurayk, R., Rivera, J.A., De Vries, W., Majele Sibanda, L., Afshin, A., Chaudhary, A., Herrero, M., Agustina, R., Branca, F., Lartey, A., Fan, S., Crona, B., Fox, E., Bignet, V., Troell, M., Lindahl, T., Singh, S., Cornell, S.E., Srinath Reddy, K., Narain, S., Nishtar, S. and Murray, C.J.L. (2019) 'Food in the Anthropocene: the EAT-Lancet Commission on healthy diets from sustainable food systems.', *Lancet (London, England)*, 393(10170), pp. 447–492. Available at: [https://doi.org/10.1016/S0140-6736\(18\)31788-4](https://doi.org/10.1016/S0140-6736(18)31788-4).
- Yang, J., Kornet, R., Diedericks, C.F., Yang, Q., Berton-Carabin, C.C., Nikiforidis, C. V., Venema, P., van der Linden, E. and Sagis, L.M.C. (2022) 'Rethinking plant protein extraction: Albumin—From side stream to an excellent foaming ingredient', *Food Structure*, 31(October 2021). Available at: <https://doi.org/10.1016/j.foostr.2022.100254>.

- Yang, J. and Sagis, L.M.C. (2021) 'Interfacial behavior of plant proteins — novel sources and extraction methods', *Current Opinion in Colloid and Interface Science*, 56. Available at: <https://doi.org/10.1016/j.cocis.2021.101499>.
- Yang, S., Zhang, Q., Yang, H., Shi, H., Dong, A., Wang, L. and Yu, S. (2022) 'Progress in infrared spectroscopy as an efficient tool for predicting protein secondary structure', *International Journal of Biological Macromolecules*, 206(October 2021), pp. 175–187. Available at: <https://doi.org/10.1016/j.ijbiomac.2022.02.104>.
- Ye, X., Hedenqvist, M.S., Langton, M. and Lendel, C. (2018) 'On the role of peptide hydrolysis for fibrillation kinetics and amyloid fibril morphology', *RSC Advances*, 8(13), pp. 6915–6924. Available at: <https://doi.org/10.1039/c7ra10981d>.
- Zhou, J., Li, T., Peydayesh, M., Uselli, M., Lutz-bueno, V., Teng, J., Wang, L. and Mezzenga, R. (2021) 'Oat Plant Amyloids for Sustainable Functional Materials', *Advanced Science*, 2104445, pp. 1–11. Available at: <https://doi.org/10.1002/advs.202104445>.

Popular science summary

There is a pressing need to produce protein-rich food products that are good for the environment and for animal welfare. One way to achieve this is to replace animal products with plant-based alternatives. Despite growing awareness of the negative impact of animal products on the global climate, the vast majority of consumers worldwide are unwilling to shift their diet to plant-based alternatives. Eating meat and dairy products is a deep-rooted tradition in many cultures worldwide, which raises the question of why people think that these food products are so good. The answer is quite complex, but a key factor for a food to be experienced as good lies in the texture. Creating plant-based alternatives that mimic the structure of highly valued animal products could be a way to get more consumers to eat more sustainably.

This thesis presents a solution for creating novel textured foods from plant protein by exploiting the internal structuring that can be achieved with formation of plant-based protein nanofibrils (PNFs). These thread-like protein structures are only a few nanometres wide, but can be up to several micrometres long. PNFs differ in terms of structure from most proteins found in plants worldwide. For example, they have a more well-organised chemical construction, making them incredibly stable and strong, which are important properties for creating texture in food.

There are several methods available for converting plant protein to PNFs. The PNFs investigated in this thesis were made by dissolving proteins in acidic solution (~pH 2), followed by heating. Fibril formation by seven different plant-based proteins was tested. The seven plant raw materials used were fava bean, mung bean, lupin, oats, rapeseed, soybean and potatoes. The

latter two were obtained as pre-extracted protein isolates, while the others were extracted by hand in the laboratory. The ability of these proteins to form PNFs was evaluated by different methods that characterised their internal and the external fibril structure. The results showed that all plant proteins that was tested here could form fibrils, but with some variation in length and morphology (either straight or curly) depending on the protein source.

Protein characterisation and extraction optimisation were performed for fava bean and mung bean protein, to identify components crucial for creating large quantities of long fibrils. These studies indicate that the purer the protein and the smaller the protein molecule, the easier it was to form PNFs. The work continued by comparing how PNFs with different lengths and appearances are structured and react to a more food-relevant pH, and how fibril morphology affects sample characteristics. The results showed that fibril length plays a vital role in the ability to create structure, that the fibrils formed at neutral pH are stable (although somewhat shorter) and that curly fibrils form more viscous samples than straight fibrils.

The ability to stabilise air bubbles is an essential property in many well-known foods, such as whipped cream, meringues and bread. In another part of the work presented in this thesis, samples with straight PNFs from fava bean and samples with curly PNFs from mung bean were whipped into foams to investigate whether fibrils can stabilise air bubbles. The height and lifetime of the foams were compared to those of foams from samples containing only dissolved protein from the same raw material. The results showed that fibrillated samples created foams with larger volume that were more stable over time and that curly fibrils were better than straight fibrils at stabilising foams at low concentrations.

Preliminary results on how plant-based fibrils can be aligned into long spider silk-like threads are summarised at the end of the thesis. These PNF-based ‘spider threads’ could be used in future plant-based meat substitutes to mimic the texture of muscle fibre. In summary, the results presented in this thesis provide a deeper understanding of how plant protein can be used to create PNFs and how these can be used in the future to improve the structure of plant-based foods.

Populärvetenskaplig sammanfattning

Det finns ett stort behov att få fram proteinrika livsmedelsprodukter som både är bra för miljön och värnar om djurens välmående. Ett sätt att åstadkomma detta är att ersätta animaliska produkter med växtbaserade alternativ. Trots en ökande medvetenhet om animaliska produkters negativa påverkan på klimatet, så är det svårt få den breda massan av konsumenter att genomföra detta skifte till växtbaserade alternativ. Att äta kött och mejeriprodukter är en djupt rotad tradition i många kulturer världen över. Så frågan man måste ställa sig är varför tycker vi dessa livsmedel är så goda? Svaret är ganska komplext, men en nyckelfaktor för att vi ska uppleva maten vi äter som god är att den har en bra textur. Så en lösning för att få fler konsumenter att äta mer hållbart är att, även i växtbaserade alternativ, försöka efterlikna texturen i våra uppskattade animaliska produkter.

I denna avhandling presenteras en möjlig lösning för att skapa nya texturerade livsmedel från växtprotein. Hypotesen var att denna strukturering kunde uppnås med växtbaserade protein nanofibriller (PNFs). Vilket är trådliknande proteinstrukturer som endast är några nanometer breda och kan bli upp till flera mikrometer långa. Det som särskiljer PNFs från majoriteten av de proteiner som kan hittas i växter världen över är en kemisk mer välorganiserad konstruktion, vilket gör dem otroligt stabila och starka, egenskaper som är viktiga för att kunna skapa textur i ett livsmedel.

Det finns flera metoder för att omvandla växtprotein till PNFs. Alla PNFs som undersöktes i detta arbete tillverkades genom att lösa upp protein i en sur lösning (~pH 2) som sedan värmdes. Fibrillerna tillverkades från sju olika växtbaserade proteiner vars förmåga att bilda PNFs utvärderades med en rad olika metoder som karakteriserade både den interna och den externa fibrill

strukturen. Resultaten visade att alla växtproteiner kunde bilda fibriller, dock med en viss variation i längd och utseende (antingen raka eller krulliga) beroende på proteinkällan.

De sju olika råmaterialen som användes var åkerböna, mungböna, lupinfrön, havre, rapsfrön, sojaböna och potatis. De två sistnämnda erhöles som redan extraherade proteinisolat medan resterande extraherades för hand i labbet. Grundläggande proteinkarakterisering och extraktionsoptimering gjordes av protein från åkerböna och mungböna för att undersöka vilka komponenter som är avgörande för att skapa stora kvantiteter av långa fibriller. Slutsatsen från denna undersökning var att desto renare proteinet är och ju mindre storlek proteinmolekylerna har desto lättare är det att bilda PNFs. Detta arbete omfattar även hur PNFs med olika längd och utseende strukturerar sig, hur de reagerar i ett mer livsmedels relevant pH samt hur fibrillernas utseende påverkar provets karaktär. Från dessa undersökningar konstaterades att längden av fibrillerna spelar en viktig roll i förmågan att skapa struktur, att fibrillerna är stabila vid neutralt pH (dock lite kortare) och att krulliga fibriller skapar mer trögflytande prov än raka.

Att kunna stabilisera luftbubblor är en viktig egenskap i många livsmedel så som vispgrädde, maränger och bröd. Genom att vispa raka PNFs från åkerböna samt krulliga PNFs från mungböna till skum och jämföra höjden och livslängden med skum med prover innehållande endast upplöst protein från samma råmaterial kunde slutsatser dras om hur bra fibriller kan stabilisera luftbubblor. Resultaten visade att fibrillerade prover skapade skum med större volym som var stabilare över tid samt att krulliga fibriller är bättre på att stabilisera skum än raka vid riktigt låga koncentrationer.

I slutet av avhandlingen redovisas även preliminära resultat på hur växtbaserade fibriller kan linjeras upp till långa trådar, liknade spindeltråd. Dessa ”spindeltrådar” skulle kunna användas i framtida växtbaserade köttsubstitut för att efterlikna texturen av muskelfiber. Sammanfattningsvis så har resultaten som redovisades i denna avhandling givit en djupare förståelse för hur växtprotein kan användas för att skapa PNFs och hur dessa i framtiden kan användas för att skapa ökad struktur i växtbaserade livsmedel.

Acknowledgements

Around five years ago, I moved from my beloved Skåne to Uppsala to start my dream job, the PhD position that was the foundation for this thesis. Now I want to take the opportunity to thank everyone who contributed to my scientific development, made me feel welcome at work and in my new hometown, and were there for me during my PhD journey.

First, I want to thank my main supervisor, Professor **Maud Langton**, for believing in me by letting me be part of this project. Thank you for always being there when I had questions and always standing up for me. Most of all, thanks for always caring about my well-being. Thanks to my co-supervisors; **Christofer** for contributing with your great knowledge and for all your help with my projects, **Bill** for your support and motivating me with your ever-cheerful attitude, and **Daniel** for all the help at the start of this PhD journey.

There are many people at SLU I want to thank, starting with the STEG group. Thanks to **Sacid** for all the support and sharing all your expertise about protein characterisation, to **Henrik** for all your help and for being so genuinely interested in my work, **Jing** for all the help and being the master of the confocal microscope, and **Galia** for sharing your best mushroom-picking spots around Uppsala. To my office-mates and fellow PhD students; thanks to **Klara** because you made working at SLU more entertaining when you arrived with your energy, impressive knowledge of wines and cheerful attitude, to **Solja** for your porridge knowledge and all the fun, and to **Mathias** for your kindness, helpfulness and being so tolerant of your office mates' constant chitchatting. To the newest recruits in the group, **Jaqueline** and **Johanna**, thanks for the great company, I wish you all the luck for your

coming PhD years! Thanks, **Hanna**, for all your support and consideration of my well-being during the writing of this thesis.

To all other people hanging out in the small fikaroom outside the D-corridor; **Elin, Yan, Troy, Marijana, Björn** and **Mathilde** thanks for the fika talks. To those who left (for the industry or other universities) but are missed, thanks to **Johnny** for contributing with all your unfiltered knowledge, and to **Frida, Fredric** and **Christina** for being part of all wild discussions. Thanks to all the others in the D-corridor, **Ani** for teaching me the fine art of macramé and **Anders** and **Corine** for all the champagne and for driving me home during the worst snowstorm I have ever experienced. I also want to thank all the other colleagues at the Department of Molecular Sciences for making working at SLU so enjoyable. Thank you **Gulaim** for all your assistance with the AFM, **Nils** for always taking time to solve all my strange IT problems, and **Jerry** for taking time off from your vacation to read my thesis. To **Laura**, thanks for your friendship - I'm looking forward to enjoying your company even more frequently now that we will soon be living in the same city again. Thanks to **Monika** for always standing up for your PhD students and always caring for our well-being. To all of you in the steering group, social group, PhD council and other committees that I have met during my work as equal opportunity representative, thanks for all the interesting discussions.

To the people at KTH; **Fredrik, Mikael, Antonio, Tomas** and **Xinchen** thanks for all the help and sharing your knowledge, and **Saeed**, thanks for the company and for teaching me to handle the flow cell. Thanks to **Anna** at Chalmers who taught me how to handle the rheometer. To the whole group, **Fredrik, Elias, Henrik, Christofer**, and **Maud**, that travelled with me to DESY in Hamburg last autumn, working all day and night with my samples on the synchrotron, thanks for all the help, I learned a lot and had a really good time! To my LiFT mentor at Lantmännen **Christian**, I want to thank you for your support and the energy you brought to our meetings. Thanks also to **Karin** and **Annelie** at Lantmännen for interesting discussions.

Tack till **Sofia** för att du har stått ut med mig i över 25 år och för att du lät dig bli övertalad att flytta till Uppsala – du är en fantastisk vän. Mitt bästa fynd i Uppsala är ju såklart dig, **Hanna** tack för alla roliga samtal, middagar och utflykter – du har verkligen gjort livet i Uppsala så mycket roligare. Tack dig **Linnea** för att du visade mig Uppsalas mysigaste område, så att vi kunde bli grannar.

Fia; tack för alla fester, semestrar och Game of Thrones-kvällar, men framförallt tack för att det är fysiskt omöjligt att ha tråkigt i ditt sällskap. Tack **Karin**, för att du gjorde min studenttid så galet rolig, det hade inte varit samma sak utan dig! Till min gamla korridorsgranne **Maria**, tack för jag fått ha kvar dig som vän trots att jag flyttade till fiende staden Uppsala.

Amanda, min vän som alltid är i något fjärran land och jobbar för att världen ska bli lite bättre och trots det alltid finns där för mig, tack för att jag får ha dig i mitt liv. Till **Caro** tack för jag får vara din vän, ser fram emot att besöka dig och lilla **Molly** i Skåne oftare nu när denna avhandling är klar. **Linda** tack för att du är en sådan inspiration, vilken bedrift att skaffa en doktorexamen och rodde två små barn på vägen! Till gänget **Joel, Björn, Raul, Lollo** och **Amanda** tack för alla fantastiska minnen från gymnasiet och den otroligt roliga resan till Degerträsk (Norrland) runt nyår 2020.

Helena tack för att du styr upp typ allt kul som händer i Malmö med omnejd. Tack till dig och resten av gänget; **Mathilda, Meggie, Frida, Sofie, Linn, Alex** och **Laura, Karin** för alla fester, resor och festivalminnen. Det är även några nyare bekanta jag vill tacka för att de gjort senaste två åren lite skojigare, **Calle, Julia** tack för den underbara fjällvandringen sommaren 2021, och tack **Johannes** och **Carina** för årets skidresa och midsommarfirandet i paradiset.

Till **Mamma och Pappa**, tack för att ni alltid har trott och hejat på mig – ni har givit mig så mycket. **Mamma**, du har jag lärt mig att alltid stå upp och kämpa för det som man tycker är fel, och av dig **Pappa** så har jag fått den tjurskallighet som nog behövdes för att klara dessa doktorandstudier.

Till de tre hundarna i mitt liv **Faxe, Nelly** och **Molly** tack för all kärlek ni gav/ger mig och för att ni alltid fått mig att längta hem till gården. Till resten av familjen **Axel, Farmor, Farfar, Mormor, Morfar, Faster Ina, Thomas, Uffe, Julia** och **Alex** tack för all kärlek och stöd ni givit mig genom åren. Som en kul (!) hobby när du blev pensionär började du doktorera på konservering av skeppet Vasa, tack gammelmyster **Gitta** för att du är en sådan inspiration.

Till killen jag träffade på tåget hem från den där resan i Norrland för drygt 2.5 år sedan, som snabbt blev den viktigaste personen i mitt liv. Tack **Fredrik**, för att du är så omtänksam och för att du får mig får mig att känna mig trygg och lycklig. Speciellt tack för att du har tagit hand om mig under månaderna jag skrivit denna avhandling, vet inte vad jag gjort utan dig (troligen haft ett betydligt grusigare golv och levt på endast pyttipanna).



Hierarchical propagation of structural features in protein nanomaterials†

Cite this: *Nanoscale*, 2022, **14**, 2502

Ayaka Kamada,^{‡a} Anja Herneke,^c Patricia Lopez-Sanchez,^{§c} Constantin Harder,^{d,e} Eirini Ornithopoulou,^a Qiong Wu,^{Ⓛf} Xinfeng Wei,^f Matthias Schwartzkopf,^{Ⓛd} Peter Müller-Buschbaum,^{Ⓛb,b,e} Stephan V. Roth,^{d,f} Mikael S. Hedenqvist,^f Maud Langton^{Ⓛc} and Christofer Lendel^{Ⓛb,*a}

Natural high-performance materials have inspired the exploration of novel materials from protein building blocks. The ability of proteins to self-organize into amyloid-like nanofibrils has opened an avenue to new materials by hierarchical assembly processes. As the mechanisms by which proteins form nanofibrils are becoming clear, the challenge now is to understand how the nanofibrils can be designed to form larger structures with defined order. We here report the spontaneous and reproducible formation of ordered microstructure in solution cast films from whey protein nanofibrils. The structural features are directly connected to the nanostructure of the protein fibrils, which is itself determined by the molecular structure of the building blocks. Hence, a hierarchical assembly process ranging over more than six orders of magnitude in size is described. The fibril length distribution is found to be the main determinant of the microstructure and the assembly process originates in restricted capillary flow induced by the solvent evaporation. We demonstrate that the structural features can be switched on and off by controlling the length distribution or the evaporation rate without losing the functional properties of the protein nanofibrils.

Received 24th August 2021
Accepted 17th January 2022

DOI: 10.1039/d1nr05571b

rsc.li/nanoscale

Introduction

Nature's own high-performance materials, such as silks and muscles, provide inspiration for the development of new materials with proteins as building blocks. Such materials could play important roles in a range of applications, from sustainable bioplastics and novel foodstuff to sophisticated biomaterials for *e.g.* regenerative medicine. The key to utilize the full potential of the proteins lies in improved knowledge of the

hierarchical assembly of the materials, from the molecular level to the macroscopic level.¹ With this in mind, it is notable that proteins show a generic ability of self-assembly into protein nanofibrils (PNF), also referred to as amyloid-like fibrils.^{2,3} These species display a highly ordered filamentous structure up to length scales of a few micrometers. The understanding about how protein molecules are transformed into PNFs has increased immensely during the last decades, mainly thanks to the central role of amyloid structures in many devastating diseases.^{4,5} Today we have a reasonably good knowledge about how the PNFs are formed from the molecular building blocks, but the ways by which the nanoscale components can be arranged into macroscopic structures remains to a large extent unexplored.⁶

Amyloid-like PNFs are characterized by a highly ordered molecular structure, observable through the cross- β pattern in X-ray fiber diffraction studies,⁷ but the PNFs also possess the ability to organize into anisotropic structures at higher length scales. Several studies describe the formation of lyotropic nematic phases in solution.^{8–11} Knowles *et al.*¹² demonstrated that films made from PNFs could display nematic order in the presence of plasticizer, in their case polyethylene glycol (PEG). Since then, several studies have explored preparation protocols for PNF-based films^{13,14–17} as well as various composite films with PNFs as one constituent.^{18–23} However, these studies do

^aDepartment of Chemistry, KTH Royal Institute of Technology, Teknikringen 30, SE-100 44, Stockholm, Sweden. E-mail: lendel@kth.se

^bHeinz Maier-Leibniz Zentrum (MLZ), Technische Universität München, Lichtenbergstraße. 1, D-85748 Garching, Germany

^cDepartment of Molecular Sciences, SLU, Swedish University of Agricultural Sciences, BioCentrum, Almas allé 5, SE-756 61, Uppsala, Sweden

^dDeutsches Elektronen-Synchrotron, Notkestr. 85, D-22607 Hamburg, Germany

^eLehrstuhl für Funktionelle Materialien, Physik-Department, Technische Universität München, James-Frank-Str. 1, D-85748 Garching, Germany

^fDepartment of Fibre and Polymer Technology, KTH Royal Institute of Technology, Teknikringen 56-58, SE-100 44, Stockholm, Sweden

†Electronic supplementary information (ESI) available. See DOI: 10.1039/d1nr05571b

‡Present address: Department of Chemistry, University of Cambridge, Lensfield Road, Cambridge CB2 1EW, UK.

§Present address: Department of Biology and Biological Engineering, Chalmers University of Technology, SE-412 96, Gothenburg, Sweden.

not address how alterations in fibril nanostructure propagate to larger length scales. Aligned structures in the form of filaments can also be created through flow-assisted assembly processes.^{24,25} Another important route to achieve macroscale structures is gel formation. For semi-flexible PNFs with high aspect ratio the critical percolation concentration for sol-gel transition is in the order of 1–2% (w/w).¹¹ Liquid crystalline structures in solution phase typically occur at lower concentrations than that.^{9,11}

A frequently studied PNF system is β -lactoglobulin from bovine whey, either in its pure form or with whey protein isolate (WPI) as starting material.²⁶ This protein can form PNFs under various conditions, including the use of additives such as alcohols²⁷ or urea²⁸ or at low pH.^{27,29,30} It has been shown that fibrillation at low pH follows upon hydrolysis of β -lactoglobulin into peptide fragments that constitute the building blocks of the PNFs.^{31,32} Furthermore, β -lactoglobulin can form PNFs of distinct morphologies depending on the initial protein concentration.^{24,32,33} These classes of fibrils differ in chemical as well as nanomechanical properties and they seem to be constructed from different compositions of molecular building blocks.³² We have shown that the different classes of fibrils also display distinct behaviors in flow-assisted assembly of protein microfibrils with different degree of alignment and substantial differences in mechanical properties of the final fibers.²⁴ The present study reports the discovery of distinct microscale features of solution cast films that appear as a consequence of variation in the nanoscale structures of the β -lactoglobulin PNFs. The process by which the microstructure is formed could reveal new clues about hierarchical material design as they connect the molecular building blocks (below 1 nm) with the microscale features (visible by the human eye).

Careful characterization of the PNF films using microscopy and synchrotron X-ray scattering reveal that the ordered structures do not originate from nematic order but rather appear as a consequence of the sol-gel transition and the length distribution of the fibrils. This opens for processing protocols in which the structural and functional properties of the PNFs can be adjusted independently.

Results and discussion

The PNFs used for film preparation were produced from WPI at pH 2 and 90 °C as described previously.^{24,32} Different fibril morphologies were obtained by varying the initial protein concentration; all other parameters were the same. Concentrations above 60 mg ml⁻¹ resulted in *curved* PNFs (Fig. 1h). These fibrils are short (typically below 500 nm), have a worm-like appearance and a short persistence length (*ca.* 40 nm).²⁴ Fibril assembly from an initial concentration below 40 mg ml⁻¹ resulted in *straight* fibrils that can measure several micrometers in length and have 50 times higher persistence length (*ca.* 1.9 μ m) (Fig. 1g).²⁴ Both classes of fibrils are amyloid-like, as the dimensions agree with the typical numbers for amyloid fibrils, they bind amyloidophilic dyes, such as thioflavin T and Congo red, and display β -sheet rich secondary structure and amyloid-associated intrinsic fluorescence.³²

Free-standing films were solution cast by letting the PNF dispersions dry on a Teflon surface. Reference films were also prepared from non-fibrillar WPI solution at the same pH. The dry films display the brittleness that is typical for protein films without plasticizer, including PNF-based films.¹² Inspections

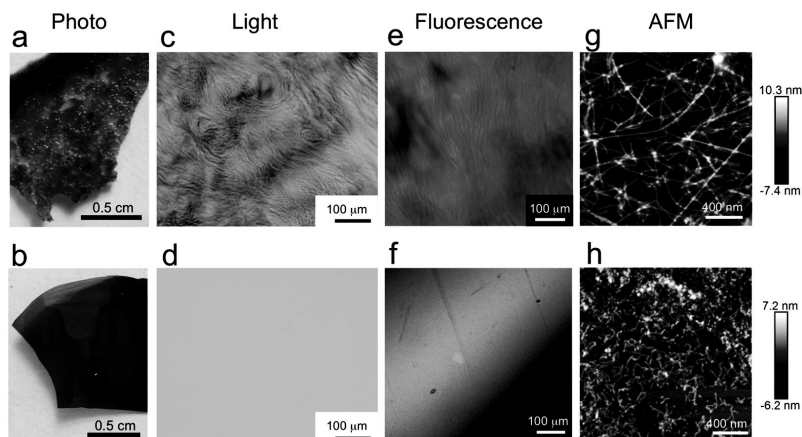


Fig. 1 Films prepared from PNFs with different morphologies result in distinct structural features. Photographs (a and b), light microscopy images (c and d) and confocal laser scanning microscopy images of ThT-stained films (e and f) reveal the presence of domains with apparent aligned structures in films made from *straight* PNFs (top row: a, c, e) while these features are absent in films made from *curved* PNFs (bottom row: b, d, f). AFM images of *straight* (g) and *curved* (h) fibrils show the nanoscale morphology of the two classes of PNFs in diluted samples (1 : 1000).

Paper

of the different films by eye and with light microscopy revealed some intriguing differences; while the films made from non-fibrillar WPI or *curved* PNFs were smooth, transparent and apparently homogenous, the films made from *straight* PNFs displayed regions with rough structures interleaved with homogenous regions that are similar to the other films (Fig. 1, Fig. S1†). The rough parts contain apparently ordered domains with resemblance of liquid crystalline polymers.³⁴ Nematic structures were indeed observed previously in plasticized films by Knowles and co-workers.¹² Our films, however, are made from protein isolate solutions without any additives. The finding is highly reproducible and substrate independent as the same results have been observed for many films made from different batches of PNFs and on different support materials (Teflon, mica, glass, plastics, silicon). We have also observed a similar surface roughness in glycerol-plasticized films cast at pH 7.²³ Film preparations from 2- or 3 times diluted solutions of *curved* fibrils (to match the lower WPI concentration in the *straight* fibril samples) did not change the appearance of the films showing that the observed differences are not an effect of mass concentration. Moreover, purification of the PNFs by dialysis (100 kDa molecular weight cut-off) did not change the structural features. Hence, the structures are a result of the PNFs themselves and not caused in cooperation with non-fibrillar components. Confocal laser scanning microscopy shows evenly distributed thioflavin T (ThT) intensity for both *curved* and *straight* PNFs (Fig. 1e and f), without any indications of spots with extremely high or low local PNF concentration.

The ordered parts appear to consist of aligned structures organized in linear parallel patterns on the micrometer scale (Fig. 1c). These features can also be observed by scanning electron microscopy (SEM) and atomic force microscopy (AFM) (Fig. 2, S2 and S3†). Both these methods show that the dry films are compact without larger cavities. The width of the aligned entities is between 50 and 100 nm, hence they are too wide to be individual PNFs. Some of the SEM images reveal fiber-like structures pointing out from the film (Fig. S2†). However, it is not clear if these ‘fibers’ are the same as the aligned species as they appear to be wider (>200 nm). To examine if the ordered domains have any orientational order, as expected if they originate from a liquid crystalline phase, we employed polarized optical microscopy but no birefringence could be observed for any of the investigated films (data not shown but similar results are shown in Fig. S4 and S5†).

To further characterize the structure of the ordered domains we performed micro-focused synchrotron X-ray diffraction experiments. The employed beam size was $20\ \mu\text{m} \times 10\ \mu\text{m}$, which allows focused measurements within the regions with anisotropic appearance. Wide angle X-rays scattering (WAXS) data of both *straight* and *curved* fibrils clearly display the amyloid associated distances of 4.6 Å and 9.1–9.2 Å (Fig. 3a and b).⁷ In addition, there are peaks at 3.7–3.8 Å corresponding to repetitive $C\alpha$ distances in β -sheets.^{35,36} However, neither the WAXS nor the small angle X-ray scattering (SAXS) experiments produced diffraction patterns with anisotropic features (Fig. 3). Hence, the scattering experiments

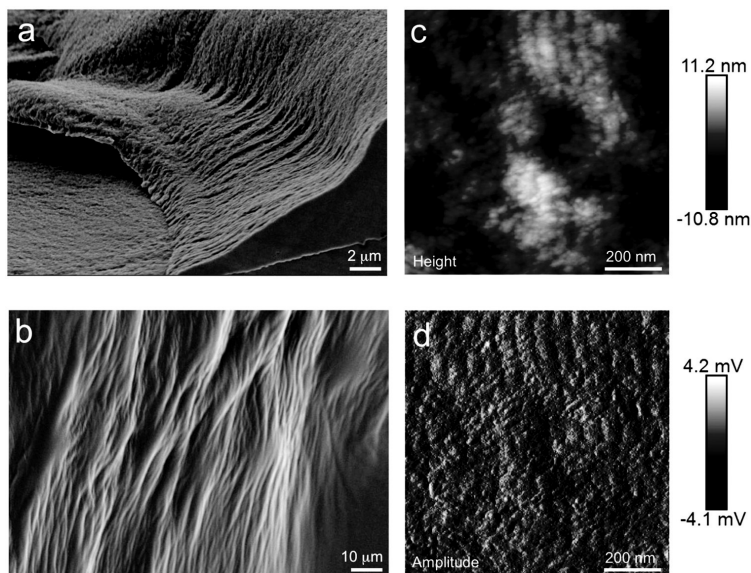


Fig. 2 SEM (a and b) and AFM (c and d) images of the structured domains in films from *straight* PNFs. (a) Fracture surface. (b) Top view of the film surface. (c and d) Height and amplitude AFM images of the same surface area, respectively.

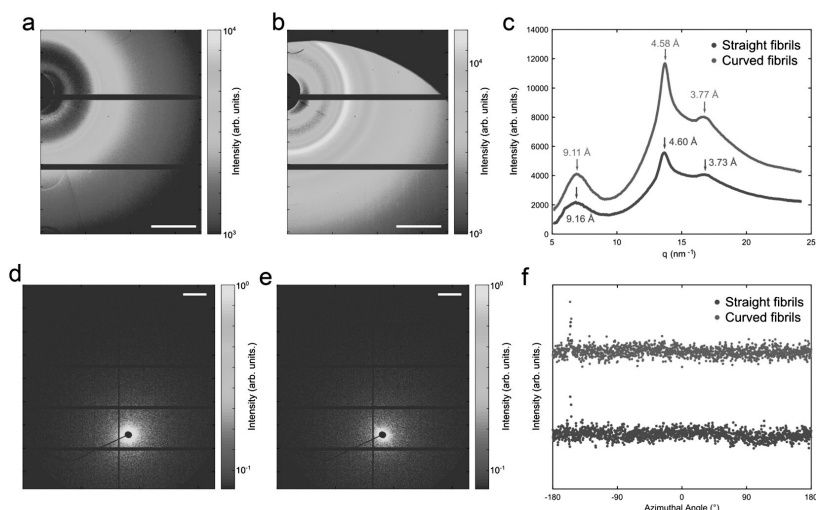


Fig. 3 Synchrotron microfocus X-ray scattering investigation of the PNF films. (a and b) WAXS scattering data for films from *straight* (a) and *curved* (b) PNFs. The scale bars are 10 nm^{-1} . (c) Radial integration of the WAXS data with the corresponding real space distances indicated. (d and e) SAXS scattering data for films from *straight* (d) and *curved* (e) PNFs. The scale bars are 0.2 nm^{-1} . (f) Azimuthal integration of the SAXS data shows isotropic arrangements (in the plane of the film) of the PNFs in both type of films.

confirm the results of the polarized microscopy that there is no overall directional order of the PNFs (in the horizontal plane of the film) for any of the films.

To summarize, the results presented so far show that *straight* PNFs form distinct macroscopic features in solution cast films compared to *curved* fibrils and non-fibrillar protein. Since the starting material and protein constituents are the same in all these films, the structural features must originate from the nanoscale structures. We also found that the structures do not originate from nematic order adopted during drying.

With a closer examination of the PNF dispersions we observed the presence of small (on the order of $100 \mu\text{m}$ in size) gel domains in the straight PNF samples even though they appeared homogenous from a macroscopic view (Fig. 4, Fig. S4 and S6a†). These domains cover at least 30% of the image area in Fig. S6a.† The occurrence of such domains in the dispersion of the curved fibrils was much less frequent accounting for less than 3% of the image area (Fig. S5 and S6b†). Following the drying process of a $100 \mu\text{l}$ droplet on a glass surface using light microscopy revealed that the ordered structures appear to form around these gel domains. However, it is not the gel domains themselves that are transformed into the aligned structures; those features instead appear between the domains (Fig. 4, S4, ESI Video S1†). Essentially no birefringence is observed during the drying process, except for some of the gel domains in the starting dispersion (Fig. S4†).

We note that stripe-like patterns with some resemblance of the ordered structures in the PNF films have previously been

observed in spray-deposited polymer colloids due to flow and rapid solvent evaporation in confined geometries.³⁷ Although the time scale for solvent evaporation in the present study is much longer (hours) it appears from the microscopy experiments that the formation of the ordered structures is associated with the drying process (Fig. 4, S4, ESI Video S1†). Drying of a colloidal solution will induce capillary flow in the bulk.³⁸ This is the origin of the “coffee ring effect” and some accumulation of material in the outer rim can indeed be observed in the films (see Fig. 1, 5 and S8†). However, far from all PNF material is transported to the rim during the drying time. *Straight* PNFs, with persistence lengths of *ca.* $2 \mu\text{m}$,²⁴ behave as rods on micrometer length scale with rotational diffusion times on the order of minutes.³⁹ As the solvent evaporation proceed, the motions will be slowed down by the inter-fibrillar contacts and the formation of a gel network. A directional capillary flow will speed up the accumulation of PNFs in certain areas, in particular if the available diffusion volume is already reduced close to the pre-formed gel domains. Based on this line of argument, we hypothesized that the appearance of the ordered structures is related to a sol-gel transition that is distorted by capillary flow in a confined space.

The sol-gel transition of the two classes of PNFs depends on their chemical and physical properties. In previous work, we have found that they do display some differences in the chemical properties and probably consist of slightly different peptide segments.³² To explore if the structural difference of the films could be related to the surface electrostatics of the PNFs their zeta-potential as function of pH was investigated.

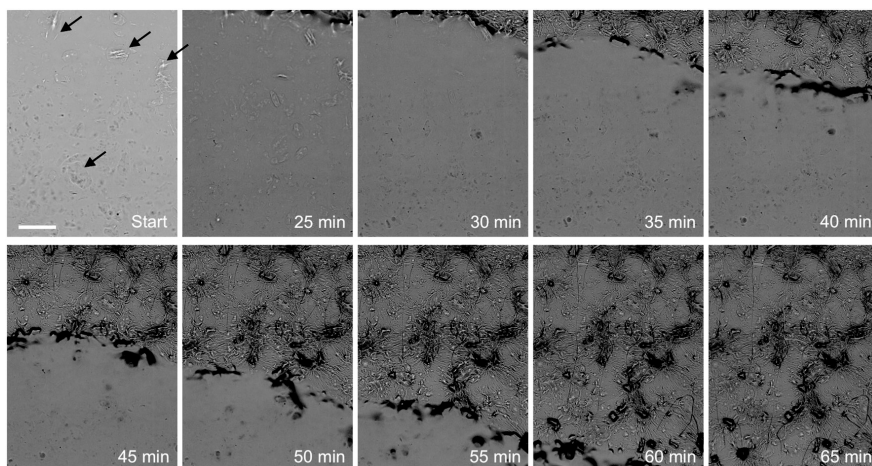


Fig. 4 Film formation (solvent evaporation) followed by light microscopy. 100 μl dispersion of *straight* PNFs were left to dry on a glass surface. Small gel domains (some indicated by the arrows) can be observed already in the start image. The start image with adjusted contrast can be found in Fig. S6A.† Scale bar is 500 μm .

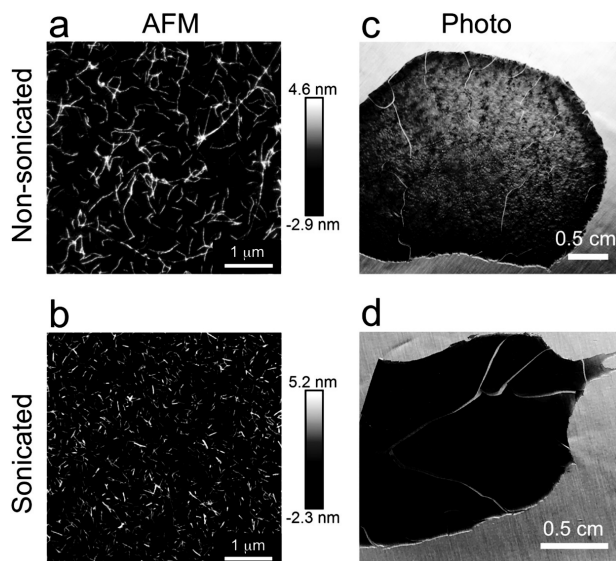


Fig. 5 Comparison of films made from *straight* PNFs without (top row) and with (bottom row) sonication. (a and b) AFM images of diluted PNF solutions. (c and d) Photographs of the dry films.

The results show that the zeta-potentials, as well as the isoelectric points, are similar for the two classes of PNFs and are not likely the reason for the observed structural differences (Fig. S7†). Moreover, preparation of films from solutions with

different pH values in the range pH 1 to pH 3 shows the same structural features (Fig. S8†).

Focusing on the physical properties, the *straight* fibrils are characterized by different length distribution and different

stiffness (persistence length, which also incorporates the thickness) compared to the *curved* fibrils. To determine which of these properties (or both) that define the macro-scale structure, we sonicated the straight fibrils (Fig. 5). This resulted in substantially shorter fibrils (but with retained internal structure and stiffness). Typical lengths before sonication was 500–700 nm with some fibrils extending to a few micrometers. After sonication, the majority of the fibrils were shorter than 200 nm. To verify that the amyloid-like structure was retained we compared the ThT fluorescence of sonicated and non-sonicated PNFs. The results show that the fluorescence intensity is in fact higher in the sonicated sample (Fig. S9†). The explanation for this may be that more surface area becomes exposed if aggregated fibrils are also to some degree separated during sonication. We then cast films from non-sonicated and sonicated *straight* PNFs. Interestingly; we found that films made from sonicated fibrils lack the described macroscopic features. Hence, we conclude that the fibril lengths are the source for the observed structures.

Finally, we explored if the appearance of the ordered structures could be omitted by applying a fast evaporation protocol for film formation that would not give the PNFs enough time to accumulate due of capillary flow. Spray deposition allows the application of a very thin layer onto the substrate. We here used a spray device⁴⁰ and deposited either straight PNFs or sonicated straight PNFs onto a silicon substrate heated to

55 °C. Deposition was done in 5 or 20 cycles and the films were thereafter investigated by light microscopy.

The microscope images in Fig. 6 and S10† show that the short (sonicated) PNFs form smoother film surfaces than the long (non-sonicated) PNFs. The color variations in the images appear when the thickness of the films corresponds to multiples of half the photon wavelength. Hence, the blue color corresponds to a thickness of *ca.* $n \times 200$ nm, and the magenta color is corresponding to a thickness of *ca.* $n \times 350$ nm, where *n* is an integer. Already at 5 pulses, larger patches of homogenous thickness (same color) are visible in the film made from short PNFs (Fig. 6b) compared to the long PNFs (Fig. 6a). Fig. S10c† shows the presence of droplets with strong coffee-ring effects confirming that drying occurs at a local scale. At 20 pulses, the color gradients in the film for short PNFs are reduced compared to long PNFs film (Fig. 6a and b) indicating a smoother surface for the sonicated material. However, none of the samples display the ordered microstructures seen in the solution cast films of long *straight* PNFs. Hence, a fast evaporation protocol allows manufacturing of thin films without these structural features, even from long *straight* PNFs.

To conclude, we demonstrated that the macroscale structure of all-protein films is defined by the nanoscale features of the building blocks. Surprisingly, polarized light microscopy and X-ray diffraction show no signs of orientational anisotropy in the apparently ordered domains of the films. Hence, the

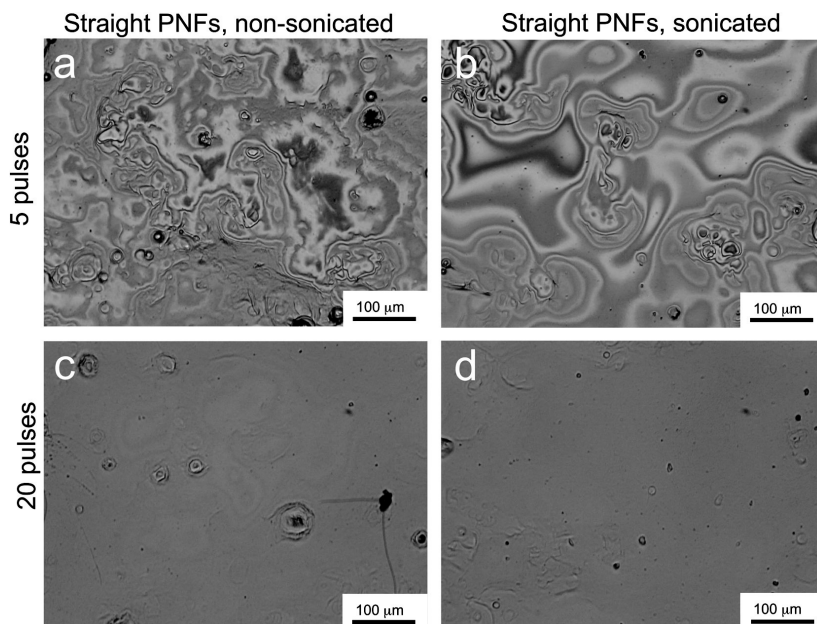


Fig. 6 Light microscopy images of the surface of spray deposited PNF films on silicon. (a and c) *Straight* long PNFs. (b and d) *Straight* short (sonicated) PNFs. (a and b) 5 spray pulses. (c and d) 20 spray pulses.

structural features do not originate from liquid crystalline phases. Rather, the results are in agreement with a mechanism where structural inhomogeneities are created from a local sol-gel transition facilitated by capillary flow during drying in a confined space. Applying a fast-drying protocol suppresses the structural features. The appearance of the macroscale features is directly related to the length distribution of the PNFs and can be switched off by fibril fragmentation. Notably, the amyloid-associated changes in photophysical properties of ThT are retained, or even enhanced, in the fragmented fibrils (Fig. S8†). Hence, controlling the length distribution of the fibrils can be used to define the macroscopic structure of the films without losing the functional properties associated with the surface structure of the PNFs.

Experimental section

Preparation of PNF films

Whey protein isolate (WPI, Lactoprodan Di-9224) was kindly provided by Arla Food Ingredients. Solutions for fibrillation reactions were prepared by dissolving WPI in 0.1 M hydrochloric acid (HCl) to a final concentration of *ca.* 100 mg ml⁻¹ and then dialyze against 0.01 M HCl (pH 2) using a membrane with 6–8 kDa molecular weight cut-off (Spectrum laboratories). The protein concentrations were then adjusted by addition of dialysis solution. Straight PNFs were obtained from an initial WPI concentration of 40 mg ml⁻¹ while curved PNFs were obtained with a starting concentration of 70–80 mg ml⁻¹. Fibrils formed during incubation at 90 °C for a period of 3 days. The yield is typically 20–30% (*i.e.* percentage of the total protein mass incorporated in the PNFs). Purified PNFs were obtained by dialysis for 3 days using a membrane with 100 kDa cut-off (Spectrum laboratories). Films were solution cast by pouring the PNF dispersions onto a poly(tetrafluoroethylene) surface (BYTAC Type AF-21, Saint-Gobain Performance Plastics). Other substrates, including glass, mica, plastics and silicon, were also explored. The films were left to dry in air at room temperature.

Fragmentation of PNFs by sonication

Solutions of straight PNFs were fragmented using a Qsonica Q500 sonicator equipped with a 6 mm micro tip. The amplitude was 20–25% and sonication was done in pulses (2 s on, 10 s off) for a total effective time of 1 or 2 min. During the process the sample was emerged in a water bath.

Film formation by spray deposition

Spray deposition was performed by a spray device (Compact JAU D55000, Spray Systems) onto a piranha-acid cleaned silicon substrate. The PNF suspension (8 mg ml⁻¹) was supplied by a siphon attached to a spray device using the setup described in ref. 40. Spray deposition was carried out by atomization of the PNF suspensions with compressed nitrogen at a gas pressure of 1 bar. The distance between the spray device and the substrate was 200 mm, which means spraying in the

very dilute regime. The silicon substrate temperature was controlled to 55 ± 3 °C and the spray protocol consisted of a 0.2 s spraying step followed by 10 s waiting time, repeated for 5 or 20 cycles. This corresponds to deposited average film thickness of *d* ≈ 0.3 μm and *d* ≈ 2 μm, for the 5 and 20 spray cycles respectively.

Light microscopy

Microscopy investigations were conducted both on pre-formed films dried on a poly(tetrafluoroethylene) surfaces, spray deposited on heated silicon substrate and *in situ* on samples drying on glass surfaces. From the pre-formed films, a piece of approximately 1 cm × 1 cm was cut and placed onto a glass slide and covered with a glass cover slide. For the *in situ* experiments, 100 μl droplets from dispersions with *straight* or *curved* PNFs were examined while drying into films under ambient conditions. A Nikon Eclipse Ni-U light microscope, with a 10× (0.3 NA) objective was used. Images (polarized and non-polarized) were captured every 5 min with a Nikon Digital Sight DS-Fi2 camera with resolution of 2569 × 1920 pixels. The images were processed with the software NIS-Elements BR (Nikon Instruments Inc.). Microscope images of the sprayed samples were obtained with a Keyence VH Z250R at 500× magnification from the sample center.

Confocal laser scanning microscopy

Films for confocal laser scanning microscopy were prepared by adding 1 mM ThT solution to the PNF samples before drying them into films. The same amount of ThT in relation to total protein content was used in all samples. Fluorescence microscopy was performed using a Zeiss, LSM 780 confocal microscope with ×10 or ×63 objectives. An argon laser was used for excitation at 405 nm and emission was monitored at 450–600 nm.

Scanning electron microscopy (SEM)

Small pieces of the films (*ca.* 1 cm × 1 cm) were sputtered with a platinum/palladium (60/40) alloy using a Cressington 208RH high-resolution sputter and then investigated in a Hitachi S-4800 field-emission SEM.

Atomic force microscopy (AFM)

AFM was carried out using a Dimension FastScan AFM instrument (Bruker). PNF morphology was investigated in tapping mode using samples that were diluted between 1:500 and 1:10 000 in 10 mM HCl. 25 μl were applied on a freshly cleaved mica surface and dried in air. Film surfaces were examined on non-diluted samples dried on a mica surface. FastScan A cantilevers (Bruker) were used for the experiments and the images were investigated in Nanoscope 1.5 software (Bruker).

Synchrotron X-ray scattering

Wide-angle X-ray scattering (WAXS) and small-angle X-ray scattering (SAXS) were performed at microfocus P03 beamline at PETRA III⁴¹ at DESY, Hamburg, Germany. WAXS intensity was recorded using a Pilatus 300k detector (Dectris, pixel size 172

× 172 mm) with the sample-to-detector distance, SDD = 154 mm. SAXS diffractogram was obtained using Pilatus 1 M detector (Dectris, pixel size 172 × 172 mm) with SDD = 6765 mm. X-ray wavelength of $\lambda = 0.95377 \text{ \AA}$ was used for both measurements. In order to analyse the structural orientation, the scattering intensity in the range of $q = 0.0335\text{--}0.4522 \text{ nm}^{-1}$ was radically integrated as a function of the azimuthal angle. The data was analysed with DPAK software.⁴²

Dynamic light scattering and zeta potential

Measurements were carried out using a Zetasizer Nano ZS dynamic light scattering instrument (Malvern Instruments). Each sample was measured five times maintaining an attenuation between 7 and 10, and the temperature at 25 °C. The samples were diluted thirty times (30×) before measurements, after first validating that dilution between 10–100× did not significantly affect the value of the zeta potential.

ThT fluorescence

Samples for thioflavin T (ThT) fluorescence measurements were prepared by mixing 0.1 ml PNF solution with 2.4 ml 50 μM ThT solution in PBS buffer. Fluorescence was measured at a Cary Eclipse Spectrofluorometer (Varian) with excitation at 440 nm and emission spectra recorded between 460 and 600 nm.

Author contributions

Ayaka Kamada, Anja Herneke, Patricia Lopez-Sanchez, Constantin Harder, Eirini Ornithopoulou, Qiong Wu, Xinfeng Wei: investigation, writing – review & editing. Matthias Schwartzkopf: investigation, methodology, writing – review & editing. Peter Müller-Buschbaum: supervision. Stephan V. Roth: conceptualization, methodology, writing – review & editing. Mikael S. Hedenqvist: conceptualization, methodology, writing – review & editing. Maud Langton: conceptualization, supervision, writing – review & editing. Christofer Lendel: conceptualization, formal analysis, funding acquisition, investigation, methodology, project administration, supervision, writing – original draft.

Conflicts of interest

There are no conflicts to declare.

Acknowledgements

This work was financially supported by Formas (grant numbers 213-2014-1389 and 2017-00396), Magnus Bergwalls stiftelse (grant number 2015-00858). Parts of this research were carried out at the light source PETRA III at DESY, a member of the Helmholtz Association (HGF).

References

- 1 T. P. J. Knowles and M. J. Buehler, *Nat. Nanotechnol.*, 2011, **6**, 469–479.
- 2 T. P. Knowles and R. Mezzenga, *Adv. Mater.*, 2016, **28**, 6546–6561.
- 3 X. Ye, C. Lendel, M. Langton, R. T. Olsson and M. S. Hedenqvist, in *Industrial Applications of Nanomaterials*, ed. S. Thomas, Y. Grohens and Y. B. Pottathara, Elsevier, 2019, ch. 2, pp. 29–63.
- 4 P. C. Ke, R. H. Zhou, L. C. Serpell, R. Riek, T. P. J. Knowles, H. A. Lashuel, E. Gazit, I. W. Hamley, T. P. Davis, M. Fändrich, D. E. Otzen, M. R. Chapman, C. M. Dobson, D. S. Eisenberg and R. Mezzenga, *Chem. Soc. Rev.*, 2020, **49**, 5473–5509.
- 5 F. Chiti and C. M. Dobson, *Annu. Rev. Biochem.*, 2017, **86**, 27–68.
- 6 C. Lendel and N. Solin, *RSC Adv.*, 2021, **11**, 39188–39215.
- 7 K. L. Morris and L. C. Serpell, *Methods Mol. Biol.*, 2012, **849**, 121–135.
- 8 A. M. Corrigan, C. Muller and M. R. H. Krebs, *J. Am. Chem. Soc.*, 2006, **128**, 14740–14741.
- 9 J. M. Jung and R. Mezzenga, *Langmuir*, 2010, **26**, 504–514.
- 10 C. Müller and O. Inganäs, *J. Mater. Sci.*, 2011, **46**, 3687–3692.
- 11 L. M. C. Sagis, C. Veerman and E. van der Linden, *Langmuir*, 2004, **20**, 924–927.
- 12 T. P. J. Knowles, T. W. Oppenheim, A. K. Buell, D. Y. Chirgadze and M. E. Welland, *Nat. Nanotechnol.*, 2010, **5**, 204–207.
- 13 L. Wang, F. G. Bäcklund, Y. Yuan, S. Nagamani, P. Hanczyk, L. Sznitko and N. Solin, *ACS Sustainable Chem. Eng.*, 2021, **9**, 9289–9299.
- 14 A. Kamada, M. Rodriguez-Garcia, F. S. Ruggeri, Y. Shen, A. Levin and T. P. J. Knowles, *Nat. Commun.*, 2021, **12**, 3529.
- 15 N. M. D. Courchesne, A. Duraj-Thatte, P. K. R. Tay, P. Q. Nguyen and N. S. Joshi, *ACS Biomater. Sci. Eng.*, 2017, **3**, 733–741.
- 16 F. G. Bäcklund, J. Pallbo and N. Solin, *Biopolymers*, 2016, **105**, 249–259.
- 17 Y. Yuan and N. Solin, *ACS Appl. Polym. Mater.*, 2021, **3**, 4825–4836.
- 18 K. J. De France, N. Kummer, Q. Ren, S. Campioni and G. Nyström, *Biomacromolecules*, 2020, **21**, 5139–5147.
- 19 C. L. Li, J. Adamcik and R. Mezzenga, *Nat. Nanotechnol.*, 2012, **7**, 421–427.
- 20 L. Wang, B. Xin, A. Elsukova, P. Eklund and N. Solin, *ACS Sustainable Chem. Eng.*, 2020, **8**, 17368–17378.
- 21 J. Zhao, B. Miao and P. Yang, *ACS Appl. Mater. Interfaces*, 2020, **12**, 35435–35444.
- 22 S. J. Ling, C. X. Li, J. Adamcik, Z. Z. Shao, X. Chen and R. Mezzenga, *Adv. Mater.*, 2014, **26**, 4569–4574.
- 23 X. Ye, K. Junel, M. Gällstedt, M. Langton, X. Wei, C. Lendel and M. S. Hedenqvist, *ACS Sustainable Chem. Eng.*, 2018, **6**, 5462–5469.

- 24 A. Kamada, N. Mittal, L. D. Söderberg, T. Ingverud, W. Ohm, S. V. Roth, F. Lundell and C. Lendel, *Proc. Natl. Acad. Sci. U. S. A.*, 2017, **114**, 1232–1237.
- 25 A. Kamada, A. Levin, Z. Toprakcioglu, Y. Shen, V. Lutz-Bueno, K. N. Baumann, P. Mohammadi, M. B. Linder, R. Mezzenga and T. P. J. Knowles, *Small*, 2019, **16**, 1904190.
- 26 S. M. Loveday, S. G. Anema and H. Singh, *Int. Dairy J.*, 2017, **67**, 35–45.
- 27 W. S. Gosal, A. H. Clark and S. B. Ross-Murphy, *Biomacromolecules*, 2004, **5**, 2408–2419.
- 28 D. Hamada and C. M. Dobson, *Protein Sci.*, 2002, **11**, 2417–2426.
- 29 G. M. Kavanagh, A. H. Clark and S. B. Ross-Murphy, *Int. J. Biol. Macromol.*, 2000, **28**, 41–50.
- 30 C. Veerman, H. Ruis, L. M. C. Sagis and E. van der Linden, *Biomacromolecules*, 2002, **3**, 869–873.
- 31 C. Akkermans, P. Venema, A. J. van der Goot, H. Gruppen, E. J. Bakx, R. M. Boom and E. van der Linden, *Biomacromolecules*, 2008, **9**, 1474–1479.
- 32 X. Ye, M. S. Hedenqvist, M. Langton and C. Lendel, *RSC Adv.*, 2018, **13**, 6915–6924.
- 33 C. C. vandenAkker, M. F. Engel, K. P. Velikov, M. Bonn and G. H. Koenderink, *J. Am. Chem. Soc.*, 2011, **133**, 18030–18033.
- 34 U. W. Gedde and M. S. Hedenqvist, *Fundamental polymer science*, Springer, 2nd edn, 2019.
- 35 M. Sunde, L. C. Serpell, M. Bartlam, P. E. Fraser, M. B. Pepys and C. C. Blake, *J. Mol. Biol.*, 1997, **273**, 729–739.
- 36 L. C. Serpell, *Biochim. Biophys. Acta*, 2000, **1502**, 16–30.
- 37 A. Buffet, M. M. Abul Kashem, J. Perlich, G. Herzog, M. Schwartzkopf, R. Gehrke and S. V. Roth, *Adv. Eng. Mater.*, 2010, **12**, 1235–1239.
- 38 R. D. Deegan, O. Bakajin, T. F. Dupont, G. Huber, S. R. Nagel and T. A. Witten, *Nature*, 1997, **389**, 827–829.
- 39 S. S. Rogers, P. Venema, L. M. C. Sagis, E. van der Linden and A. M. Donald, *Macromolecules*, 2005, **38**, 2948–2958.
- 40 C. J. Brett, N. Mittal, W. Ohm, M. Gensch, L. P. Kreuzer, V. Korstgens, M. Månsson, H. Frielinghaus, P. Müller-Buschbaum, L. D. Söderberg and S. V. Roth, *Macromolecules*, 2019, **52**, 4721–4728.
- 41 A. Buffet, A. Rothkirch, R. Döhrmann, V. Körstgens, M. M. A. Kashem, J. Perlich, G. Herzog, M. Schwartzkopf, R. Gehrke, P. Müller-Buschbaum and S. V. Roth, *J. Synchrotron Radiat.*, 2012, **19**, 647–653.
- 42 G. Benecke, W. Wagermaier, C. H. Li, M. Schwartzkopf, G. Flucke, R. Hoerth, I. Zizak, M. Burghammer, E. Metwalli, P. Müller-Buschbaum, M. Trebbin, S. Forster, O. Paris, S. V. Roth and P. Fratzl, *J. Appl. Crystallogr.*, 2014, **47**, 1797–1803.

Protein Nanofibrils for Sustainable Food—Characterization and Comparison of Fibrils from a Broad Range of Plant Protein Isolates

Anja Herneke,* Christofer Lendel, Daniel Johansson, William Newson, Mikael Hedenqvist, Saied Karkehabadi, David Jonsson, and Maud Langton



Cite This: *ACS Food Sci. Technol.* 2021, 1, 854–864



Read Online

ACCESS |



Metrics & More



Article Recommendations



Supporting Information

ABSTRACT: Protein nanofibrils (PNFs) from plant-based protein sources have great potential for use in new sustainable food applications or biobased materials. Plant-based proteins from seven different sources (fava bean, mung bean, lupin, oat, rapeseed, soybean, and potato) were evaluated here for their ability for forming PNFs and compared with whey protein PNFs. Formation of PNFs was studied under incubation at acidic conditions (pH 2) and heat (85–90 °C) for 24–96 h. Presence of PNFs was detected using thioflavin T, circular dichroism spectroscopy, Fourier-transform infrared spectroscopy, and atomic force microscopy. The results showed that all plant-based proteins were able to form PNFs. For some of the plant protein isolates in this study, nanofibril formation is reported for the first time. We also describe and compare the distinct features associated with each protein source and the morphological alterations of the nanoscale structures. Finally, we describe how PNF production can be enhanced by purifying the fibril-forming protein component. Taken together, our study suggests that the structural and functional variation within plant protein nanofibrils can be exploited in future scaled-up food or material applications.

KEYWORDS: *fava bean, mung bean, lupin, oat, rapeseed, amyloid*

■ INTRODUCTION

With the growing global population, the need for developing more sustainable foods has been stressed.¹ Shifting from eating animal-based proteins to proteins from plant-based sources is one way of reducing the pressure on the environment from food production.² Meat consumption has a strong cultural element,³ and this cultural bond makes it difficult for many people to give up their old meal patterns centered around meat,³ despite increasing awareness of the effects of meat production on the environment. One way of encouraging consumers to choose a more sustainable protein source is to replace meat with a similar foodstuff in terms of texture and appearance, such as a meat analogue made from plant proteins.⁴ Designing such products has proven to be a challenging task for material science.

Using amyloid protein nanofibrils (PNFs) made from plant proteins to create new textured foodstuffs is an approach with good potential.⁵ PNFs are characterized by a high content of β -sheets, packed in a cross- β structure and linked together with a strong network of hydrogen bonds.⁶ The chemical properties of PNFs make them one of the most stable polypeptide structures.⁷ The good mechanical properties of PNFs have attracted the interest of researchers in material sciences,⁸ with demonstrated applications in, e.g., water purification and bioorganic electronics. Rheological studies indicate that PNFs can decrease gelation time and increase the firmness of a gel system.⁹

Naturally occurring PNFs were first discovered within the pathological patterns of several diseases such as Alzheimer's, Parkinson's, Creutzfeldt-Jakob's disease, and some categories of type 2 diabetes.¹⁰ However, naturally occurring nanofibrils

are not only linked to pathological diseases but are also found in a wide span of biologically functional systems from bacteria and yeasts to humans. They function as mechanical protection and adhesion in the form of biofilms, transfer epigenetic information between generations, and can be used as scaffolds for cell growth.¹¹ An ability to form PNFs with no connection to any natural function has been documented for a wide range of proteins.¹² Goldschmidt et al. reported that the ability to form PNFs is a generic feature for almost all proteins (<98.7%),¹³ which opens the door to endless possibilities for novel renewable materials (edible or nonedible). To date, no toxic effect of PNFs not naturally occurring in biological systems has been reported.¹⁴

The mechanical and rheological properties, together with the absence of documented toxic effects, make PNFs manufactured from plant proteins good candidates for use in production of new textured foodstuffs or plant-based biomaterials.¹² The majority of published data on plant-derived PNFs are on specific fractions of storage proteins from cereals and legumes.¹² There are a limited number of reports on plant-based PNFs generated from whole protein isolates, and to our knowledge, only soybean,^{15,16} pea,¹⁷ potato,¹⁸ cowpea, chickpea, lentils,¹⁹ and fava bean²⁰ have been studied. The study made on PNFs from fava bean was focusing on the

Received: January 22, 2021

Revised: April 24, 2021

Accepted: May 4, 2021

Published: May 14, 2021



interaction between PNFs and nanoparticles. There is still a great need to understand the characteristics of plant-based PNFs before adding them to more complex systems such as a food gel.

Some commonly used methods for detection and characterization of PNFs are thioflavin T (ThT) fluorescence, circular dichroism (CD) spectroscopy, Fourier-transform infrared spectroscopy (FTIR), and atomic force microscopy (AFM). ThT is a fluorescent dye with a high affinity to β -sheets and is one of the most frequently used methods for detection of the β -sheet-rich PNFs.²¹ CD and FTIR are used as complementary methods for detection of the secondary structure, while AFM is used for morphological characterization of PNFs.¹²

The aim of this study was to compare the ability of different classes of plant-based protein isolates to form PNFs and to evaluate the characteristics of these PNFs with relevant methods (ThT, CD, FTIR, and AFM). We successfully generated and characterized PNFs from extracted protein isolates from seven different plant sources, mung bean, lupin, rapeseed, and oat, for which data are reported for the first time, and fava bean, soybean, and potato. The features of the plant-based PNFs were compared with those of well-studied^{1,2} food-related PNFs made from whey protein.

MATERIALS AND METHODS

Fava bean (*Vicia faba* minor; cv. Gloria) cultivated in Sweden was kindly provided by RISE (Research Institutes of Sweden). Mung bean (*Vigna radiate*) cultivated in Myanmar was kindly provided by Lantmännen (Sweden). Lupin seeds (*Lupinus angustifolius*, cv. Boregine) were bought from Italy. Milled, defatted, and air-classified oat (*Avena sativa* cv. Mathilda) flour was kindly provided by Lantmännen (Sweden). Commercial oilseed rape (*Brassica napus*) was kindly provided by Gunnarshögs Gård (Sweden). Potato (*Solanum tuberosum*) protein isolate (85043, Batch 1502000052), was kindly provided by Lyckeby Starch AB (Sweden). Soybean (*Glycine max*) protein isolate (SUPRO 120 IP) was kindly provided by Solae Belgium N.V. Whey protein isolate (Lacprodan DI-9224) was obtained from Arla Food Ingredients (Denmark). Hydrochloric acid (HCl, VWR, France), sodium chloride (NaCl, VWR, Belgium), thioflavin T (Sigma, India), heptane (Merck), and guanidinium chloride (GuCl, Merck, Germany) were purchased from commercial sources.

Protein Extraction and Isolation. A dehulling machine (Lu Cao Hi-Tech Machinery Manufacturing Co. Ltd., China) was used to remove the hulls of fava bean and lupin seed. Mung beans, dehulled lupin seeds, and fava beans were milled in an Ultra-Centrifugal Mill (ZM-1, Retsch GmbH, Germany) with a 500 μ m mesh. The protein extractions for the mung bean protein isolate (MPI), fava bean protein isolate (FPI), and lupin seed protein isolate (LPI) were obtained according to the following procedure: The flour was dispersed in deionized water at a ratio of 1:10 (w/w) at 20 °C. The pH of the mixture was adjusted with 2 M NaOH to 9.0 for fava bean and 8.0 for mung bean and lupin. The mixture was then incubated with stirring at room temperature (20 \pm 2 °C) for 1 h, followed by centrifugation at 3700 g for 15 min for lupin, and 30 min for mung bean and fava bean. The difference in pH was based on earlier in-house optimization studies (not shown). After centrifugation, the supernatant was collected, and the pH was adjusted with 1 M HCl to pH 4.6 for mung bean and lupin and 4.0 for fava bean (the pH was chosen based on protein yield). The mixture was incubated with continuous stirring at room temperature for 2 h for lupin, 1 h for fava bean, and 40 min for mung bean and then centrifuged at 3700 g (20 °C, 15 min). The pellet was collected and dispersed in deionized water at a ratio of 1:10 (w/w) with pH adjustment to 4.6 (lupin and mung bean) and 4.0 (fava bean), followed by centrifugation at 3700 g for 15 min. All pellets were then freeze-dried for 24 h. Due to its high fat content, LPI was defatted using 95% EtOH at a ratio of 1:10 (LPI

to EtOH) with continuous stirring at 45 °C. The defatting process was repeated twice. The fat content of the extracted protein isolate was 3.58% for MPI, 4.44% for FPI, and 0.38% for the defatted LPI, measured by a Soxtec 8000 Extraction Unit (Foss Analytical A/S Hillerød, Denmark).

The extraction of oat protein isolate (OPI) was made according to the method previously described by Wu et al.,²² with the only modification that the oat flour used was air-classified. The defatted, air-classified oat flour was dispersed in deionized water at a flour to water ratio of 1:6 (w/v). The pH of the mixture was adjusted to 9.2 with 2 M NaOH, and the mixture was incubated at room temperature (20 \pm 2 °C) for 25 min with stirring, followed by filtration through cheesecloth. The filtered mixture was centrifuged at 3700 g for 15 min. After centrifugation, the supernatant was collected, and the pH was adjusted to pH 5.0 with 1 M HCl. The mixture was incubated with stirring at room temperature for 1 h and then centrifuged at 3700 g (20 °C, 15 min). The pellet was collected and dispersed in deionized water at a ratio of 1:6 (w/w) with pH adjusted to 5.0, followed by centrifugation at 3700 g for 15 min. All pellets were then freeze-dried for 24 h.

The production of rapeseed protein isolate (RPI) was carried out through mildly alkaline aqueous separation of protein, hulls, and free oil followed by isoelectric precipitation of the aqueous phase.²³ Residual oil in the precipitate was removed with heptane. Whole rapeseeds were milled in a Krups 75 coffee grinder (Krups GmbH, Germany) at 2 \times 10 s, with manual scraping of the bowl between pulses. Then, 100 g of ground meal were dispersed in 1.5 L of deionized water and hydrated overnight at 5 °C. The pH of the dispersion was adjusted to 8 with 1 M NaOH, and the dispersion was incubated for 1 h at room temperature. The dispersion was mixed for 1 min in a Bosch Clevermix food processor (Robert Bosch GmbH, Germany) in four batches and coarse-filtered through four layers of surgical gauze. The solids were re-extracted in 500 mL of deionized water at pH 8 by incubation for 30 min and mixed and filtered as in the previous step. The combined filtrate was placed in a separatory funnel, and the quickly sedimenting seed hull particles were immediately removed with separation proceeding overnight at 5 °C. After separation, the sediment and liquid phase was removed from the oleosome containing cream. The liquid phase was centrifuged at 10 000 g for 30 min, and the remaining cream was removed; the liquid phase was decanted from the remaining solids. A small amount of free oil remained in the liquid phase, which was removed in a separatory flask overnight at 5 °C. The resulting liquid was recentrifuged at 10 000 g for 30 min, and the middle phase was removed by siphoning. The pH of the liquid phase was adjusted to 5 with 1 M HCl, and it was incubated at room temperature for 30 min and centrifuged 30 min at 10 000 g. The precipitate was redispersed in 250 mL of deionized water with pH adjusted to 8 and incubated for 60 min, followed by reprecipitation at pH 5. The supernatant was decanted, and the precipitate was dispersed in 50 mL of deionized water, adjusted to pH 7 with 1 M NaOH, and lyophilized. The lyophilized precipitate was dispersed in 50 mL of heptane and centrifuged at 1500 g for 15 min, and the precipitate was similarly re-extracted twice with 25 mL of heptane and dried in a fume hood at room temperature overnight.

The protein content of the extracted FPI, MPI, LPI, OPI, and RPI was determined by the Dumas method (Flash 2000 Analyzer), with a conversion factor of 6.25. The protein content was FPI 90.8%, MPI 84.5%, LPI 96.2%, OPI 89.0%, and RPI 68.0%. According to the manufacturers, the potato protein isolate (PPI) had a protein content of 81%, and the whey protein isolate (WPI) had a protein content of 92%, the soy protein isolate (SPI) had a protein content of 90.0%.

Preparation of PNFs. The FPI, MPI, LPI, OPI, and RPI were dissolved in 0.01 M HCl, and the pH was adjusted to 2.0 with 2 M HCl. To improve the solubility of RPI, guanidine chloride (GuCl) was added to the solution to a final molarity of 7 M. The FPI, MPI, and LPI solutions were stirred for 1 h, while OPI and RPI were stirred overnight at room temperature, followed by centrifugation at 3700 g (20 °C, 30 min). The mixture with RPI was dialyzed for 24 h against

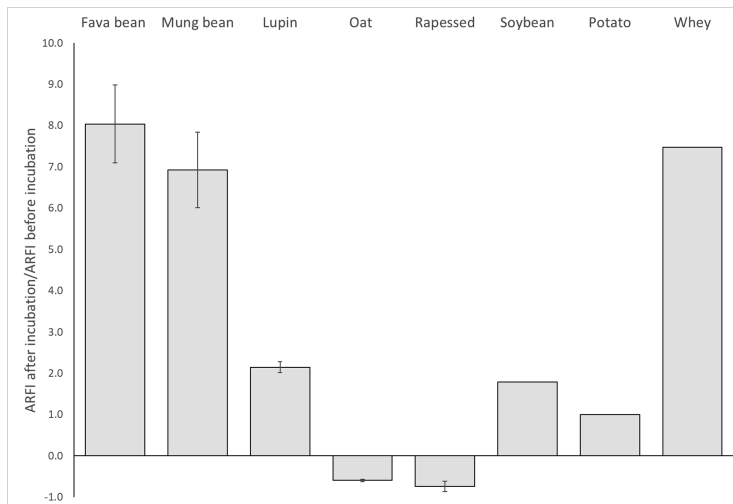


Figure 1. Proportional increase in average relative fluorescence intensity (ARFI) after incubation (ARFI after incubation/ARFI before incubation) for fava bean, mung bean, lupin, oat, and rapessed protein. Proportional increase in ARFI for soybean, potato, and whey protein after incubation is taken from Josefsson et al.,¹⁶ Josefsson et al.,¹⁸ and Ye et al.,²³ respectively.

0.01 M HCl (pH 2), using a membrane with 6–8 kDa molecular weight cutoff, before being recentrifuged.

The supernatants were recovered, pH-adjusted to 2.0 if required, and filtered through a 0.45 μm nylon syringe filter (Merck Millipore/Ireland). The filtrates from dissolved FPI, MPI, LPI, OPI, and RPI were concentrated using a spin filter with a 10 kDa cutoff (Sartorius/UK). Protein content was estimated by dry weight measurement; 1 mL from each sample containing dissolved and concentrated FPI, MPI, LPI, and OPI was dried at 105 $^{\circ}\text{C}$ for 3 h. The protein content was adjusted based on the dry weight measurement to 20 mg/mL for the dissolved and concentrated FPI, LPI, and OPI samples and to 10 mg/mL for the MPI sample. The different protein concentrations were selected based on earlier studies (not published), to avoid gelation during heating. RPI concentration was estimated by UV absorbance at 280 nm, and the concentration was adjusted to 2 mg/mL. This concentration was selected due to low quantities of RPI. The pH 2 solutions containing dissolved and concentrated FPI, MPI, LPI, OPI, and RPI were then incubated at 85 $^{\circ}\text{C}$ in a heating block without agitation for 24 h.

The PNF preparation method for SPI, PPI, and WPI was as previously published,^{16,18,23} where the setup for fibrillation was similar to the process described above, with some minor differences in concentration, incubation time, and temperature during fibrillation. Dissolved SPI, PPI, and WPI were adjusted to a concentration of 14 mg/mL (SPI and PPI) or 40 mg/mL (WPI) before incubation for 96 h (PPI) or 72 h (SPI and WPI) in an oven at 90 $^{\circ}\text{C}$. For more details on the setup used for fibrillation of SPI, PPI, and WPI, see Josefsson et al.,¹⁶ Josefsson et al.,¹⁸ and Ye et al.,²³ respectively.

Before CD and FTIR measurements and AFM imaging, PNFs made from FPI, MPI, LPI, OPI, RPI, and SPI were purified by passage through a spin filter with a 100 kDa molecular weight cutoff membrane (Sartorius/UK) spun at 1500 g, followed by dilution to initial volume. The PNFs made from PPI and WPI were dialyzed with a 100 kDa molecular weight cutoff membrane, instead of purification by a spin membrane. The dialyzed WPI and PNFs were only used for FTIR measurements and AFM imaging.

Thioflavin T Fluorescence. Thioflavin T fluorescence assay was used to detect any increase in β -sheet content due to fibril formation. To measure the content of PNFs made from FPI, MPI, LPI, OPI, and RPI, the following procedure was used: A ThT stock solution of 1

mM was prepared by diluting ThT in phosphate buffer (10 mM phosphate, 150 mM NaCl, pH 7.0). The stock solution was filtered through a 0.2 μm nylon syringe filter (VWR, USA) and stored covered in aluminum foil at -21°C . On the day of analysis, the stock solution was diluted in phosphate buffer to make a 50 μM working solution. A 100 μL sample was mixed with 900 μL of the ThT working solution and incubated for 10 min at room temperature before testing. Fluorescence intensity was measured using a multimode microplate reader (Polarstar Omega, BMG Labtech, Germany) at an excitation wavelength of 440 nm (slit width = 10.0 nm) and an emission wavelength of 480 nm (slit = 10.0 nm). The ThT working solution without addition of a protein sample was used as a blank.

A similar method was used for measuring the content of PNFs made from SPI, PPI, and WPI, with only a few modifications. For these, the measurements were made with a Varian Cary Eclipse Spectrofluorometer at emission spectra between 460 and 600 nm, instead of at a fixed wavelength of 480. For more details about the ThT measurements on SPI, PPI, and WPI, see Josefsson et al.,¹⁶ Josefsson et al.,¹⁸ and Ye et al.,²³ respectively.

Circular Dichroism Spectroscopy. Conformational changes to the secondary protein structure during fibrillation were investigated with CD spectroscopy, using a Jasco J-810 spectropolarimeter (Jasco Corp., Japan) for the FPI, MPI, LPI, OPI, and RPI samples and a Chirascan CD spectrometer (Applied Photophysics) for the SPI, PPI, and WPI samples.

The protein concentration in all samples was adjusted to 0.1 mg/mL with 0.01 M HCl before analysis. At these conditions, the proteins are 100% soluble. Spectra were obtained at 25 $^{\circ}\text{C}$ for the range 190–270 nm (190–260 for Chirascan CD), using a quartz cuvette with an optical path length of 1 mm. The spectral resolution was 1 nm, with a response time of 1 s at a bandwidth of 2 nm (spectral resolution 0.5 nm, response time 0.5 s, and bandwidth 1 nm for Chirascan CD). Ten scans (5 scans for Chirascan CD) were accumulated and averaged, and the baseline (0.01 M HCl) was subtracted.

Fourier-Transform Infrared Spectroscopy. Purified PNFs made from FPI, MPI, LPI, OPI, RPI, SPI, and PPI were flash-frozen in liquid nitrogen and subsequently freeze-dried for 24 h, while dialyzed PNFs made from WPI were dried into a film at 40 $^{\circ}\text{C}$ for 48 h. The dry powders/film were then investigated using a PerkinElmer

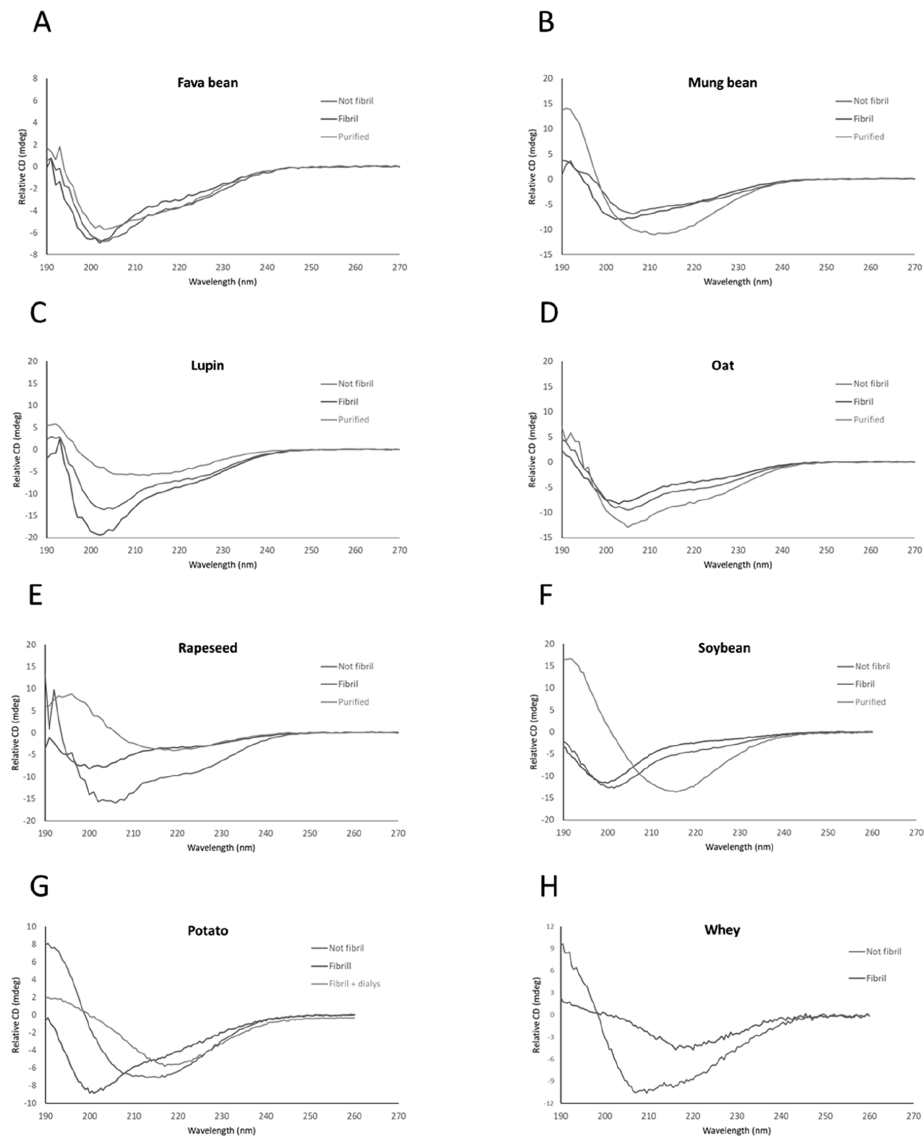


Figure 2. Circular dichroism spectra of nonfibrillated protein (blue), fibrils (red), and purified fibrils/dialyzed (green) from (A) fava bean, (B) mung bean, (C) lupin, (D) oat, (E) rapeseed, (F) soybean, (G) potato, and (H) whey. The CD spectra for soybean, potato, and whey protein are taken from Josefsson et al.,¹⁶ Josefsson et al.,¹⁸ and Ye et al.,²³ respectively.

Spectrum 400 FTIR imaging system (PerkinElmer, USA) equipped with a Specac Golden Gate germanium attenuated total reflection (ATR) crystal (Specac, UK). The IR absorption spectra were recorded in ATR image mode for the region between 600 and 4000 cm^{-1} , with 16 scans and a resolution of 4 cm^{-1} . The IR spectra were deconvoluted using the Spectrum 10.5.1 software, with an enhancement factor (γ) of 2 and a smoothing filter of 70%. Secondary structures were examined in the amide-I band (1580–1700 cm^{-1}) due to its sensitivity to C=O stretching. Origin software (version 9.1)

was used with the peak analyzer for baseline subtraction and multiple peaks fit for fitting Gaussian curves to the spectrum. The peak positions and assignments of the Gaussian curves were based on those stated by Cho et al.,²⁴ and the height and width of the curves were iteratively fitted to align with the spectrum. The content of secondary structures was calculated from the integral of the Gaussian curves, using the peak analyzer tool. Before the measurements, the purified PNFs made from FPI, MPI, LPI, OPI, RPI, SPI, and PPI were dried in a desiccator containing silica gel for at least 2–3 days.

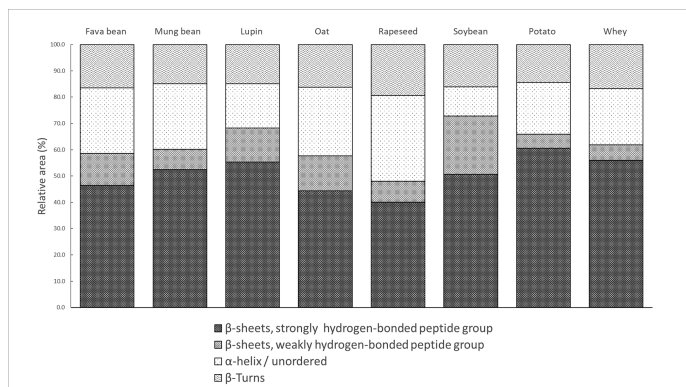


Figure 3. Relative size of resolved IR peaks from purified PNFs from fava bean, mung bean, lupin, oat, soybean, potato, and whey, grouped into those from strongly hydrogen-bonded β -sheets, weakly hydrogen-bonded β -sheets, α -helix/unordered, and β -turns. The IR peaks from purified PNFs from potato and whey protein are taken from Josefsson et al.¹⁸ and Ye et al.,²³ respectively.

Atomic Force Microscopy. AFM imaging was carried out using a Bruker Dimension FastScan instrument operating in tapping mode. The samples were diluted between 1:50 and 1:500 in 0.01 M HCl, and 15 or 25 μ L were applied on freshly cleaved mica surfaces and dried in air. FastScan A cantilevers from Bruker were used for the experiments, and the micrographs were analyzed with Gwyddion 2.48 (<http://gwyddion.net/>).

SDS-PAGE. To compare the protein profiles of the seven different protein isolates used to form PNFs, one-dimensional SDS-PAGE was performed on Mini-PROTEAN TXG, 4–20% gels. Each protein isolate was dispersed in 0.01 M HCl, and the pH was adjusted to 2 with 2 M HCl. The dispersions were filtered through 45 μ m sterile nylon syringe filters, and the concentration was adjusted to 1 mg/mL for all protein isolates (estimated with UV-absorbance, 280 nm). The samples were run under reducing conditions.

Size Exclusion Chromatography. A small amount of extracted MPI was dissolved in deionized water, and the pH was measured to be 4.2. To ensure complete dissolution of MPI, NaCl was added to a final concentration of 0.6 M. The protein solution was then centrifuged at 3500 g for 5 min, and the supernatant was filtered through a 45 μ m sterile nylon syringe filter. The extracted 8S was diluted in 25 mM Bicine pH 8.7, 200 mM NaCl. The protein solution was then vortexed thoroughly and run through a PD-10 column using the same buffer. Each of the prepared protein solutions (0.1 mL) were loaded onto a Superdex-200 Hiloal 10/300 size exclusion column with 25 mM Bicine pH 8.7, 200 mM NaCl as running buffer.

RESULTS AND DISCUSSION

PNF formation was initiated after the protein isolates were dissolved at pH 2 and incubated at 85–90 °C for 24–92 h. The secondary structure of the PNFs was analyzed using ThT fluorescence, CD spectroscopy, and FTIR spectroscopy. The morphology was evaluated using AFM.

All Isolates Are Able to Form Amyloid-Like PNFs.

Thioflavin T. ThT is a fluorescent dye that has a strong attraction for mature PNFs, due to the proposed mechanism of the dye binding to the surface side-chain grooves that run parallel to the long axis of the fibrils.²⁵ For this reason, ThT fluorescence spectroscopy is a widely used method for detection of both naturally occurring and synthetic PNFs.¹²

Figure 1 shows the relative increase in average fluorescence for all protein isolates after incubation, compared with before incubation. The change in fluorescence for the protein isolates after incubation was 8.0-fold for FPI, 6.9-fold for MPI, 2.1-fold

for LPI, 0.5-fold for OPI, 0.7-fold for RPI, 1.8-fold for SPI, 1.0-fold for PPI, and 7.5-fold for WPI. There was an increase in fluorescence after incubation for all plant-based protein isolates except OPI and RPI, which is in line with previously published data on detection of PNFs from plant-based protein isolates with ThT.^{15,17} However, there was great variation in the relative change in fluorescence among the different protein isolates after incubation compared with before incubation (Figure 1). This was due to some protein isolates (LPI, SPI, and PPI) having a relatively high fluorescence intensity already before incubation (Supporting Information, SI, Figure S1C,F,G). The decrease in OPI (0.6-fold) and RPI (0.7-fold) was due to the fluorescence peaks being higher before incubation (Figure S1D,E). Despite the general belief that ThT dye binds specifically to PNF structures and should not interact with soluble proteins in their native or partly unfolded stage, there are some contradictory findings.²⁵ For instance, serum albumin in its native state from several different species has been reported to have a high affinity to ThT dye.²⁶ These observations indicate that ThT dye should not be used as the sole method for detection of PNFs but should be used together with other verification methods.

A possible explanation for the high ThT fluorescence peaks is that reactive native protein or protein aggregates existed before fibril formation and that the denaturation and hydrolysis under PNF formation conditions (pH 2, 85 °C) eliminated these native proteins/aggregates, while PNFs were formed. In this case, the drop in ThT fluorescence from native protein/aggregate destruction was larger than the ThT fluorescence coming from PNF formation, leading to an overall reduction in ThT fluorescence. Most storage proteins are rich in β -sheets,²⁷ as has been demonstrated with FTIR measurements on oat protein isolate; e.g., one study found that OPI consisted of approximately 74% β -sheets.²⁸ Similar studies conducted on cruciferin (the major storage protein in rapeseed) have found a 45.6% β -sheet content (at pH 7).²⁹ Thus, the native protein/aggregates that interact with the ThT signaling in these cases might be due to undissolved storage proteins. In the present study, FPI was the protein source that showed the highest increase in fluorescence after incubation (8.0-fold). The high ThT fluorescence increase for MPI fibrils formed at pH 2 and

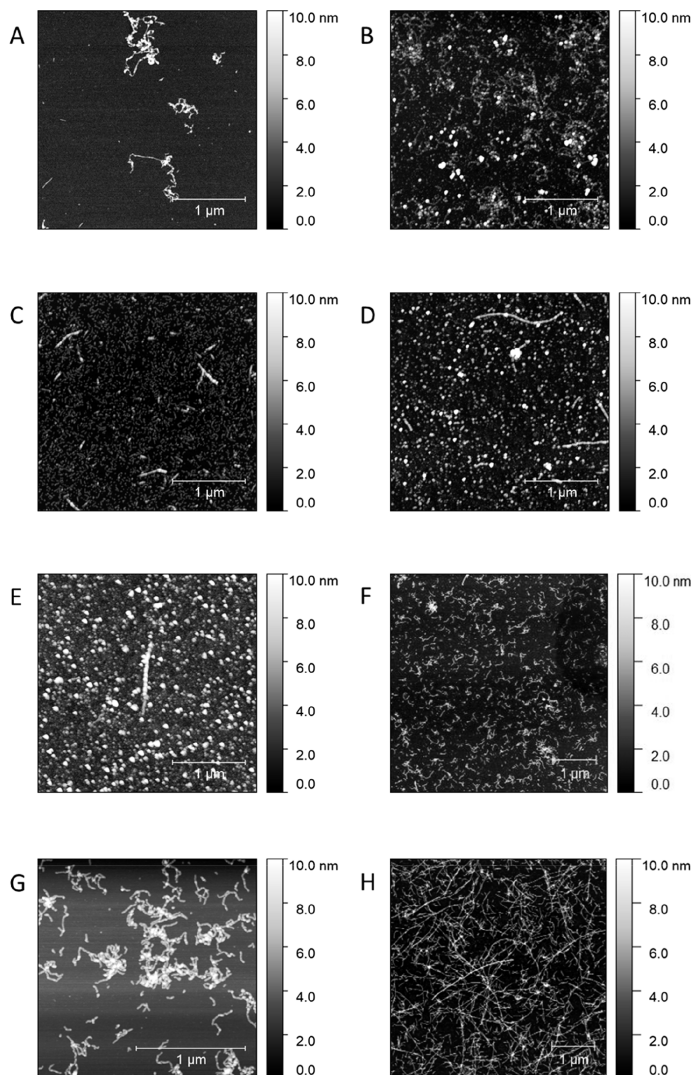


Figure 4. Atomic force microscopy images of PNFs from (A) fava bean, (B) mung bean, (C) lupin, (D) oat, (E) rapeseed, (F) soybean, (G) potato, and (H) whey, the scale bar is 1 μm in all images.

85 $^{\circ}\text{C}$ (6.9-fold) is in line with earlier published data in a study investigating the ability of vicilins (7S/8S globulins) from mung beans, red beans, and kidney beans to form PNFs.³⁰ That study concluded that vicilin from mung bean had the highest maximum fluorescence peak among the three proteins.³⁰

Circular Dichroism Spectroscopy. CD spectroscopy was used to analyze the secondary structure for all plant-based protein isolates before incubation (not fibril), after incubation (fibril), and after purification/dialysis (purified/fibril + dialys) (Figure 2). For the WPI samples, the CD spectra are the same as those published in Ye et al.²³ and only contained data before

incubation (not fibril) and after incubation (fibril). For disordered proteins, the minimum in the curve should be around 195 nm; for α -helix, there are two minima at around 222 and 208 nm, and for β -sheet structures, the minimum should be around 218 nm.³¹ The CD spectra containing proteins and nonpurified fibrils might have some interactions with nonprotein molecules; however, these possible interactions should not be applicable for the samples containing purified fibrils.

The fava bean, mung bean, lupin, oat, rapeseed, and soybean samples (Figure 2A–F) before incubation (not fibril) had a minimum peak between 201 and 206 nm, indicating

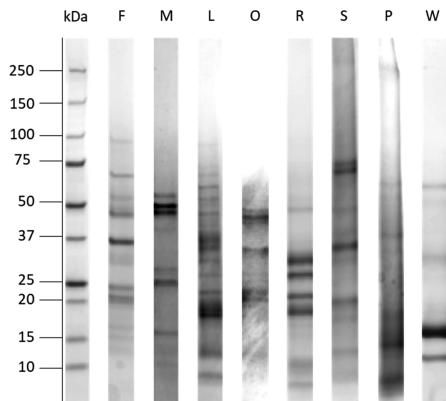


Figure 5. Electrophoretic pattern of protein isolates from fava bean (F), mung bean (M), oat (O), rapeseed (R), lupin (L), soybean (S), potato (P), and whey (W), separated by SDS-PAGE under reducing conditions.

disordered secondary structure. This behavior was observed for all protein samples except potato (Figure 2G), which had a minimum peak for the “not fibril” sample at 213 nm. Potato showed a similar pattern for the “not fibril” sample as the CD analyses on whey (Figure 2H), with a minimum at 209 nm, indicating that there could have been some ordered structures in the starting material of PPI. The indication of ordered structures in oat and rapeseed samples before incubation seen in ThT fluorescence analysis (Figure 1, Figure S1D,E in SI) was not confirmed by the CD measurements (Figure 2D,E) (not-fibril), confirming the need for complementary measurements to ThT dye in PNF detection.

After incubation (fibril), the potato sample (Figure 2G) shifted to a more disordered structure, with a minimum at 200 nm. This shift was in line with all the other plant-based samples (Figure 2A–F). For the whey sample, a clear shift to a spectrum indicating β -sheet structure was observed already after the incubation (Figure 2H) (fibril), but this was not the case for any of the plant-based samples (Figure 2A–G).

The proposed mechanism for PNF formation is that the globular protein is denatured by low pH and high temperature, which contributes to the formation of PNFs.^{32,35} Partial degradation of the polypeptide chain due to acid-induced hydrolysis is also suggested to occur. Only a small part of the polypeptide chain is beneficial for constructing PNFs, resulting in a mixture of PNFs and hydrolyzed peptides in the fibrillated sample.³⁴ This mixture of PNFs and peptides gave CD curves with a disordered structure after heat incubation for all the plant-based proteins studied (Figure 2A–G) (fibril), indicating that the majority of the samples consisted of disordered hydrolyzed peptides.

All plant-based samples had curves with a shift to the right after purification with a 100 kDa spin membrane or dialysis (Figure 2A–G) (purified/fibril + dialysis). This shift was probably due to small disordered peptides being removed by the purification and to larger ordered structures with a high amount of β -sheet remaining, which indicates that the samples contained PNFs.

Fourier-Transform Infrared Spectroscopy. FTIR spectroscopy was used to further analyze the secondary structure of

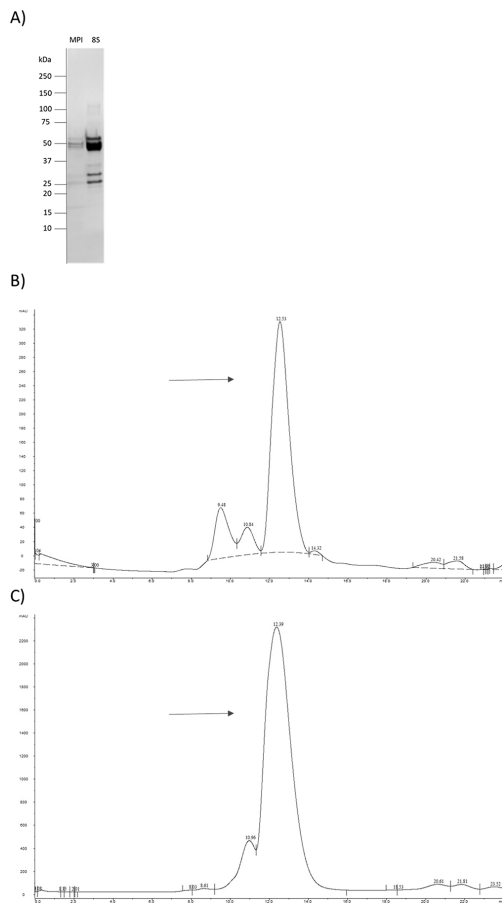


Figure 6. Electrophoretic pattern of MPI and the purified 8S fraction from mung bean protein (A). Size exclusion chromatography of MPI (B) and the purified 8S fraction (C) red arrows indicate 8S.

purified PNFs, and the values were divided into four groups: strongly hydrogen-bonded β -sheets, weakly hydrogen-bonded β -sheets, α -helix/unordered, and β -turns (Figure 3, Table S1 in SI).

All the purified PNFs made from protein isolate from legumes (fava bean, mung bean, lupin, and soybean) had a high content of strongly hydrogen-bonded β -sheets (range 46.4–55.3%). Among the plant-based PNFs, potato had the highest amount of strongly hydrogen-bonded β -sheets (60.5%) and had a low amount of weakly hydrogen-bonded β -sheets (5.4%). These results are similar to the FTIR measurements on the purified whey PNFs, which had 71.6% strongly bonded and 3.2% weakly hydrogen-bonded β -sheets. Purified PNFs from oat and rapeseed contained, respectively, 44.4 and 40.3% strongly hydrogen-bonded β -sheets and 13.3 and 8.0% weakly hydrogen-bonded β -sheets. One possible reason why both the potato and whey samples had high quantities of strongly hydrogen-bonded β -sheets is that they were dialyzed with a 100 kDa membrane, instead of filtered with a spin membrane

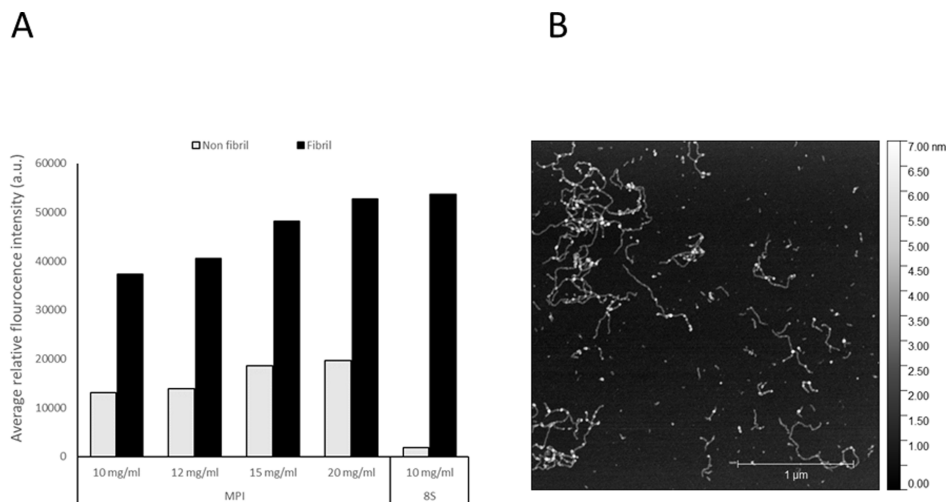


Figure 7. (A) Average relative fluorescence intensity for nonfibrillated (Nonfibril) and fibrillated (Fibril) samples from MPI at concentrations of 10, 12, 15, and 20 mg/mL and 8S at a concentration of 10 mg/mL (single measurement). (B) Atomic force microscopy image of PNFs from 8S.

at the same cutoff. The dialysis might have resulted in a purer sample compared with the plant-based PNFs (except potato), and thus, the FTIR measurements on potato and whey are not completely comparable with the results from the purified plant-based PNFs. Despite this, the results for the purified and dialyzed plant-based samples were still in alignment with the CD measurements, indicating an increased amount of β -sheet structure after purification/dialysis.

PNFs Display Variations in Nanoscale Morphologies.

Atomic force microscopy was used to determine the morphology of the PNFs. The PNFs made of protein isolate from fava bean, mung bean, lupin, oat, rapeseed, soybean, and potato were purified with a 100 kDa cutoff filter before imaging.

Fibril structures were detected in all samples after incubation (Figure 4). All PNFs had a similar height within the range 2.7–5.3 nm. The longest PNF measured within the samples was ~720 nm for fava bean, ~550 nm for mung bean, ~390 nm for lupin, ~760 nm for oat, ~910 nm for rapeseed, ~220 nm for soybean, ~340 nm for potato, and several micrometers (μ m) for whey. Some morphological differences were detected between the samples from different protein sources. PNFs made from FPI (Figure 4A), MPI (Figure 4B), SPI (Figure 4E), and PPI (Figure 4G) had a curly structure and were entangled with each other, which made their size difficult to determine. Incubated LPI (Figure 4C), OPI (Figure 4D), and RPI (Figure 4E, Figure S2) produced PNFs with a straighter shape compared with FPI, MPI, SPI, and PPI. The sample made from LPI (Figure 4C) seemed to consist mainly of small PNFs, with an average length of ~60 nm. Under the experimental conditions used in this study, none of the plant-based PNFs had the ability to form PNFs of the same length as the incubated WPI (Figure 4H). The PNFs made from WPI were generated at a higher concentration (40 mg/mL) than the PNFs made from plant-based protein isolates (2–20 mg/mL). This concentration variation is a possible explanation for the considerably longer fibers made from WPI

than from the plant-based PNFs. Secondary structure determination of the WPI-based PNFs showed CD curves that had a clear shift to the right already after fibrillation (Figure 2H) and the largest content of strongly hydrogen-bonded β -sheets among the proteins investigated (Figure 3, Table S1 in SI). This indicates that WPI has the best ability in this condition to form PNFs among the proteins investigated, which is why whey is the most commonly used protein source for studies of food-related PNFs.

Due to the small quantity of RPI available, this sample was incubated at 2 mg/mL, which can explain the low amount of PNFs detected with AFM imaging (Figure 4E, Figure S2). In the fibrillated OPI (Figure 4D) and RPI (Figure 4E, Figure S2) samples, many small spherical (~70 nm) protein aggregates were detected along with PNFs. Similar spherical structures, but in lower amounts, were observed in the fibrillated MPI sample (Figure 4B). OPI and RPI did not increase in ThT fluorescence after fibrillation compared with the untreated protein isolate (Figure 1), which could be due to undissolved β -sheet-rich protein aggregates. The small spherical structures observed in the AFM images of fibrillated and purified PNFs from OPI and RPI may be connected to the inconclusive ThT assay results. The CD analysis of both OPI and RPI showed a shift to the right after fibrillation and purification (Figure 2D,E), even though the shift for OPI was very small. However, the FTIR measurements showed that the fibrillated and purified OPI and RPI (Figure 3) had a lower amount of β -sheet-rich structures than the other protein isolates. This contradicts the hypothesis that the small spherical structures observed in the AFM images are the same aggregates that generated strong ThT fluorescence in the OPI and RPI samples before fibrillation. The hypothesis is also contradicted by the fact that similar spherical structures were seen in the fibrillated MPI sample, which had the second highest increase in ThT fluorescence after incubation.

Purity and Size of Protein May Have an Impact on PNF Formation. The features that make WPI superior to

plant-based proteins in terms of ability to form PNFs are not clear, but the quality of the isolate is one possible explanation. Another potential reason could be that the small proteins in the whey protein isolate are more soluble than the larger proteins within the plant-based protein isolates, which could be beneficial for PNF formation. Whey protein consists of two major monomeric proteins, mainly β -lactoglobulin (18.3 kDa) and α -lactalbumin (14.2 kDa).³⁵ In the SDS-PAGE analysis of the protein isolate (Figure 5), WPI had two bands between 10 and 20 kDa, indicating that this sample contained β -lactoglobulin and α -lactalbumin. None of the plant-based protein isolates contain proteins as small as those in the whey. The isolate closest in size was potato, which consists of two main relatively small protein groups, patatin (40–42 kDa) and protease inhibitors (7–21 kDa).³⁶ SDS-PAGE analysis confirmed that both patatin and protease inhibitors were present within the PPI sample (Figure 5). The PNFs made from PPI had the largest amount of strong β -sheets (Figure 3), supporting the theory that isolates containing small proteins have benefits in the formation of PNFs.

The major globular proteins in fava bean, oat, rapeseed, and soybean are 11S or 12S which have a molecular weight ranging from 320 to 360 kDa.^{37–40} For lupine, the protein content is more equally divided between the two major proteins 7S with a molecular weight of 143–260 kDa and 11S with a molecular weight between 330 and 430 kDa.⁴¹ For mung bean, the major protein (~89%) is 8S with a molecular weight of 200 kDa.⁴² The fact that the main part of the mung bean protein consists of a smaller protein (8S) than fava bean, lupine, oat, rapeseed, and soybean might be a possible explanation for MPI having the third highest relative increase in ThT fluorescence after PNF formation; only fava bean and whey had a larger increase (Figure 1). This theory is contradicted by the fact that the fava bean had the highest relative increase ThT fluorescence after PNF formation. However, the fava bean PNFs were made at a higher protein concentration (20 mg/mL) than the PNFs made from MPI (10 mg/mL) which might be a reason for the high increase in ThT fluorescence.

An alternative method to improve the PNF formation might be to pre-expose the protein isolate for enzymatic proteolysis to form smaller peptides. This has been reported to alter the formation of PNFs made from soybean protein isolate when treated with papain selective for β -conglycinin (7S), compared with whole protein isolate.⁴³ Pre-exposure of the protein isolate to proteolytic enzymes requires further investigation but might be a good method to enhance the ability of plant protein isolates to form PNFs.

Both the size and the purity of the protein isolate might be possible explanations to why WPI was superior to the other proteins in this study to form PNFs. The SDS-PAGE results (Figure 6A) show that the MPI contains similar bands as the 8S fraction, indicating that the 8S is the dominating protein in MPI. This was further confirmed with size exclusion chromatography (Figure 6B,C) where both samples had well-defined peaks (Figure 6B,C) (red arrows) at volumes (12.53 and 12.39 mL) close to 200 kDa which is the reported molecular weight of 8S.⁴² Additionally, two other peaks were observed within the MPI sample. There is one at 10.84 mL corresponding to 400 kDa which is similar to the reported weight of the 11S fraction from mung bean at 360 kDa and one at 14.32 mL corresponding to 70 kDa which is approximately half of the reported weight of the 7S fraction at 135 kDa. The reason why the assumed 7S fraction is smaller than earlier

reports is not clear, but it might be due to variations in the protein profile or variations in the preparation of the sample before the analysis. ThT fluorescence measurements show that the 8S fraction is superior to the MPI's ability to form PNFs (Figure 7A). The 8S sample has approximately the same average relative fluorescence intensity after PNF formation at a concentration of 10 mg/mL as the MPI sample had at a concentration of 20 mg/mL. Before initiating the PNF formation, the MPI sample had a higher average relative fluorescence intensity compared to the 8S fraction; the reason for this is not fully understood, but some compound within the MPI sample was interacting with the ThT dye. AFM image of the PNFs formed from the 8S fraction (Figure 7B) shows that the PNFs have the curly morphology as observed for PNFs formed from MPI (Figure 4B). When comparing the dissolved samples of MPI and 8S after PNF formation with the naked eye, there were clear differences in the color of the samples (Figure S3). The MPI sample had a brown color, whereas the sample containing 8S was transparent. The compounds that are coloring the MPI sample may be the same compounds obstructing the PNFs formation. These results indicate that the ability of the protein extract to form PNFs is increasing when the PNF-forming proteins are purified. However, this needs to be further investigated before any conclusions can be drawn.

In conclusion, this study compared the characteristics of PNFs made from seven different plant-based protein isolates (from fava bean, mung bean, lupin, rapeseed, soybean, potato, and oat). Using ThT fluorescence spectroscopy, PNFs were detected in all protein isolates except OPI and RPI. However, AFM imaging, CD spectroscopy, and FTIR measurements revealed presence of PNFs in all samples including the OPI and RPI samples, indicating limitations with using the ThT assay as the only detection method for PNFs. Using CD spectroscopy, we detected a shift to more β -sheet-rich structures for all protein isolates after PNF incubation (pH 2, 85–90 °C) and purification with a 100 kDa cutoff. This indicates that we successfully generated PNFs, with their characteristic high β -sheet content. This was confirmed by FTIR spectroscopy, which successfully quantified the content of β -sheet structures in all fibrillated protein isolates. There was some divergence in the proportion of β -sheets between the different plant-based proteins, with potato having the highest quantities. Visualization of the PNFs using AFM confirmed that we were able to generate PNFs from all protein isolates. PNFs generated from different plant-based protein sources showed distinct morphologies in terms of PNF straightness, length, and proportion of PNFs to spherical nanosized aggregates. We hypothesize that the size and purity of the protein isolate could affect the ability to form PNFs, where low molecular weight and pure isolate could be more suitable for PNF formation. Thus, PNFs can be manufactured from plant protein isolates under realistic conditions for industrial production, with their morphology depending on the protein source. Structural features such as a high aspect ratio and waviness make plant-based PNFs promising candidates for tailoring the properties of meat analogues or as a stabilizing additive.

■ ASSOCIATED CONTENT

Supporting Information

The Supporting Information is available free of charge at <https://pubs.acs.org/doi/10.1021/acsfoodscitech.1c00034>.

Average relative fluorescence intensity for nonfibrillated and fibrillated samples, table with relative content of secondary structure in the amide I region for all proteins, two additional AFM images of rapeseed PNFs, and an image of MPI and 8S samples after PNF formation (PDF)

AUTHOR INFORMATION

Corresponding Author

Anja Herneke – Department of Molecular Sciences, Swedish University of Agricultural Sciences (SLU), 750 00 Uppsala, Sweden; orcid.org/0000-0003-4646-7725; Email: anja.herneke@slu.se

Authors

Christofer Lendel – Department of Chemistry, Royal Institute of Technology (KTH), 100 44 Stockholm, Sweden; orcid.org/0000-0001-9238-7246

Daniel Johansson – Department of Molecular Sciences, Swedish University of Agricultural Sciences (SLU), 750 00 Uppsala, Sweden

William Newson – Department of Plant Breeding, Swedish University of Agricultural Sciences (SLU), 230 53 Alnarp, Sweden; orcid.org/0000-0003-4949-7567

Mikael Hedenqvist – Department of Fiber and Polymer Technology, School of Engineering Science in Chemistry, Biotechnology and Health, KTH Royal Institute of Technology, SE-100 Stockholm, Sweden; orcid.org/0000-0002-6071-6241

Saeid Karkehabadi – Department of Molecular Sciences, Swedish University of Agricultural Sciences (SLU), 750 00 Uppsala, Sweden

David Jonsson – Department of Fiber and Polymer Technology, School of Engineering Science in Chemistry, Biotechnology and Health, KTH Royal Institute of Technology, SE-100 Stockholm, Sweden

Maud Langton – Department of Molecular Sciences, Swedish University of Agricultural Sciences (SLU), 750 00 Uppsala, Sweden

Complete contact information is available at: <https://pubs.acs.org/10.1021/acsfoodscitech.1c00034>

Funding

This project was financially supported by Formas (grant no. 2018-01869 and grant no. 2017-00396), Lantmännen Research Foundation (grant no. 2017F003 and grant no. 2018F004), Trees and Crops for the Future (TC4F), a Strategic Research Area at SLU, supported by the Swedish Government, and the Faculty of Natural Resources and Agricultural Sciences at the Swedish University of Agricultural Sciences (SLU).

Notes

The authors declare no competing financial interest.

REFERENCES

- Willett, W.; Rockström, J.; Loken, B.; et al. Food in the Anthropocene: the EAT–Lancet Commission on healthy diets from sustainable food systems. *Lancet* **2019**, *393* (10170), 447–492.
- Davis, K. F.; Gephart, J. A.; Emery, K. A.; Leach, A. M.; Galloway, J. N.; D’Odorico, P. Meeting future food demand with current agricultural resources. *Glob Environ. Chang.* **2016**, *39*, 125–132.
- Graça, J.; Calheiros, M. M.; Oliveira, A. Moral Disengagement in Harmful but Cherished Food Practices? An Exploration into the Case of Meat. *J. Agric. Environ. Ethics.* **2014**, *27* (5), 749–765.
- Apostolidis, C.; McLeay, F. Should we stop eating like this? Reducing meat consumption through substitution. *Food Policy.* **2016**, *65*, 74–89.
- Jansens, K. J. A.; Rombouts, I.; Grootaert, C.; et al. Rational Design of Amyloid-Like Fibrillary Structures for Tailoring Food Protein Techno-Functionality and Their Potential Health Implications. *Compr. Rev. Food Sci. Food Saf.* **2019**, *18* (1), 84–105.
- Sipe, J. D.; Benson, M. D.; Buxbaum, J. N.; et al. Amyloid fibril proteins and amyloidosis: chemical identification and clinical classification International Society of Amyloidosis 2016 Nomenclature Guidelines. *Amyloid* **2016**, *23*, 6129.
- Fitzpatrick, A. W.; Knowles, T. P. J.; Waudby, C. A.; Vendruscolo, M.; Dobson, C. M. Inversion of the balance between hydrophobic and hydrogen bonding interactions in protein folding and aggregation. *PLoS Comput. Biol.* **2011**, *7* (10), No. e1002169.
- Ye, X.; Lendel, C.; Langton, M.; Olsson, R. T.; Hedenqvist, M. S. Protein Nanofibrils: Preparation, Properties, and Possible Applications in Industrial Nanomaterials. *Industrial Applications of Nanomaterials* **2019**, 29–63.
- Mohammadian, M.; Madadlou, A. Technological functionality and biological properties of food protein nanofibrils formed by heating at acidic condition. *Trends Food Sci. Technol.* **2018**, *75* (July 2017), 115–128.
- Chiti, F.; Dobson, C. M. Protein Misfolding, Functional Amyloid, and Human Disease. *Annu. Rev. Biochem.* **2006**, *75* (1), 333–366.
- Knowles, T. P. J.; Mezzenga, R. Amyloid fibrils as building blocks for natural and artificial functional materials. *Adv. Mater.* **2016**, *28* (31), 6546–6561.
- Cao, Y.; Mezzenga, R. Food protein amyloid fibrils: Origin, structure, formation, characterization, applications and health implications. *Adv. Colloid Interface Sci.* **2019**, *269*, 334–356.
- Goldschmidt, L.; Teng, P. K.; Riek, R.; Eisenberg, D. Identifying the amyloids, proteins capable of forming amyloid-like fibrils. *Proc. Natl. Acad. Sci. U. S. A.* **2010**, *107* (8), 3487–3492.
- Lassé, M.; Ulluwishewa, D.; Healy, J.; et al. Evaluation of protease resistance and toxicity of amyloid-like food fibrils from whey, soy, kidney bean, and egg white. *Food Chem.* **2016**, *192*, 491–498.
- Akkermans, C.; Van Der Goot, A. J.; Venema, P.; et al. Micrometer-sized fibrillar protein aggregates from soy glycinin and soy protein isolate. *J. Agric. Food Chem.* **2007**, *55* (24), 9877–9882.
- Josefsson, L.; Cronhamn, M.; Ekman, M.; Widehammar, H.; Emmer, Å.; Lendel, C. Structural basis for the formation of soy protein nanofibrils. *RSC Adv.* **2019**, *9* (11), 6310–6319.
- Munialo, C. D.; Martin, A. H.; Van Der Linden, E.; De Jongh, H. H. J. Fibril formation from pea protein and subsequent gel formation. *J. Agric. Food Chem.* **2014**, *62* (11), 2418–2427.
- Josefsson, L.; Ye, X.; Brett, C. J.; et al. Potato Protein Nanofibrils Produced from a Starch Industry Sidestream. *ACS Sustainable Chem. Eng.* **2020**, *8*, 1058.
- Li, T.; Wang, L.; Zhang, X.; Geng, H.; Xue, W.; Chen, Z. Assembly behavior, structural characterization and rheological properties of legume proteins based amyloid fibrils. *Food Hydrocolloids* **2021**, *111* (October 2020), 106396.
- Li, J.; Pylypchuk, L.; Johansson, D. P.; Kessler, V. G.; Seisenbaeva, G. A.; Langton, M. Self-assembly of plant protein fibrils interacting with superparamagnetic iron oxide nanoparticles. *Sci. Rep.* **2019**, *9* (1), 1–18.
- Gade Malmos, K.; Blancas-Mejia, L. M.; Weber, B.; et al. ThT 101: a primer on the use of thioflavin T to investigate amyloid formation. *Amyloid* **2017**, *24* (1), 1–16.
- Wu, Y. V.; Sexson, K. R.; Cluskey, J. E.; Inglett, G. E. Protein Isolate From High-Protein Oats: Preparation, Composition and Properties. *J. Food Sci.* **1977**, *42* (5), 1383–1386.

- (23) Ye, X.; Hedenqvist, M. S.; Langton, M.; Lendel, C. On the role of peptide hydrolysis for fibrillation kinetics and amyloid fibril morphology. *RSC Adv.* **2018**, *8* (13), 6915–6924.
- (24) Cho, S. W.; Gällstedt, M.; Johansson, E.; Hedenqvist, M. S. Injection-molded nanocomposites and materials based on wheat gluten. *Int. J. Biol. Macromol.* **2011**, *48* (1), 146–152.
- (25) Biancalana, M.; Koide, S. Molecular mechanism of Thioflavin-T binding to amyloid fibrils. *Biochim. Biophys. Acta, Proteins Proteomics* **2010**, *1804* (7), 1405–1412.
- (26) Sen, P.; Fatima, S.; Ahmad, B.; Khan, R. H. Interactions of thioflavin T with serum albumins: Spectroscopic analyses. *Spectrochim. Acta, Part A* **2009**, *74* (1), 94–99.
- (27) Marcone, M. F.; Kakuda, Y.; Yada, R. Y. Salt soluble seed globulins of dicotyledonous and monocotyledonous plants II. Structural characterization. *Food Chem.* **1998**, *63* (2), 265–274.
- (28) Liu, G.; Li, J.; Shi, K.; et al. Composition, secondary structure, and self-assembly of oat protein isolate. *J. Agric. Food Chem.* **2009**, *57* (11), 4552–4558.
- (29) Perera, S. P.; McIntosh, T. C.; Wanasundara, J. P. D. Structural properties of cruciferin and napin of *Brassica napus* (canola) show distinct responses to changes in pH and temperature. *Plants* **2016**, *5* (3), 64–74.
- (30) Liu, J.; Tang, C. H. Heat-induced fibril assembly of vicilin at pH2.0: Reaction kinetics, influence of ionic strength and protein concentration, and molecular mechanism. *Food Res. Int.* **2013**, *51* (2), 621–632.
- (31) Greenfield, N. J. Using circular dichroism spectra to estimate protein secondary structure. *Nat. Protoc.* **2006**, *1* (6), 2876–2890.
- (32) Aymard, P.; Nicolai, T.; Durand, D.; Clark, A. Static and Dynamic Scattering of β -Lactoglobulin Aggregates Formed after Heat-Induced Denaturation at pH 2. *Macromolecules* **1999**, *32* (8), 2542–2552.
- (33) Tang, C. H.; Wang, C. S. Formation and characterization of amyloid-like fibrils from soy β -conglycinin and glycinin. *J. Agric. Food Chem.* **2010**, *58* (20), 11058–11066.
- (34) Akkermans, C.; Venema, P.; van der Goot, A. J.; et al. Peptides are building blocks of heat-induced fibrillar protein aggregates of β -lactoglobulin formed at pH 2. *Biomacromolecules* **2008**, *9* (5), 1474–1479.
- (35) Madureira, A. R.; Pereira, C. I.; Gomes, A. M.P.; Pintado, M. E.; Xavier Malcata, F. Bovine whey proteins - Overview on their main biological properties. *Food Res. Int.* **2007**, *40* (10), 1197–1211.
- (36) Lokra, S.; Strætkvern, K. O. Industrial Proteins from Potato Juice. A Review. *Food* **2015**, 88.
- (37) Langton, M.; Ehsanzamir, S.; Karkehabadi, S.; Feng, X.; Johansson, M.; Johansson, D. P. Gelation of faba bean proteins - Effect of extraction method, pH and NaCl. *Food Hydrocolloids* **2020**, *103*, 105622.
- (38) Mäkinen, O. E.; Sozer, N.; Ercili-Cura, D.; Poutanen, K. Protein From Oat: Structure, Processes, Functionality, and Nutrition. *Sustainable Protein Sources* **2017**, 105.
- (39) Yonsel, S. Extraction of Protein Mixture from Rapeseed for Food Applications. MSc Thesis, 2018.
- (40) Barac, M.; Stanojevic, S.; Jovanovic, S.; Pesic, M. Soy protein modification: A review. *Acta Period. Technol.* **2004**, *280* (35), 3–16.
- (41) Duranti, M.; Consonni, A.; Magni, C.; Sessa, F.; Scarafoni, A. The major proteins of lupin seed: Characterisation and molecular properties for use as functional and nutraceutical ingredients. *Trends Food Sci. Technol.* **2008**, *19* (12), 624–633.
- (42) Mendoza, E. M. T.; Adachi, M.; Bernardo, A. E. N.; Utsumi, S. Mungbean [*Vigna radiata* (L.) Wilczek] globulins: Purification and characterization. *J. Agric. Food Chem.* **2001**, *49* (3), 1552–1558.
- (43) Xia, W.; Zhang, H.; Chen, J.; et al. Formation of amyloid fibrils from soy protein hydrolysate: Effects of selective proteolysis on β -conglycinin. *Food Res. Int.* **2017**, *100*, 268–276.

ACTA UNIVERSITATIS AGRICULTURAE SUECIAE

DOCTORAL THESIS NO. 2022:44

This thesis explores the potential of protein nanofibrils (PNFs) as an ingredient to generate structure in food. Proteins from whey and plants were used to form PNFs, focusing on proteins extracted from plants. The secondary structure and nanostructure of all PNFs were characterised and results showed that all seven plant-proteins investigated formed PNFs. The ability of PNFs to stabilise foams and form microfibers was explored. Results showed that PNFs could improve foaming properties, and could align into relatively stable microfibers.

Anja Herneke received her graduate education at the Department of Molecular Sciences, SLU, Uppsala. She received her B.Sc. and M.Sc. degree in Biomedicine at Lund University, Sweden.

Acta Universitatis Agriculturae Sueciae presents doctoral theses from the Swedish University of Agricultural Sciences (SLU).

SLU generates knowledge for the sustainable use of biological natural resources. Research, education, extension, as well as environmental monitoring and assessment are used to achieve this goal.

ISSN 1652-6880

ISBN (print version) 978-91-7760-963-6

ISBN (electronic version) 978-91-7760-964-3